The Invariable Variability of Alpha Oscillations: Alterations in Power and Peak Frequency

Inaugural thesis

presented to the Faculty of Mathematics and Natural Sciences

of Heinrich Heine University Düsseldorf

for the degree of

Doctor of Philosophy in Natural Sciences

Submitted by

Vaishali Balaji

from Vellore, India

Düsseldorf, February 2026

From the Institute of Clinical Neuroscience and Medical Psychology
of Heinrich Heine University Düsseldorf

Printed by permission of the
Faculty of Mathematics and Natural Sciences
of Heinrich Heine University Düsseldorf

Examiners:

1. PD Dr. Joachim Lange
2. Prof. Dr. Eckart Zimmermann

Date of oral defence: 19.05.26

ACKNOWLEDGMENTS

I would like to express my deepest gratitude to my supervisor, Dr. Joachim Lange, whose calm and resolute guidance has shaped this research in fundamental ways. I would also like to extend my sincere thanks to Prof. Alfons Schnitzler for his invaluable support and encouragement. Additionally, this endeavour would not have been possible without the generous support of the Deutsche Forschungsgemeinschaft, which funded my research.

I could not have undertaken this journey without the unwavering enthusiasm of my dear colleagues, who have become friends and more along the way. Thanks should also go to my study participants for their cooperation.

Lastly, I would like to mention my parents. This thesis is dedicated to them, as all of my achievements in life are.

TABLE OF CONTENTS

LIST OF ABBREVIATIONS

PSP Postsynaptic Potentials

EPSP Excitatory Postsynaptic Potentials

IPSP Inhibitory Postsynaptic Potentials

MRI Magnetic Resonance Imaging

CT Computerised Tomography

MEG Magnetoencephalography

EEG Electroencephalography

SQUID Superconducting Quantum Interference Device

BEM Boundary Element Model

FEM Finite Element Model

CSF Cerebro Spinal Fluid

LCMV Linearly Constrained Minimum Variance

ERD Event-Related Desynchronisation

APF Alpha Peak Frequency

PAC Phase Amplitude Coupling

NIBS Non-Invasive Brain Stimulation

TMS Transcranial Magnetic Stimulation

TES Transcranial Electrical Stimulation

tDCS Transcranial Direct Current Stimulation

tACS Transcranial Alternating Current Stimulation

STDP Spike Timing Dependent Plasticity

LTP Long-Term Potentiation

LTD Long-Term Depression

SSR Steady State Response

SUMMARY

Alpha oscillations are a defining feature of the brain's rhythmic activity. Although they were initially dismissed as an idle rhythm, a growing body of evidence indicates that they play an essential role in perception and cognition. Given their functional relevance, the alpha rhythm is unlikely to be static; rather, both its strength and speed are dynamically adjusted. In this thesis, I aimed to elucidate the extent of their flexibility by actively modulating the amplitude of alpha oscillations using weak electrical stimulation in Study 1, and by characterising spontaneous variability in alpha dynamics in Study 2.

In Study 1, we modulated oscillatory alpha activity in the right somatosensory cortex using short trains of transcranial alternating current stimulation (tACS). During simultaneous magnetoencephalography (MEG) recordings, participants received intermittent tACS or no stimulation, which served as a control. Stimulation was administered in 10 s and 30 s trains at an individually-adapted stimulation frequency (ISF), selected to approximate each participant's alpha peak frequency (APF) at rest. We observed elevations in oscillatory power following tACS relative to control, most prominently around the ISF, with additional effects extending into the beta range. These effects were distributed bilaterally across somatosensory and frontal regions. Notably, 10 s trains produced a greater increase in power than 30 s trains, demonstrating that even very brief periods of tACS can robustly modulate alpha-band activity.

Study 2 was motivated by a key limitation identified in Study 1, namely the difficulty of aligning ISF with each participant's endogenous APF. Using resting-state MEG data from the control sessions of Study 1, we characterised spontaneous fluctuations in APF at a fine temporal scale across the cortex. We found that variability in APF increases systematically along the posterior-to-anterior cortical axis, from occipital to frontal regions. Comparisons with amplitude-matched simulated data confirmed that this gradient could not be explained by measurement noise alone. Across cortical regions, APFs exhibited poor temporal reliability, suggesting that APF reflects a transient state rather than a stable trait.

In Study 1, we demonstrated that alpha power can be modulated through brief bouts of electrical stimulation, whereas in Study 2, we showed that alpha frequency fluctuates substantially even in the absence of external modulation. Overall, this work contributes to a broader understanding of alpha oscillations, highlighting that variability is a fundamental characteristic of their dynamics, rather than mere noise.

1 INTRODUCTION

Alpha oscillations are inherently dynamic, exhibiting spontaneous fluctuations in power and frequency as well as sensitivity to external modulation. The malleable nature of alpha activity is thus as an intrinsic property of its ongoing neural dynamics. Such malleability is also thought to underlie the brain's flexibility in information processing and cognition. In this thesis, I investigated the adaptable nature of alpha oscillations by applying weak electric currents to the brain to modify the amplitude of these oscillations and quantified the spontaneous changes in alpha frequency while at rest. In this introduction, I will outline the theoretical groundwork necessary to understand the appended studies. In section **1.1**, I will introduce neural oscillations and its presumed role in cognition. Next, in section **1.2**, I will detail how techniques such as Magnetoencephalography measure neural oscillations and elaborate on how the sources of neural activity are determined. In section **1.3**, I will focus on alpha oscillations. I will briefly discuss its role in brain functioning and highlight its variable nature. Finally, in section **1.4**, I will explain how neuromodulation techniques such as transcranial Alternating Current Stimulation can be used to vary oscillatory activity and in turn behaviour.

1.1 Neural Oscillations

Nearly a century ago, Bishop (1932) demonstrated that the excitability of the rabbit optic pathway undergoes cyclic variations. Following an initial stimulus, he observed a transient reduction in responsiveness, which was then followed by a phase of heightened excitability. These early findings provided compelling evidence that neural excitability is subject to temporal modulation. Since then, a growing body of research has shown that neuronal oscillations play a central role in organizing local and long-range cortical dynamics, offering a temporal scaffold for perception, cognition, and behaviour. Neuronal oscillations are pervasive across mammalian cortical networks. Their presence across species and behavioural states reflects their involvement in the basic dynamics of nerve cells and neural circuits (Buzsáki & Draguhn, 2004). As such, understanding the role of oscillatory activity has become essential to understanding brain function itself.

1.1.1 Neuron, Spike Activity and Oscillations

Neurons are the fundamental building blocks of the brain. Their dendrites enable them to receive inputs from numerous other neurons via synaptic connections. The soma, or cell body, houses the nucleus along with other essential organelles that support cell functions. Extending from the soma is the axon, a crucial structure responsible for carrying information toward the synapse, where communication with other neurons occurs through synaptic transmission (Dayan & Abbott, 2005). In addition to their structural features, neurons also exhibit unique physiological properties. One of the most significant is the presence of diverse ion channels embedded in their membranes. These channels regulate the movement of key ions, such as sodium (Na^+), potassium (K^+), calcium (Ca^{2+}), and chloride (Cl^-), in-and-out of the neuron. They function by opening or closing in response to shifts in membrane voltage (Cotman & McGaugh, 1980a).

In a resting state, the difference in voltage between the inside of a neuron and the surrounding extracellular fluid, known as the resting membrane potential, is typically around -70 millivolts, indicating that sodium ions (Na^+) are more concentrated outside the neuron, whereas potassium ions (K^+) are more abundant inside. These ionic imbalances drive ion movement across the membrane. When positively charged ions exit the neuron or negatively charged ions enter, the inside becomes more negative—a phenomenon known as hyperpolarization. Conversely, when positive ions enter the cell, reducing the negative charge or even making the inside positive, the process is called depolarization (Barnett & Larkman, 2007). When a neuron's membrane

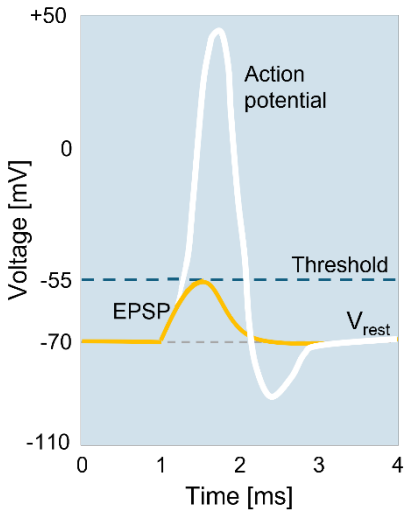

Figure. 1 Action potential. EPSPs (yellow) depolarise the membrane; when the summed effect of multiple EPSPs reaches threshold (blue dashed line), an action potential (white) is triggered. The resting potential (V_{rest}) is indicated by the grey dashed line. Original work by Vaishali Balaji, 2025.

potential becomes sufficiently depolarized and crosses a certain threshold, it triggers a positive feedback loop that leads to the generation of an action potential (Fig. 1). This event involves a rapid change of approximately 100 millivolts in the membrane potential and typically lasts around 1 millisecond. The ability to generate a new action potential also depends on the neuron's recent activity. Immediately after an action potential, the neuron enters an absolute refractory period—a brief time during which initiating another spike is nearly impossible (Cotman & McGaugh, 1980a). Axons end at synapses, where the arrival of an action potential triggers the opening of ion channels. This allows calcium ions (Ca^{2+}) to enter the neuron, prompting the release of neurotransmitters. These neurotransmitters then bind to receptors on the postsynaptic neuron, leading to the opening of ion-conducting channels (Cotman & McGaugh, 1980b). This induces graded changes in the membrane potential, known as postsynaptic potentials (PSPs; Purves, 2008). Excitatory postsynaptic potentials (EPSP) make the postsynaptic neuron more likely to fire an action potential by depolarising the cell whereas inhibitory postsynaptic potentials (IPSP) decrease the likelihood of an action potential by hyperpolarising the cell. Membrane potential experiences just a slight depolarization of ~0.1 to 10 mV from a single EPSP, which is not sufficient to trigger an action potential. Instead, the postsynaptic neuron linearly integrates PSPs over time or space, and the cumulative effect of several EPSPs may cause an action potential (Purves, 2008).

Neurons do not function in isolation; instead, they operate in synchrony as a part of cell assemblies (Hebb, 1949). The constituent neurons, namely pyramidal and interneurons, are interconnected by feedforward and feedback loops (Buzsáki et al., 1983; Whittington et al., 2000). Inhibitory interneurons, by means of negative feedback loops, generate alternating windows of responsiveness to inputs: periods of increased excitability, during which action potentials are likely to occur, alternate with periods of low excitability (Fries et al., 2007). As such, excitatory neurons drive inhibitory neurons, which in turn inhibit the same excitatory cells by generating IPSPs (Bishop, 1932; Buzsáki et al., 2013; Lindsley, 1939). This reciprocal antagonism produces rhythmic activity in both cell populations (Buzsáki & Wang, 2012).

At the peak of increased excitability, incoming EPSPs are highly likely to summate and trigger action potentials, whereas in the subsequent phase of heightened inhibition, EPSPs do not combine effectively and the neuron's membrane potential does not reach the firing threshold due to hyperpolarization (Purves, 2008). Thus, oscillations periodically modulate the ability of cell populations to relay signals, whereby there are shorter windows of opportunity at higher oscillation frequencies. The oscillation's frequency and regularity depend on several interacting factors, including synaptic kinetics (EPSPs, IPSPs), conduction delays of the feedback loops, and the excitatory drive of the circuits in the assembly (Amzica & Lopes da Silva, 2011).

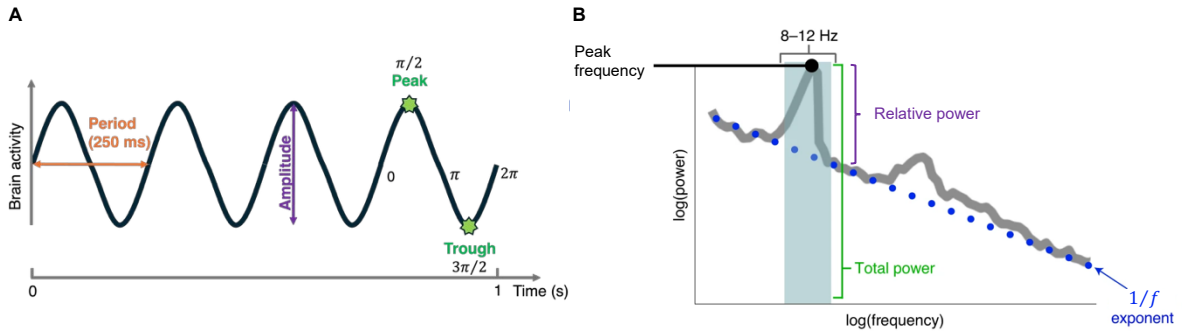

Figure 2. Oscillatory parameters. A) A 4 Hz oscillation is represented. One cycle takes 250 seconds, and four cycles are completed in one second. The phase varies from 0 to 2π along one cycle. The peak and the trough correspond to the maximum and minimum activity respectively, and the amplitude is the distance between minimum and maximum activity. Original work by Vaishali Balaji, 2025. B) Example neural power spectrum with a prominent alpha peak (8–12 Hz, blue-shaded region). Total power (green bars in the inset) reflects the total power in this range, and relative power (purple bars in the insets) reflects relative power of the peak above the 1/f component (dotted blue line). Adapted from Donoghue et al. (2020).

Neural oscillations, whether measured at micro-, meso-, or macro scales, are described by the following parameters (Fig. 2A). The period refers to the time taken to complete one oscillatory cycle, while the frequency indicates how many such cycles occur per second, expressed in hertz (Hz). The amplitude captures the magnitude of fluctuations between the minimum and maximum activity, and the power corresponds to the square of the amplitude, providing a measure of signal strength. Finally, the phase specifies the position within the oscillatory cycle at a given time, typically expressed in radians (0–2π). The power of the signal shows a characteristic 1/f distribution (Fig. 2B; Nunez & Srinivasan, 2006), reflecting that slow oscillations produce large, synchronous membrane-potential fluctuations across widespread networks, while fast oscillations involve smaller, localized changes within limited neural volumes (He et al., 2008).

1.1.2 Functions of Oscillations

Neural oscillations serve fundamental computational needs for the effective processing of time and information (Buzsáki et al., 2013). They span several orders of magnitude in frequency i.e., from infra-slow (<0.01 Hz), delta (0.2–3.5 Hz), theta (4–7.5 Hz), alpha (8–13 Hz), beta (14–30 Hz), gamma (30–90 Hz), to ultra-fast oscillations (>90 Hz). The frequency bands, along with their temporal dynamics, and their links to behaviour, are present even in other mammalian species (Buzsáki & Draguhn, 2004).

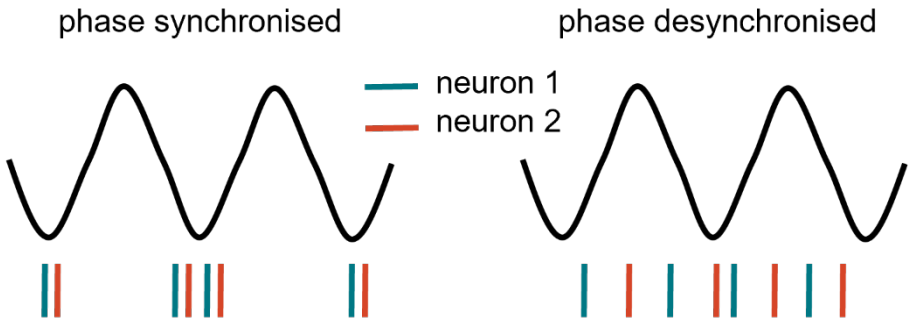

Figure 3. Example of spike-phase synchronisation. The oscillatory traces on top depict two cycles of a hypothetical oscillatory signal of a narrow frequency band. The spiking activity of two example neurons is shown in red and blue, illustrating a synchronized state, in which spikes are aligned with the oscillatory troughs, and desynchronized state, in which spikes are distributed across different oscillatory phases. Adapted from Esghaei et al., (2018).

When populations of neurons become entrained to an oscillation, their spikes tend to cluster in time, forming bursts that are phase-locked to the underlying rhythm (Fig. 3; Voloh & Womelsdorf, 2018). This temporal clustering enhances the saliency of neural signals (Gray & McCormick, 1996) by increasing the likelihood of postsynaptic activation, without necessarily raising the overall spike count (Larkum, 2013). Oscillatory synchronization thus provides a temporal scaffold for organizing neural discharges into coherent sequences. This dramatically expands the coding capacity of neural circuits (Masquelier et al., 2009). Neurons may fire in perfect synchrony (zero phase lag) or with systematic phase delays relative to one another, effectively encoding ordered information streams through phase coding—a mechanism that supports temporally structured processes such as speech (Assaneo & Orpella, 2024).

Beyond local coordination, oscillations regulate the selective transmission of information between brain regions. The “communication through coherence” framework (Fries, 2005) posits that the alignment of oscillatory phases determines the efficiency of information exchange between neuronal populations: when their rhythms are aligned, synaptic inputs coincide with periods of high excitability, whereas misalignment suppresses communication (Fig. 4). In this way, the brain can dynamically route signals across fixed anatomical pathways

without altering synaptic strength. Khamechian et al., (2024), for example, showed that the coupling strength between the phase of beta oscillations and the power of high-gamma activity (reflecting local neuronal firing) predicts the speed of perceptual reports in rhesus monkeys. Such findings (also see Luczak et al., 2013) reveal that oscillatory dynamics gate the transmission of sensory information in accordance with behavioural demands.

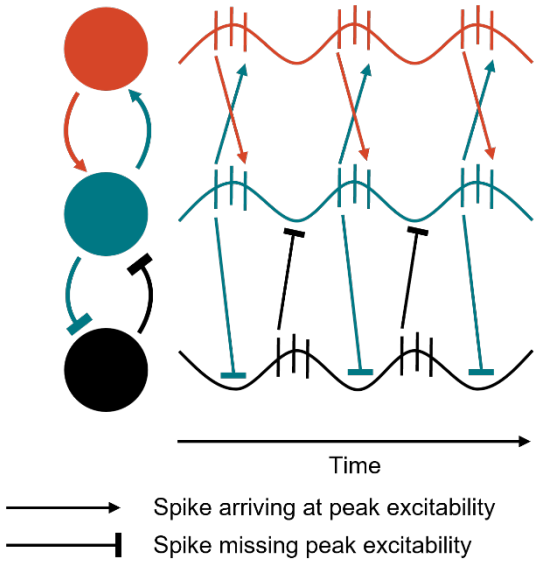

Figure 4. A schematic illustration of communication through coherence. The red and blue neuronal groups are phase-locked such that spiking in one set of cells will coincide with the excitatory phase in the other cells, enabling effective communication. In contrast, the phase relationship between the red and black groups is misaligned, causing incoming spikes to miss the excitatory phase and thereby preventing information transfer. Spikes that arrive during periods of peak excitability are shown with pointed arrowheads, whereas spikes that miss these peaks have blunt arrowheads. The red and green neuronal groups undergo coherent excitability fluctuations, and their communication is therefore effective. The red and green groups thus exhibit coherent excitability fluctuations that support communication, while the black group's incoherent fluctuations inhibit it. Reproduced from Fries (2005).

Oscillatory synchrony also provides a mechanism for rapid and flexible reconfiguration of functional networks. By transiently binding distributed cortical areas, oscillations allow the brain to assemble and dissolve task-relevant coalitions of neurons on demand (Von Der Malsburg et al., 2010). Evidence from multi-electrode recordings in monkeys shows that neurons in the prefrontal cortex exhibit synchronized oscillatory activity in the low-β range during the delay period preceding stimulus presentation (Liang et al., 2002), consistent with a role for oscillations in maintaining task-relevant information. Complementary findings from Zareian et al., (2020) indicate that phase coherence in the middle temporal area increases when attention is directed toward a neuron's receptive field. This attentional enhancement of phase coherence correlated with both increased stimulus-evoked firing and faster behavioural responses, highlighting how synchronization serves as an anticipatory mechanism for optimizing neural processing.

Despite extensive evidence linking oscillations to cognition, their causal role remains heavily debated. Critics argue that they may be epiphenomenal rather than mechanistically relevant (see Singer, 2018), citing three main concerns: (1) analytical tools such as Fourier- and wavelet-based methods assume that oscillations are frequency-stable and persist over many cycles, while commonly used stimulus paradigms (e.g., drifting gratings) preferentially elicit sustained

oscillations, together inflating their apparent prevalence (Ray & Maunsell, 2010, 2015); (2) oscillatory synchrony may be incompatible with the temporal constraints of natural vision and active behaviour, which unfold over a few hundred milliseconds (e.g., the ~250 ms between saccades; Maldonado et al., 2008). Moreover, oscillatory synchrony often weakens or disappears under more ecologically valid conditions, such as cluttered scenes or low-contrast images (Lima et al., 2010), and its frequency and power vary systematically with stimulus contrast, motion speed, eccentricity, and complexity. Such variability is viewed as fundamentally at odds with theories that posit oscillations as stable vehicles of neural coding, including binding-by-synchrony (Singer, 1993; Singer & Gray, 1995) and communication-through-coherence (Fries, 2005); and (3) even if synchrony enhances sparse and noisy spiking (Singer, 1999; VanRullen et al., 2001, 2005), its volatility undermines its reliability as a neural code (Averbeck et al., 2006). Together, these critiques suggest oscillations may reflect emergent network dynamics rather than causal mechanisms of cognition, underscoring the need for methods that capture their transient, context-dependent nature.

1.2 Electrophysiology

The structure of the brain can be studied in detail via autopsy specimens or in vivo with Magnetic Resonance Imaging (MRI) and Computerised Tomography (CT). But to understand how the brain functions i.e., how it coordinates activity in space, time, and across oscillatory frequencies, requires tools that go beyond anatomy (Supek & Aine, 2019). Electrophysiology uniquely enables the direct measurement of neural dynamics with the temporal precision required to study brain function (Fig 5).

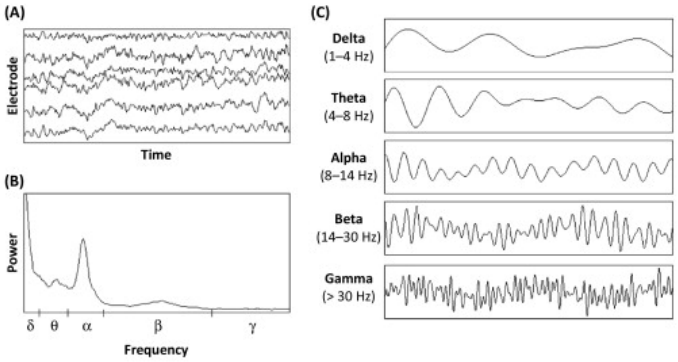

Figure 5. Electrophysiological signals. (A) EEG data recorded from six electrodes positioned on the scalp. (B) A plot of the power of specific oscillatory frequencies (δ, delta; θ, theta; α, alpha; β, beta; γ, gamma) in resting-state EEG data. (C) Electrophysiological data band-pass filtered into the delta, theta, alpha, beta, and gamma bands. Reproduced from Clayton et al. (2015).

Electroencephalography (EEG; Berger, 1929) records electrical fields generated by neuronal activity, while magnetoencephalography (MEG; Cohen, 1972) registers corresponding magnetic fields. Both reflect the same underlying sources—postsynaptic currents in populations of neurons, and are unique among non-invasive techniques, as they offer direct measures of neuronal activity with a millisecond temporal resolution (Hämäläinen et al., 1993). Their temporal frequency spans from under 1 Hz to over 100 Hz, providing insight into rapid brain rhythms and frequency-dependent interactions underlying cognition (Baillet et al., 2001; Supek & Aine, 2019).

Though EEG and MEG share temporal resolution, MEG offers several advantages. First, magnetic fields pass through skull and scalp with minimal distortion, unlike electrical potentials, which are smeared by intervening tissues (Baillet et al., 2001). This property means MEG requires less precise modelling of head-tissue conductivities to localize sources reliably. Second, MEG does not need a reference electrode (as EEG does), which reduces ambiguity in signal interpretation (Baillet, 2017). Together, these features enable more accurate spatial localization of neuronal generators.

Used alone or in combination with MRI, MEG contributes uniquely to our understanding of both regional and large-scale neural dynamics. It enables investigation of spontaneous and event-related activity, the mechanisms of functional connectivity between regions, and modes of network communication in the brain.

1.2.1 Magnetoencephalography

In MEG, the electrochemical currents circulating within and between neurons generate magnetic induction. When presynaptic neurotransmitter release generates dendritic PSPs, transmembrane ionic currents flow along the soma–dendritic axis i.e., from the negative pole (sink) to the positive pole (source), generating a primary intracellular current (Fig. 6B) accompanied by an extracellular return current (Lopes da Silva, 2013). In populations of neurons with aligned dendritic trees, such as cortical pyramidal cells, these microscopic currents summate to form a macroscopic current dipole (Hari & Puce, 2023). Because pyramidal neurons are organized in parallel "palisades", the longitudinal components of their intracellular currents add constructively, while transverse components cancel. The resulting laminar current generates both an electric field (recorded by EEG) and a magnetic field encircling the current axis (recorded by MEG; Amzica & Lopes da Silva, 2011; Hämäläinen et al., 1993).

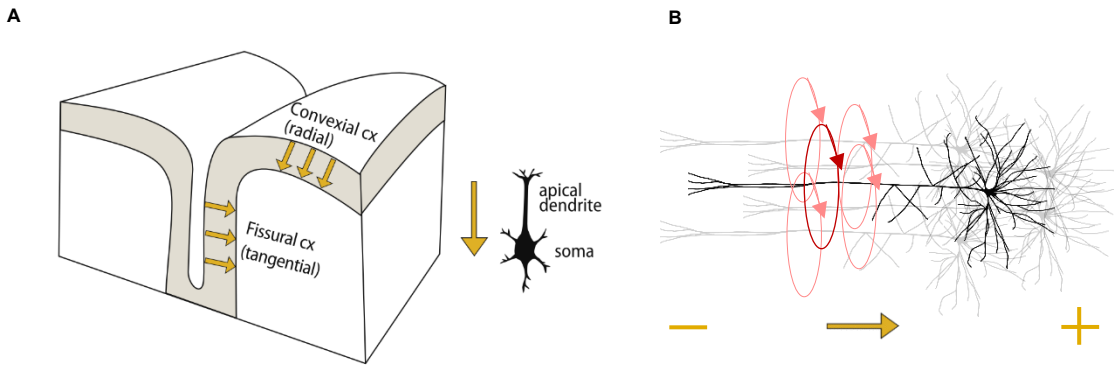

Figure 6. Radial and tangential cortical currents and their contribution to MEG signals. A) Schematic illustration of current orientations within the cortex. Neuronal populations on the surface of the gyri produce radial current dipoles, whereas those along the walls of the sulci generate tangential dipoles (yellow arrows show the orientation of the current). MEG is sensitive to tangential sources; therefore, activity within the fissural cortex contributes most strongly to the recoded magnetic fields. Reproduced from Hari & Puce (2023). B) Illustration of pyramidal neurons in the fissural cortex. When a population of pyramidal neurons are synchronously activated, their intracellular (primary) currents and associated extracellular return currents summate, producing a net magnetic field as per the right-hand thumb rule, which is detectable outside the head. Original work by Vaishali Balaji, 2025.

The magnetic fields detected by MEG primarily reflect the synchronous activity of thousands of such dipoles. These fields are strongest when the dipoles are oriented tangentially to the skull, typically within cortical sulci, making MEG particularly sensitive to sources in these regions (Fig. 6A). The corresponding magnetic field of the radial dipole remains within the cranial cavity and thus cannot be detected by sensors on the outside (Hari & Puce, 2023). However, magnetic field strength decays rapidly with distance, rendering MEG relatively insensitive to deep or subcortical generators (Hari et al., 2018).

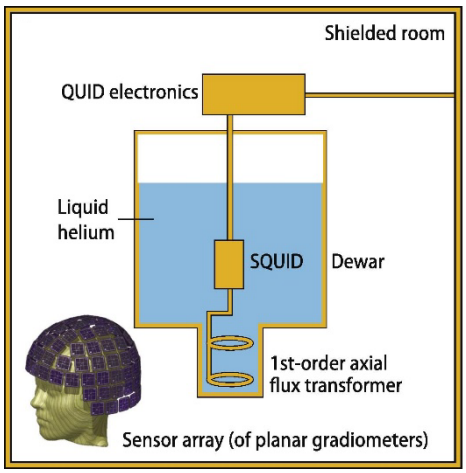

Figure 7. Schematics of MEG instrumentation. A single-channel axial gradiometer and associated SQUID inside a *dewar* filled with liquid helium. Bottom depicts the sensor array of a 306-channel MEG helmet where each sensor unit contains two orthogonal planar gradiometers and one magnetometer. Modified from Hari & Puce (2023).

The magnetic fields generated by neuronal currents are in the nanoampere (10^{-9} A) range, producing extracranial signals on the order of femtoteslas (10^{-15} T), which is roughly 10^{7}–10^{8} times weaker than the Earth's magnetic field (Gross, 2019). Detecting such weak signals requires highly sensitive instrumentation based on superconducting quantum interference devices (SQUIDs; Fig.7). SQUIDs function as an ultra–low-noise magnetic flux–to–voltage converter, enabling detection of brain magnetic fields from DC up to and beyond 1 kHz, with a flat noise spectrum above ~1 Hz and bandwidths exceeding 10 kHz (Hämäläinen et al., 1993).

In state-of-the-art whole-head MEG systems, approximately 300 SQUID sensors are arranged in a helmet-shaped cryogenic vessel, or dewar, which is filled with 70–100 L of liquid helium and maintained near –269 °C to ensure superconductivity and minimize thermal noise. The entire setup operates within a magnetically and electrically shielded room to suppress environmental interference, allowing reliable measurement of cortical signals as small as 100 fT—several orders of magnitude below even the heart's magnetic field (Gross, 2019; Hari et al., 2018).

1.2.2 Detection and Reconstruction

A SQUID consists of a closed superconducting loop interrupted by two Josephson junctions—ultrathin insulating barriers that separate superconducting regions (Hari & Puce, 2023). When cooled to cryogenic temperatures (using liquid helium), the material enters a superconducting state in which electrons form Cooper pairs that move coherently without resistance (Clarke, 2010). When an external magnetic field, such as one produced by neuronal currents, slightly perturbs the flux through the loop, it alters the phase difference of the superconducting wavefunctions across the Josephson junctions. This phase shift changes the interference pattern of the supercurrents flowing through the two junctions, modulating the total current that can circulate in the loop. By applying a constant bias current, the SQUID operates at a point where these phase-dependent changes are translated into a voltage signal (Clarke, 2010; Hämäläinen et al., 1993).

Each SQUID is coupled to a flux transformer (Fig. 8), or pickup coil, that links the neuromagnetic field to the SQUID (Hari et al., 2018). The simplest flux transformer is a magnetometer made from a single turn (or few turns) of superconducting wire. However, a magnetometer is sensitive to various artifacts and external noise, which decreases its specificity to brain signals. The most commonly used flux transformer is the first-order gradiometer, made by adding a second coil wound in the opposite direction (Hari & Salmelin, 2012). Depending on their relative displacement, the coils form either axial gradiometers (coils separated along the coil's normal axis) or planar gradiometers (coils offset within the plane). These 'gradiometers' are particularly sensitive to a gradient in magnetism from nearby (i.e., neuronal) sources, but subtract out signal from distant external (and thus artefactual) sources, as these appear similar to both coils (Hari & Puce, 2023).

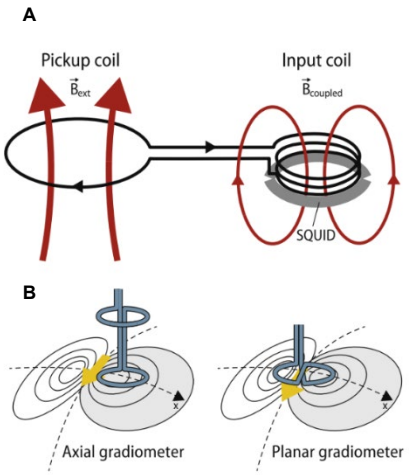

Figure 8. Flux transformer and SQUID. A) The pickup coil detects the external neuromagnetic field (B_{ext}) and induces a superconducting current that couples magnetically into the SQUID via the input coil ($B_{coupled}$). B) Two common gradiometer geometries are shown: the axial gradiometer, sensitive to fields normal to the scalp, and the planar gradiometer, sensitive to tangential field gradients. Modified from Hari & Puce (2023).

MEG data reconstruction is inherently complex due to the so-called inverse problem—the challenge of accurately localizing the neural sources that give rise to the recorded magnetic fields in three-dimensional (3D) space. Because multiple configurations of brain activity can produce indistinguishable sensor signals, the inverse problem is mathematically ill-posed; without additional constraints, it has no unique solution (Baillet et al., 2001; Hämäläinen et al., 1993)

To address this challenge, MEG source analysis relies on two fundamental concepts—the forward and inverse problems. The forward problem models how magnetic fields arise at known sensor locations from electrical currents of known position, orientation, and strength within the brain. Solving it requires an accurate head model that describes how electromagnetic fields propagate through tissues of different conductivities (Hari et al., 2018). Realistic head models are typically derived from individual anatomical MRIs and implemented as boundary element models (BEMs) which represent tissue boundaries, or finite element models (FEMs) which model tissue volumes throughout the head (Gross, 2019). Advanced FEMs can distinguish among skin, skull, cerebrospinal fluid (CSF), and grey and white matter, each with their own conductivity values (Vorwerk et al., 2014).

The forward model is often solved for an equivalent current dipole—a small, localized current element representing a neural source. The resulting lead field matrix describes how each possible source contributes to the magnetic field measured at each sensor (Hillebrand & Barnes, 2005). Once this mapping is known, the inverse problem aims to estimate the spatial distribution, orientation, and time course of the underlying neural currents that best explain the measured magnetic fields.

Because the inverse problem has infinitely many valid solutions, meaningful estimates depend on the application of anatomical, physiological, and mathematical constraints. Anatomical priors can restrict sources to the cortical grey matter and constrain their orientations to be tangential to the cortical surface, consistent with the alignment of pyramidal neurons (Baillet et al., 2001). Physiological or statistical regularization techniques further stabilize solutions by allowing small deviations between the measured and predicted data to reduce the influence of noise (Baillet et al., 2001).

Several classes of inverse models exist, among these, scanning approaches evaluate statistical metrics (e.g., power or coherence) at candidate source locations to infer likely sources without directly reconstructing current distributions. The linearly constrained minimum variance (LCMV) beamformer (Van Veen et al., 1997) is a prominent example of this type. The LCMV beamformer constructs a spatial filter for each potential source location that linearly combines sensor signals to "pass" activity originating from that location while minimizing contributions from all others (Fig. 9). This is achieved by enforcing a unit-gain constraint on the target source; mathematically, this corresponds to minimizing the projected sensor covariance under the constraint that the filter has unit sensitivity to the lead field of the candidate source (Hillebrand & Barnes, 2005).

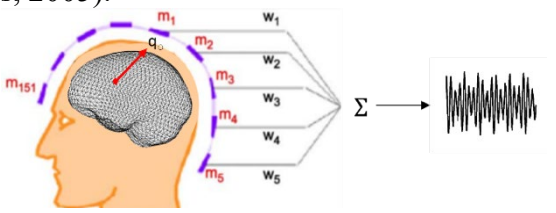

$$vs = m_1w_1 + m_2w_2 + m_3w_3 + \ldots +$$

Figure 9. Beamforming in MEG/EEG. m_1 to m_{151} are MEG sensors. The weights w_1 to w_{151} is assigned to each sensor. A different set of weights is computed for each dipole location. The neuronal source at a location of interest is constructed as a weighted sum of the MEG sensors—denoted as virtual sensor (vs). The weights are chosen so as to enhance the neural signal from q0 and suppress or attenuate the signals from elsewhere. Modified from Hillebrand and Barnes (2005).

In practice, the beamformer uses the sensor covariance matrix, estimated from the data, to adaptively weight the sensors according to the spatiotemporal characteristics of the ongoing brain activity and noise. This allows it to provide high spatial selectivity and robustness against correlated sensor noise. However, beamformers are less effective when sources are temporally correlated, such as during synchronized oscillatory activity, because mutual interference between correlated sources can lead to signal cancellation (Hillebrand & Barnes, 2005).

1.3 Alpha Oscillations in Brain Functioning

Features of oscillations are subtle and difficult to pinpoint in real time EEG or MEG recordings. Typically, they emerge after spectral decomposition and averaging across many trials, revealing brain activity patterns hidden within measurement noise. Yet there is one exception that stands out—when a person closes their eyes, a clear and sustained oscillation arises from the background signal (Fig. 10). This rhythm, known as alpha oscillations, strongest over parieto-occipital regions and ranging between 8 and 13 Hz, has been a topic of interest since its discovery in the early EEG recordings of Hans (Berger, 1929). Alpha oscillations were initially thought to reflect a state of rest or cortical idling, given their attenuation with eye opening, visual stimulation, and heightened attentiveness (Lundqvist et al., 2013; Pfurtscheller et al., 1996).

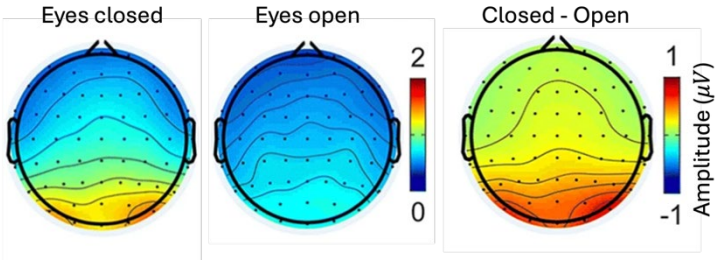

Figure 10. Scalp topographies of EEG alpha-band activity during eyes-closed and eyes-open resting-state conditions. Alpha amplitudes are markedly higher in the eyes-closed condition, particularly over parieto-occipital regions, reflecting increased cortical synchronization when visual input is reduced. The right panel shows the difference in amplitude (eyes-closed minus eyes-open). Adapted from Zhang, Wang, et al. (2019).

Early interpretations of alpha as a passive marker of disengagement gradually gave way to the idea that it might serve an active inhibitory function, shaping information flow across the cortex. According to this hypothesis, large-amplitude alpha rhythms reflect the functional suppression of task-irrelevant regions, whereas localized reductions in alpha power, termed event-related desynchronization (ERD), mark areas engaged in sensory or cognitive processing (Klimesch, 2012; Pfurtscheller et al., 1996). More recent work has further transformed our understanding of alpha rhythms. Far from representing a passive state, alpha activity appears to play an active role in sculpting perception and cognition. Both the power and phase of alpha oscillations have been shown to modulate cortical excitability, influencing how sensory information is processed and integrated (Haegens, Händel, et al., 2011; Jensen & Mazaheri, 2010; Mathewson et al., 2009). In this framework, alpha rhythms act as a dynamic control signal, rhythmically regulating neuronal communication within and between brain areas (Sadaghiani & Kleinschmidt, 2016; Van Ede et al., 2015). Studies investigating pre-stimulus amplitude, phase consistency at stimulus onset, and long-range phase coupling have demonstrated that ongoing alpha activity can bias perceptual outcomes and coordinate large-scale neural interactions (Busch et al., 2009; Hanslmayr et al., 2013; Palva & Palva, 2007).

1.3.1 Frequency, Power and Phase

The generation of alpha rhythms arises from multiple, interacting neural circuitries rather than a single anatomical source. Classical models attribute posterior alpha activity to recurrent interactions within thalamo-cortical loops, where rhythmic bursting in thalamic relay and reticular neurons entrains cortical populations (Lopes Da Silva et al., 1973, 1974). But Alpha oscillations can also emerge from local cortical microcircuits, particularly within the deep layers of the neocortex (Bollimunta et al., 2011; Haegens et al., 2015). These locally generated rhythms interact across distributed cortical territories, forming large-scale networks in which alpha synchrony supports inter-areal communication and top-down feedback signalling (Michalareas et al., 2016; Von Stein et al., 2000). Moreover, alpha traveling waves appear to propagate across cortical surfaces, providing a spatiotemporal scaffold for coordinating information flow (Alamia & VanRullen, 2019). Collectively, alpha is not a unitary rhythm but rather a network-level phenomenon emerging from the integration of local and long-range oscillatory processes.

The precise frequency of alpha oscillations is governed by biophysical parameters such as synaptic conduction delays, intrinsic membrane time constants, and the balance between excitatory and inhibitory neurotransmission (Schoffelen et al., 2024). Individual variability in these parameters gives rise to characteristic differences in alpha peak frequency (APF), rendering it a trait-like neural marker that evolves gradually across the lifespan (Tröndle et al., 2023). Nevertheless, APF is also dynamically modulated by moment-to-moment fluctuations in physiological and cognitive state. Changes in arousal, emotional context, attention, or working memory load can induce rapid shifts in APF (Klimesch, 1999; Mierau et al., 2017). While researchers frequently define the alpha range using canonical boundaries, it is increasingly common to determine each individual's APF, as it allows for flexible comparisons of intra- and inter- individual differences in behaviour and cognition (Baumgarten et al., 2023). In addition, resting-state MEG and EEG studies demonstrate a posterior-to-anterior gradient, with alpha oscillations slowing toward frontal regions (Mahjoory et al., 2020).

Increases in alpha power are associated with reduced spiking activity and lower cortical excitability in the corresponding brain regions, an effect often described as pulsed inhibition (Jensen & Mazaheri, 2010; Mathewson et al., 2009). Rather than reflecting a sustained suppression, this inhibition is inherently rhythmic, fluctuating across the alpha cycle: neuronal excitability reaches its nadir at the alpha peak and its maximum near the trough.

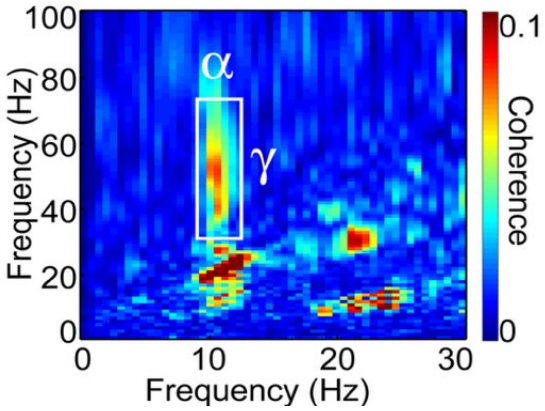

Figure 11. Coupling between alpha and gamma activity. Cross-frequency interaction in ongoing human MEG signals during eyes closed. The highlighted area indicates increased coherence between alpha activity (along the x-axis) and the power of the gamma activity (along the y-axis). Reproduced from Osipova et al., (2008).

Empirical evidence from intracranial recordings and MEG demonstrates that both high-frequency gamma power (>30 Hz) and neuronal firing rates are phase-locked to the troughs of alpha oscillations (Bahramisharif et al., 2013; Osipova et al., 2008). This interplay manifests as cross-frequency phase–amplitude coupling (PAC), whereby the phase of slower alpha oscillations modulates the amplitude of faster gamma activity (Fig. 11; Jensen & Colgin, 2007).

Through this mechanism, alpha oscillations temporally segment cortical processing into discrete excitatory windows, orchestrating when and where neural ensembles can engage in high-frequency information transmission (Jensen & Colgin, 2007). Conversely, reductions in alpha power correspond to a release from this rhythmic inhibition, allowing for more continuous and flexible neural processing. Alpha power thus dynamically gates the flow of sensory and cognitive information, functioning as a spatiotemporal filter that balances cortical inhibition and excitation. At the population level, high alpha power reflects increased phase synchrony across neuronal ensembles, leading to coherent bouts of inhibition and segmentation of incoming input into discrete temporal parcels (Pfurtscheller et al., 1996; Van Diepen et al., 2019). On the other hand, alpha desynchronization i.e., ERD, corresponds to a breakdown of phase alignment, reducing global inhibition and permitting enhanced local processing. From this perspective, alpha power indexes not the mere presence of inhibition, but the degree of network synchronization, underlying cyclic gain control (Klimesch et al., 2007; Pfurtscheller et al., 1996). Baseline alpha levels, in turn, may represent the default allocation of processing resources within a sensory system, with task-induced changes signifying dynamic redistribution rather than simple suppression (Van Diepen et al., 2019).

Conceptualizations of alpha have thus evolved substantially from early interpretations emphasizing passive inhibition toward a more nuanced view of rhythmic gating and resource allocation.

1.3.2 Attention and Perception

As outlined earlier, alpha-band oscillations regulate cortical excitability, and this regulation is subject to top-down control. Increasing evidence now supports the view that these physiological mechanisms play an active role in cognitive regulation and control.

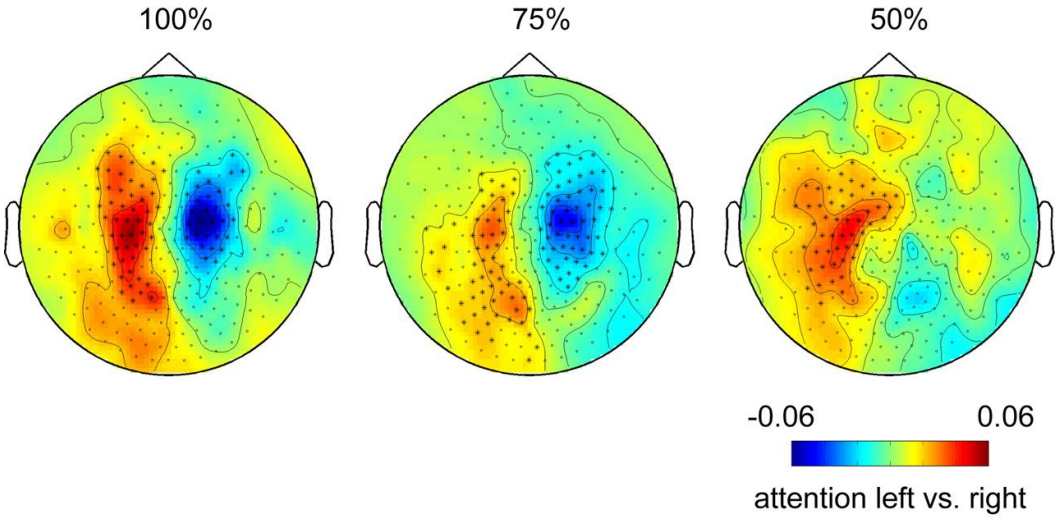

Figure 12. Prestimulus somatosensory alpha lateralization increases with cue reliability. Topographic plots showing prestimulus ($t = -1$ to 0 s) alpha power (8–14 Hz) lateralization over sensorimotor regions, for each of cue reliability conditions (100%, 75%, 50%). Sensors showing significant modulation due to attention ($p < 0.05$) are marked with asterisks. All plots are showing power as a contrast between attention left and attention right. Reproduced from Haegens, Händel et al. (2011).

During selective attention, reductions in alpha power occur in spatially specific cortical regions responsible for processing attended stimuli, as shown in both invasive (De Pesters et al., 2016; Haegens, Nácher, et al., 2011) and non-invasive recordings (Gould et al., 2011; Rohenkohl & Nobre, 2011). For instance, when participants anticipate a visual target at a cued location, alpha power decreases over occipitoparietal EEG sites contralateral to the attended hemifield (Gould et al., 2011). Similarly, when attention is directed toward left or right hand, alpha power is selectively reduced over the contralateral somatosensory cortex (Fig. 12; Haegens, Händel, et al., 2011). Such local alpha suppression enhances cortical excitability, which in turn facilitates neural responsiveness and perceptual sensitivity to relevant stimuli (Haegens, Händel, et al., 2011). Beyond its role in spatial attention, alpha power has also been associated with sustained attention and vigilance. In tasks requiring continuous monitoring, elevated alpha power often corresponds to lapses in attention or reduced task engagement. For example, during monotonous auditory detection, periods characterized by frequent missed targets coincide with broad increments in alpha power (Makeig & Inlow, 1993). Similarly, in sustained attention tasks such as breath-counting, moments of mind-wandering correspond to increased occipital alpha activity (Braboszcz & Delorme, 2011).

In addition to power, the phase of alpha oscillations has a marked influence on perceptual processing. Because neural excitability fluctuates rhythmically with the alpha cycle, the timing of stimulus presentation relative to this cycle modulates perceptual outcomes (Mathewson et al., 2009; M. T. Sherman et al., 2016). In meta-contrast masking paradigms, for instance, the probability that a visual stimulus reaches conscious awareness depends on its alignment with the ongoing alpha phase over posterior regions (Mathewson et al., 2009). Moreover, alpha phase dynamics are themselves modulated by cognitive control processes, reflecting top-down adjustments (Samaha et al., 2015; M. T. Sherman et al., 2016). The functional significance of alpha phase extends to its synchronization across distant cortical regions. Long-range phase-locking in the alpha band has been shown to support integrative processing across perceptual and cognitive domains (Klimesch et al., 2007; Palva & Palva, 2011). Empirical evidence from EEG (Sauseng et al., 2005), MEG (Doesburg et al., 2016; Palva et al., 2010), and intracranial recordings (Saalmann et al., 2012) indicate that stronger inter-regional phase coherence accompanies effective performance in tasks ranging from perceptual discrimination to working memory, particularly when top-down control demands are high. For example, in delayed match-to-sample paradigms, alpha-band phase-locking increases during the retention interval as a function of working memory load (Palva et al., 2010). Together, these observations suggest that alpha-oscillations are an instrument of information processing and cognition instead of an epiphenomenon of passive idling.

A growing body of research indicates that alpha-band oscillations play a fundamental role in segmenting continuous sensory input into discrete perceptual windows (Cecere et al., 2015; Samaha & Postle, 2015; VanRullen, 2016). In rhythmic perception, each alpha cycle defines a temporal integration window within which sensory information is combined into a single perceptual event. Stimuli occurring within the same alpha cycle are thus likely to be integrated, whereas those separated by different cycles are perceived as distinct. Consequently, APF determines the temporal precision of perception: faster oscillations (shorter cycles) are associated with narrower temporal binding windows and finer perceptual resolution.

Empirical findings provide converging support for this hypothesis. Cecere et al., (2015) demonstrated that APF predicts the width of the audiovisual temporal binding window; participants with slower alpha rhythms integrated asynchronous auditory and visual inputs over longer intervals, whereas those with faster rhythms showed enhanced temporal discrimination.

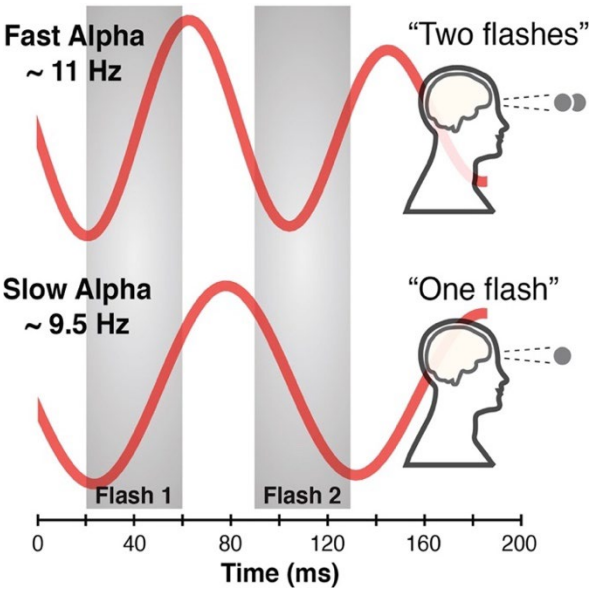

Figure 13. Schematic illustration of the relationship between individual alpha frequency and the temporal resolution of visual perception, as indexed by the two-flash fusion paradigm. When alpha oscillations are faster (~11 Hz), their shorter cycles enable finer temporal parsing of sensory input, allowing two closely spaced flashes to be perceived as distinct events. Conversely, slower alpha rhythms (~9.5 Hz) correspond to longer perceptual cycles, increasing the likelihood that successive flashes are integrated into a single percept. Reproduced from Samaha & Postle (2015).

Similarly, Samaha & Postle (2015) reported that higher APF correlated with superior performance in visual temporal order judgments, indicating that alpha frequency constrains the brain's temporal sampling capacity (Fig. 13). Complementary evidence from VanRullen, (2016) suggests that perceptual experience is discretely sampled in synchrony with ongoing neural oscillations, with alpha activity functioning as a perceptual clock that structures the temporal flow of sensory processing. Moreover, when sensory inputs fail to reset ongoing oscillations, for instance, when stimuli are weak or ambiguous, the phase of the ongoing alpha rhythm can determine whether successive signals are integrated into a single percept or segregated into separate events.

Together, these findings suggest that alpha oscillations are not merely correlates of perceptual or cognitive states, but constitute an active neural mechanism that governs the temporal organization of perception. Through their frequency and phase dynamics, alpha rhythms define the temporal resolution at which conscious experience unfolds.

1.4 Neuromodulation

Neuroimaging techniques such as M/EEG are predominantly correlational approaches. The observation of neural activity in a specific region or frequency band during the performance of a given cognitive task is not sufficient to establish causality, on the contrary, it could be a mere epiphenomenon. Since oscillatory activity could be an incidental byproduct of circuit dynamics, but not serve any computational role (see Section 1.1.2). To establish the causal relevance of neural oscillations for some cognitive process or behavioural outcome necessitates the external manipulation of relevant oscillatory frequencies (Vosskuhl et al., 2018). In animal models, external perturbation of brain activity is achieved by means of invasive methods such as pharmacological interventions, targeted micro-stimulation and optogenetics. These techniques enable spatially precise inferences regarding brain-function relationships at the cell, circuit and systems level. In healthy humans, non-invasive methods of brain stimulation (NIBS; Fig. 14) offer a feasible alternative to temporarily modulate cortical activity (Bergmann et al., 2016). As a result, the observed alterations in neural activity and in turn cognition can be directly attributed to the external manipulation.

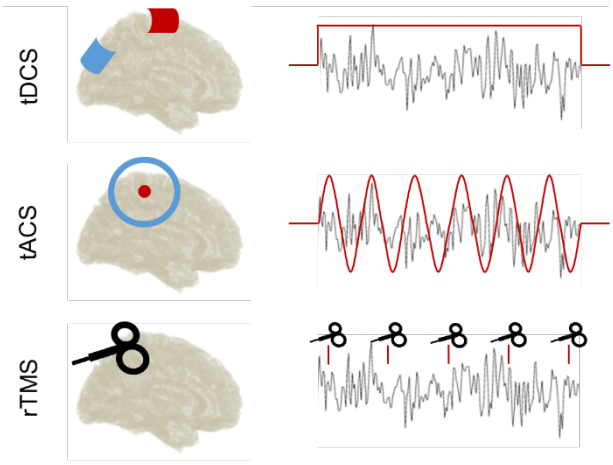

Figure 14. Standard types of non-invasive brain stimulation (NIBS) techniques. In the left panel, figures illustrate how transcranial electric stimulation (tES) methods, such as transcranial direct current stimulation (tDCS) and transcranial alternating current stimulation (tACS) are applied via electrodes to the scalp, whereas repetitive transcranial magnetic stimulation (rTMS) is applied to the scalp using a figure-eight coil. The right panel represents the stimulation signal (red) relative to MEG (black), and the rTMS pulses are depicted with red vertical bars. Adapted from Vosskuhl et al. (2018).

Among others, the most widely recognized NIBS methods are transcranial magnetic stimulation (TMS) and transcranial electrical stimulation (tES). TMS involves the application of a strong magnetic field (lasting less than 1 millisecond) which induces a current in cortical neurons aligned parallel to the magnetic coil (Hallett, 2000, 2007). In tES, a weak electric current is applied via electrodes mounted on the scalp (Paulus, 2011). There are two variants of tES: in the first type, a direct current (transcranial direct current stimulation, tDCS; Nitsche & Paulus, 2000) is applied whereas, in the second type, the electrodes alternate as the anode and cathode, creating alternating sinusoidal currents (transcranial alternating current stimulation, tACS; Antal et al., 2008).

1.4.1 Mechanisms of Action

Although TMS and tES mediate cognition by inducing an electric-field on brain tissue, they have different mechanisms of action, and the resulting effects differ drastically. The high-amplitude electric field gradients generated by TMS (lasting less than 300 µs) are strong enough to fully depolarize the membrane potential of cortical neurons, leading to the immediate generation of action potentials (suprathreshold stimulation; Groppa et al., 2012). On the other hand, the weaker, oscillating electric fields produced by tACS are thought to only slightly adjust the membrane potential of neurons, thereby influencing the probability of generating spontaneous action potentials (subthreshold stimulation; Antal & Herrmann, 2016). As tACS changes polarity rhythmically, the targeted population of oscillations synchronise to the same phase and frequency as the externally applied current – this is referred to as entrainment (Lakatos et al., 2019). Entrainment is thought to be particularly effective when the stimulation frequency matches the endogenous frequency. However, at higher stimulation intensities, a wider range of frequencies can be entrained (Fig. 15). This triangular region, referred to as an Arnold tongue, denotes susceptibility to entrainment, and is determined by intensity and frequency of the external stimulation (Herrmann et al., 2016; Pikovsky et al., 2001). Entrainment can also happen at harmonic (e.g., 2 x endogenous frequency) and subharmonic (e.g., endogenous frequency / 2) frequencies. For example, in a large-scale model of a cortical network, Ali et al., (2013) showed that stimulating at 6 Hz was effective in entraining the network, same as stimulating at the endogenous frequency of 3 Hz (i.e., 1:2 synchronization).

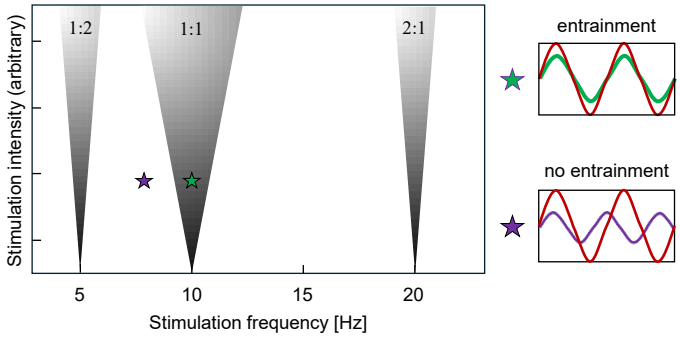

Figure 15. The Arnold tongue

The dark grey triangular regions represent the frequency range which is subject to entrainment at various stimulation intensities. The panels on the right illustrate the relationship between the endogenous oscillation and stimulation signal in the regions marked by the green and purples stars. If external stimulation is administered at the endogenous frequency (indicated by "1:1"), the endogenous oscillation (in green) couples in phase and frequency to the stimulation signal (in red), even at low stimulation intensities. If the stimulation frequency falls outside the Arnold tongue, the endogenous oscillation (in purple) remains unaffected by stimulation signal (in red). At higher stimulation intensities, the external rhythm can entrain a wider frequency of oscillations, resulting in the characteristic triangular shape of the Arnold tongue. Entrainment can also occur at harmonics and subharmonics of the endogenous frequency (indicated by "2:1" and "1:2", respectively). Original work by Vaishali Balaji, 2025

Entrainment persists only for a few cycles after the stimulation has ceased (Halbleib et al., 2012; Hanslmayr et al., 2014), but the behavioural and electrophysiological effects of stimulation can continue for several hours, due to spike-timing dependent plasticity (STDP). As per this mechanism, synaptic strength tends to increase when a pre-synaptic spike precedes post-synaptic potential (i.e., long-term potentiation; LTP). In contrast, when a post-synaptic potential precedes a pre-synaptic spikes, synaptic strength decreases, (i.e., long-term depression; LTD; Bi & Poo, 1998). Zaehle et al. (2010) illustrate this principle using a simple neural network composed of one excitatory neuron receiving feedback through multiple recurrent circuits. When the neuron receives rhythmic input (e.g., tACS at 10 Hz), only the circuits with less than 100 ms delays undergo synaptic strengthening. This occurs because feedback from the loop precedes the stimulation-driven spike. These changes in synaptic strength persist after stimulation, leading to heightened neural activity at the circuit's resonance frequency. tDCS modulates neuronal excitability in a tonic (sustained) manner by shifting the membrane voltage, whereas tACS may lead to frequency-specific modulation through entrainment and STDP (Vogeti et al., 2022).

The distribution of the electric field within the brain is significantly influenced by the spatial arrangement and conductivity of tissue, such as grey matter, white matter, and cerebrospinal fluid (Windhoff et al., 2013). Unlike TMS, which bypasses the scalp and skull (Opitz et al., 2011), in tES, the current passes through these structures thereby attenuating it with only a fraction of the current reaching the cortical surface (Opitz et al., 2015). The unavoidable shunting of current strongly supports a different mechanism altogether—transcutaneous stimulation (Asamoah et al., 2019). When tACS is administered in humans (with typical amplitudes of ~1 mA), the resultant electric field in the cortex is under 1 V/m—too weak to entrain neurons (Huang et al., 2017; Vöröslakos et al., 2018). Notably, the electric field at the skin surface can be 20-100 times stronger—sufficient to stimulate peripheral nerves (So et al., 2004), potentially leading to indirect entrainment of brain activity, similar to sensory entrainment methods (e.g., tones or flickering lights). On the contrary, more recent findings have shown that blocking somatosensory input with a topical anaesthetic does not abolish the effects of tACS, supporting a more direct cortical mode of action (Brus et al., 2024; Burke et al., 2025; Fiene et al., 2022; Vieira et al., 2020).

1.4.2 Modulating Alpha Oscillations via tACS

Both TMS and tES can be used in conjunction with neuroimaging and electrophysiological techniques to assess the changes in oscillatory activity and in turn cognition. In humans, while the stimulation is ongoing, it is difficult to measure changes in oscillatory features (i.e., online effects) due to stimulation-induced artefacts, which are stronger than the brain signals of interest (Noury et al., 2016). Therefore, the primary evidence of oscillatory modulation comes from observed changes in oscillatory power, phase or frequency, or measures of functional connectivity, between pre- and post- stimulation electrophysiological recordings (i.e., offline effects; Fig. 16).

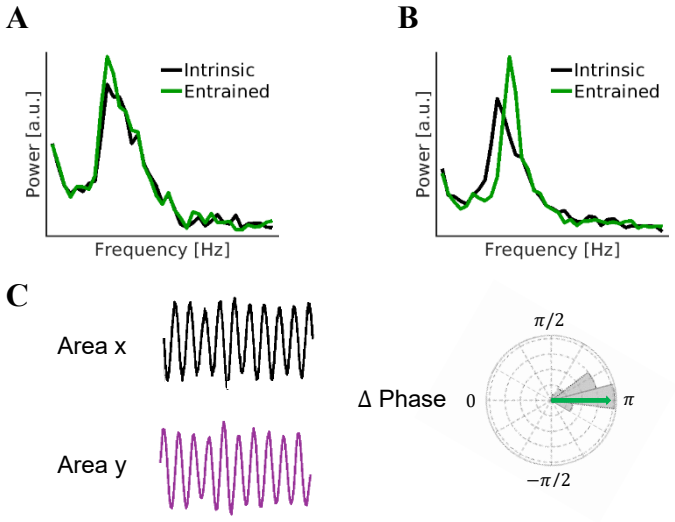

Figure 16. Effects of tACS on electrophysiological signals

Figures illustrate changes in oscillatory parameters, as measured by M/EEG, on applying tACS. **A)** Power of the endogenous oscillations increases. **B)** There is a shift in peak frequency. **C)** Endogenous oscillations of two cortical areas (x and y) synchronise in phase. Original work by Vaishali Balaji, 2025

Frequencies in the alpha range are an easy target for modulation via tACS, given its dominant presence in the parieto-occipital region (see Section 1.2). Several studies have shown that applying alpha-frequency tACS over visual areas for a few minutes can lead to increased alpha power (Zaehle et al., 2010; Neuling et al., 2013; Helfrich et al., 2014; Kasten et al., 2016) and enhanced phase coherence between cortical regions (Helfrich et al., 2016; Schwab et al., 2019). Various findings support that modulation of endogenous alpha oscillations, as evidenced by M/EEG, have a corresponding effect on perceptual tasks. Fiene and colleagues (2022) demonstrated that the effect of tACS on steady-state response (SSR) amplitudes varied depending on the phase-shift between the applied stimulation and flickering visual stimulus (see Gundlach et al., (2016) and Helfrich et al., (2014) for similar phase-dependent interactions with tACS). Cecere et al., (2015), on the other hand, manipulated the frequency of endogenous alpha oscillations. They reported that administering tACS at -2Hz or +2Hz, relative to APF, respectively enlarged and shrunk the temporal window for perceiving a sound-induced illusion

(see Zhang, Yanzu, et al., (2019) for a similar example of APF-dependent manipulation of perception). As for power modulations, two studies showed that tACS enhanced alpha power in the left-parietal cortex and induced an analogous leftward shift in attention (Kemmerer et al., 2020; Schuhmann et al., 2019).

Notably, depending on the stimulation parameters (duration, intensity, frequency, site(s) of stimulation, electrode montage etc.), there is substantial variability in outcomes. Stimulation duration appears to determine the emergence of offline effects: short trains of stimulation (1-6 s) are vastly unsuccessful at modulating power (Sliva et al., 2018; Strüber et al., 2015; Zarubin et al., 2020). Even when the duration is kept constant, the intensity of tACS determines the longevity of aftereffects (De Koninck et al., 2021). Stimulation at APF is regarded as the optimal frequency based on the principle of the Arnold Tongue; however, matching stimulation frequency to endogenous alpha frequency has proven to be challenging (Stecher & Herrmann, 2018; Vossen et al., 2015). Moreover, the efficacy of fixed versus closed-loop stimulation protocols is under debate (Stecher et al., 2021). Given that electrode placement alters current flow and in turn electrophysiological activity, it is uncertain whether the above-mentioned effects (mainly replicated with occipital alpha) extend to somatosensory regions (Cabrera-Álvarez et al., 2023; Mehta et al., 2015). For example, Krause et al., (2022) found that displacing the electrodes by approximately 3–4 cm was sufficient to completely abolish entrainment. Further, internal factors like brain states (Neuling et al., 2013; Kasten et al., 2016) together with external factors like ambient light during stimulation (Stecher et al., 2017) have an impact on the efficacy of tACS.

The literature is rife with null effects stemming from inter-individual variability. Knowing where, when and how (or even, how long to stimulate) is not trivial. Therefore, it is imperative that critical assumptions (e.g., electric field strength at cortical surface) are modelled and confounds (e.g., peripheral stimulation) are experimentally controlled to harness the full-potential of tACS to uncover cause–effect relationships.

2 OBJECTIVES

The objectives of this thesis are twofold: first, to investigate whether short-period tACS modifies alpha power in the somatosensory cortex; and second, to quantify the spontaneous variability in alpha frequency along the posterior-to-anterior axis.

Motivated by the paucity of evidence showing power modulation using short durations of stimulation, in Study 1 we, the authors of the following two studies, administered short trains of tACS to the right somatosensory cortex while simultaneously recording electrophysiological signals using the MEG. Participants received 10- and 30-second stimulation trains in two separate blocks. We contrasted tACS-induced power changes with a control condition in which no tACS was applied. We hypothesised that short-period tACS will enhance alpha power at the stimulation frequency within the somatosensory cortex relative to control.

Study 2 stemmed from a key limitation of Study 1, where we were unable to align the stimulation frequency with each participant's alpha peak frequency (APF) in roughly two-thirds of the sample. Here we used the same dataset from Study 1 but restricted our analysis to recordings obtained from the control session. We characterised the magnitude of fluctuations in APF from the caudal-end to rostral-end of the cortex. We hypothesised that APF varies spontaneously and that this variation is heterogenous across the cortex. We aimed to investigate whether APF more closely resembles a state rather than a trait.

3 STUDY 1

Title: Modulating Somatosensory Alpha Oscillations Using Short-period Transcranial Alternating Current Stimulation

Article information: Published on 21st March 2025 in Imaging Neuroscience

DOI: https://doi.org/10.1162/imag_a_00531

Author names and contributions:

Vaishali Balaji: Formal Analysis, Investigation, Writing – Original Draft, Writing – Review & Editing, Visualisation. **Alfons Schnitzler:** Conceptualisation, Methodology, Resources, Writing – Review & Editing, Project administration. **Joachim Lange:** Conceptualisation, Methodology, Resources, Writing – Review & Editing, Supervision, Project administration, Funding acquisition.

Abstract

Transcranial Alternating Current Stimulation (tACS) appears to modulate neuronal oscillations at the frequency of stimulation. Longer periods of stimulation with tACS (10-40 minutes) have shown to produce persistent changes, especially in alpha power (~ 8-12 Hz), whereas the efficacy of shorter periods of tACS (1-8 seconds) is less known. Thus, we investigated whether short periods of tACS applied to the somatosensory cortex elicits changes in alpha power following stimulation. With this aim, during simultaneous acquisition of MEG, we administered tACS and control (no-tACS) on separate days. We applied short trains of stimulation for durations of 10 s and 30 s at an individually adapted stimulation frequency (ISF). Each stimulation-train was followed by a 15 s interval. We calculated power changes in the post-stimulation intervals, relative to a baseline period, and the resulting Δpower was used to statistically test the difference between tACS and control conditions. We found significant elevations in power at ISF following tACS compared to control. The extent of this effect spanned bilaterally over the somatosensory and frontal regions. While the observed increase in power was most prominent around ISF (i.e., in the alpha band), power modulations were also observed in the beta-band. When comparing the two stimulation durations, 10 s of tACS produced greater increases in power (at ISF) than 30 s of tACS. This study validates that 10 s of tACS produces robust elevations of power in the somatosensory cortex at ISF, thereby establishing its potential for use in future studies.

Introduction

The use of electrical stimulation to study the cerebral cortex has a long-standing history in neuroscience (Fritsch & Hitzig, 1870). A non-invasive electrical stimulation method that has gained traction in recent years is transcranial Alternating Current Stimulation (tACS). This method involves the application of sinusoidal currents to the scalp with the aim of modulating neuronal oscillations, and in turn, functionally relevant behaviour. Animal studies propose that tACS acts via entrainment; a mechanism by which oscillations synchronise to the phase and frequency of the externally applied current (Fröhlich & McCormick, 2010; Ozen et al., 2010). Whereas, effects of tACS that persist beyond the period of stimulation have been attributed to spike-timing dependent plasticity (Schwab et al., 2021; Vossen et al., 2015; Wischnewski et al., 2019; Zaehle et al., 2010). An opposing view is that oscillations are indirectly entrained via stimulation of peripheral nerves on the scalp (Asamoah et al., 2019). The exact mechanisms underlying the interaction between tACS-induced electric fields and the targeted neuronal oscillations remains a matter of contention (Vogeti et al., 2022).

tACS is often targeted at oscillations in the alpha range (~8-12 Hz) given its relevance in the parieto-occipital region (Buzsáki et al., 2013; Hari et al., 1997) for perception and cognition (Baumgarten et al., 2016; Jensen & Mazaheri, 2010; Klimesch et al., 2007; Samaha & Postle, 2015; Van Dijk et al., 2008). Modulation of alpha oscillations affects perception (Battaglini et al., 2020; Cecere et al., 2015; Fiene et al., 2022; Harada et al., 2020; Kemmerer et al., 2020), motor learning and consolidation (Schubert et al., 2021), and functional connectivity between cortical regions (Gundlach et al., 2020; Randolph F. Helfrich et al., 2014; Schwab et al., 2019). Typically, these studies used long stimulation durations (of 10-40 minutes), yielding long-lasting power enhancements that persist for several minutes post-stimulation (Randolph F. Helfrich et al., 2014; Kasten et al., 2016; Neuling et al., 2013; Zaehle et al., 2010). Stecher & Herrmann (2018) found no evidence of power modulation following blocks of 1 to 10 minutes of stimulation, which was attributed to low illumination and a mismatch between stimulation frequency and endogenous alpha frequency. Besides this study, there have been no systematic investigations of the duration-dependent effects of tACS. Therefore, it is unclear whether longer periods of stimulation are beneficial for eliciting electrophysiological after-effects.

Short-intermittent tACS offers the potential to manipulate power immediately before stimulus presentation i.e., within task-relevant timescales. However, the reported effects of short stimulation periods (in the range of seconds) are not well established. Vossen et al., (2015)

found that stimulation at individual alpha frequency for trains of 8 seconds, but not 3 seconds, increased alpha power compared to sham (replicated by Stecher et al., 2021). One study demonstrated an increase in stimulus-evoked power using 1 to 1.8 second stimulation trains, with a fixed frequency of 7 Hz (Stonkus et al., 2016). Ruhnau and others (2016) showed that 2 seconds of stimulation amplified steady-state responses, but only when frequency of the flickering stimulus and tACS matched. Overall, shorter train durations may not enhance power (Strüber et al., 2015; Zarubin et al., 2020). In addition to stimulation duration, frequency and intensity of applied current differ between the above-mentioned studies; therefore, it is difficult to pinpoint the reason for the reported differences in results. Furthermore, most studies targeted visual alpha with complementary electrode placements (typically Cz and Oz). While augmenting alpha oscillations should affect perception in visual and somatosensory modalities alike, only a few studies have shown concomitant alterations in tactile perception (Gundlach et al., 2016; Saito et al., 2021; Sliva et al., 2018), whereas others reported null findings (Manzo et al., 2020; Wittenberg et al., 2019). Notably, only one study tested for increments in power after stimulation (Sliva et al., 2018). Given the paucity of evidence for power modulation in the somatosensory domain, our goal was to assess the suitability of short-period tACS for prospective studies.

In this study, we acquired magnetoencephalography (MEG) simultaneously during tACS. We applied tACS over the right primary somatosensory cortex (S1) at the individuals' alpha frequency. In contrast to most tACS studies, we employed a ring electrode montage for more focal stimulation (Datta et al., 2008). Additionally, we anaesthetised the region on the scalp underneath the electrodes to control for indirect entrainment via transcutaneous stimulation. We administered tACS for periods of 10 and 30 seconds, followed by a post-stimulation interval. Since trains of 1 to 6 seconds are unsuitable, we chose 10 seconds as a starting point. We included an additional train-duration (30 seconds), as longer stimulation durations revealed promising results. To assess after-effects of tACS, we compared power in the post-stimulation intervals to resting-state baseline and a control condition.

Methods

Participants

Twentysix volunteers participated in the study. A sample of 20 to 24 participants was deemed fit based on studies by Vossen et al., (2015) and Stecher et al. (2021). Two participants were excluded from the analysis; one due to poor performance on the vigilance task and the other

because of a broken Head Position Indicator (HPI) coil. 24 participants were included in the final analyses (11 female, age 25.33 ± 2.81 [mean ± SD] years). We excluded one block (in participant no. 15), as we failed to record the baseline period. Participants had normal or corrected-to-normal vision and met standard inclusion criteria for MEG experiments. No participant had a history of epilepsy or other neurological or psychiatric conditions.

The study was approved by the ethics committee (ethics vote no. 4965) of Heinrich Heine University Düsseldorf, Germany. Participants gave written informed consent and received a monetary compensation of 10€/h.

General procedure

Participants attended two experimental sessions conducted on separate days. We administered tACS in one session and the other session served as a control. Prior to this, we acquired anatomical T1-weighted MRIs using a 3T Siemens scanner (Siemens Magnetom Tim Trio 3T, Siemens, Germany).

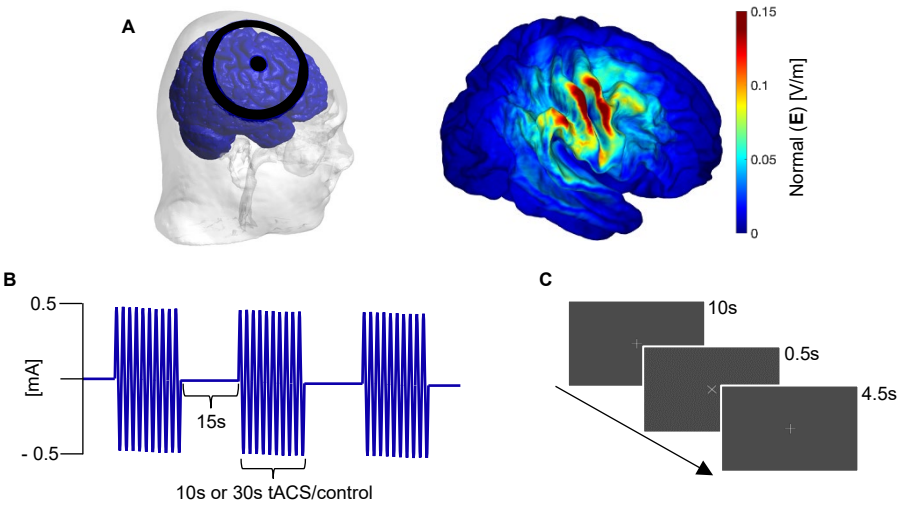

Figure 17. Electrode montage and stimulation protocol
A) Illustration of electrode placement and simulation results. A ring electrode montage was attached to the scalp corresponding to right S1 (left panel). Grand-mean of the normal field component (right panel) projected in FsAverage space. The maximum electric field strength was approximately 0.14 V/m. **B)** Stimulation protocol. All participants underwent 10 s *tACS,* 30 s *tACS,* and control sessions in separate blocks. Train duration was 10 s in one *tACS* block and 30 s in the other. Trains were followed by a 15 s interval of no stimulation. tACS was applied at 0.5 mA (zero-to-peak) amplitude. No stimulation was applied in the control condition. **C)** Schematic representation of a single 15 s-post-stimulation interval. A fixation cross was present through the entire duration of the experiment. In any 9/20 inter-stimulation intervals, the fixation cross rotated for 500 ms. Participants were instructed to press a button to indicate seeing the rotation. After 4.5 s, the next stimulation train started.

The experimental procedure was identical in tACS and control sessions. First, we individually localised the right primary somatosensory cortex (S1) using the Visor2 neuro-navigation system (ANT Neuro, Netherlands) and participants' MRI. Next, we applied a topical anaesthetic (Anesderm cream; Prilocaine 25 mg/g and Lidocaine 25 mg/g) corresponding to the site of S1 on the scalp (Fig. 17A, left). About one hour after applying the cream, we attached the tACS electrodes to the anaesthetised region using Ten20 conductive paste (Weaver & Co., USA). At

the end of each session, participants reported feelings of ‘alertness’, ‘contentedness’ and ‘calmness’ on Bond and Lader’s Visual Analogue Scale (BL-VAS; Bond & Lader, 1974). Participants also indicated if they felt any sensations on the scalp during the experiment (with yes/no) and rated their level of confidence (on a scale of 1 to 10) for having received tACS stimulation.

Stimulation protocol

Participants were seated upright in a dimly lit magnetically shielded room while we acquired MEG simultaneously during tACS or no-tACS (control session). We administered tACS via a ring electrode montage (Fig. 17A, left), with a small circular electrode (Ø: 2 cm) and a larger concentric electrode (outer Ø: 11 cm; inner Ø: 9 cm; NeuroConn, Germany). The stimulation currents were generated by a battery-operated stimulator (DC Stimulator, NeuroConn, Germany), whereas the timing of stimulation was controlled by Presentation (Neurobehavioral Systems, USA). We maintained electrode impedance below 15 kΩ. Simulations of electric fields were set-up using SimNIBS 4 MATLAB functions (Thielscher et al., 2015). We used Gmsh to visualise the position of the electrode (Geuzaine & Remacle, 2009). We averaged the normal (or strength) of the electric field across participants (Saturnino et al., 2018), and projected the results in FreeSurfer’s FsAverage brain template (Fig. 17A, right).

We administered two stimulation blocks per session. In each block, following a two-minute resting-state baseline measurement, we applied 20 trains of stimulation in an intermittent fashion (Fig. 17B; adapted from Vossen et al., 2015). The duration of each stimulation-train was 10 s in one block and 30 s in the other, and we counterbalanced the order of blocks between participants. Each stimulation-train was followed by a 15 s inter-stimulation interval. In the tACS session, amplitude of the current was kept constant at 1 mA (peak-to-peak), whereas the frequency of stimulation was individually adapted (see below section). No stimulation was applied in the control session.

To maintain attention, participants performed a vigilance task (Fig. 17C). We projected a white fixation-cross on a black background (PT-DW700E, Panasonic, Japan) at a distance of ~57 cm from the participant. The fixation-cross (of 2° visual angle) rotated 10 s after stimulation offset by 45° for a short period of 500 ms. The rotation was triggered during any 9 out of 20 inter-stimulation intervals per block. We instructed participants to press a button using their right index finger within 2 s of the rotation.

Individual Stimulation Frequency (ISF)

To determine the frequency of stimulation, we estimated alpha peak frequency for each participant from a two-minute resting-state measurement. We tapered the data with a single Hanning window and applied a Fast Fourier Transformation for frequencies from 4-40 Hz in steps of 1 Hz. We averaged spectral power across a fixed set of right parietal channels ('MEG2412+2413', 'MEG2422+2423', 'MEG2432+2433', 'MEG2442+2443', 'MEG2612+2613', 'MEG2622+2623', 'MEG2632+2633', 'MEG2642+2643'). From this averaged spectrum, we determined the peak frequency, i.e., the frequency with maximal power, within a broad alpha range (7-14 Hz; Table S1).

MEG data acquisition and preprocessing

We recorded neural activity using a 306-channel MEG system (MEGIN Oy, Finland) at a sampling frequency of 1000 Hz. We used the Polhemus Fastrak system (Polhemus, USA) to digitise HPI coils, fiducial markers, and ~50-100 additional points. We recorded electrooculogram (EOG) to monitor blinks and eye movements.

We performed preprocessing and analysis of MEG data offline using the Fieldtrip toolbox (v20210825) (Oostenveld et al., 2011) and custom-made MATLAB scripts (R2019b; The MathWorks, Inc., USA). We first segmented the continuous MEG recording into trials. We segmented the 20 inter-stimulation intervals, succeeding tACS or control, into 6.2 s-epochs; 3.8 s to 10 s relative to stimulation offset (henceforth referred to as post-stimulation trials).

The stimulation device systematically produced two artefacts around 10 ms and 3.8 s after every train of stimulation. We observed a power decrease (relative to baseline), resembling a DC offset, in the period between the two artefacts. Therefore, the first 3.8 s of data were unusable. It is likely that the artefacts are a result of the impedance measurement performed by the stimulator in preparation for the next train of stimulation. We also rejected the last five seconds of every inter-stimulation period to avoid movement-related artefacts due to the vigilance task. We restricted further preprocessing to 204 gradiometer channels. We applied a band-pass filter of 4-150 Hz and removed the linear trends and mean of every trial. Segments of trials containing artefacts (e.g., SQUID jumps, head and muscle movements) were removed via a semi-automatic artefact detection approach implemented in Fieldtrip. Additionally, we removed noisy channels and trials containing artefacts after visual inspection. We used Independent Component Analysis (ICA) to remove remnant electro-cardio and electro-ocular artefacts.

Finally, we cut the post-stimulation trials into 5.5 s-epochs, from 4.2-9.7 s, to remove edge effects introduced during preprocessing. Further, we removed the last 10 s of the baseline period to avoid device-related artefacts and obtain a uniform number of baseline trials. The remaining 110 s were then segmented into 20 trials, each 5.5 s long.

MEG source projection

To project sensor-level data into source space, we employed the Linearly Constrained Minimum Variance (LCMV; Van Veen et al., 1997) beamformer technique.

To construct individual grids, participants' anatomical MRIs were co-registered with their MEG data through fiducial markers and the brain was segmented. From the segmented MRI, we generated a single-shell volume conduction model (Nolte, 2003). Then we applied a regular 3D-grid (5 mm resolution) to the MNI template brain (Montreal Neurological Institute, Canada). We computed individual grids by nonlinearly warping participants' MRI on the MNI template brain, and then applied the inverse of this warp to the MNI template grid. We restricted the individual grid to cortical grid points defined by the AAL atlas (Tzourio-Mazoyer et al., 2002), resulting in 8793 grid points.

We computed the covariance matrix from concatenated baseline and post-stimulation trials. Then, the covariance matrix, the individual grid, and the volume conduction model were used to build LCMV filters. To obtain time-series for each grid point, we multiplied these filters with sensor time-series data.

MEG time-frequency analysis

We performed time-frequency analysis for all cortical grid points for frequencies from 5-40 Hz (1 Hz resolution) by applying a Hanning taper to sliding time windows (with seven cycles per time window; *100 ms step-size*), followed by a Fast Fourier Transformation.

Subsequently, we adjusted the Time Frequency Representations (TFRs) of both sessions so that stimulation frequencies were aligned across participants. For each participant, the frequencies ranged from 'ISF−2' to 'ISF+26' Hz.

Statistical analyses of tACS

For each grid point of a participant, we calculated change in power relative to baseline, (i.e., Δpower) using independent t-tests. Prior to this calculation, we averaged power across all 20 trials for baseline and post-stimulation periods respectively, and we averaged power across

timepoints for the baseline period to obtain a single power value for each frequency. The resulting Δpower provided a measure of power change following tACS or control:

$$\Delta power_{tacs/control} = \frac{power_{post} - power_{baseline}}{pooled\ standard\ error}$$

To investigate Δpower on group-level, we performed a non-parametric cluster-based permutation test (Maris & Oostenveld, 2007). In single participants, we first averaged $\Delta power_{tACS}$ and $\Delta power_{control}$ over time. Then, $\Delta power_{tACS}$ for the 10 s-block and $\Delta power_{tACS}$ for the 30 s-block were pooled together and likewise for $\Delta power_{control}$. On group-level, we performed paired t-tests for each of the 8793 grid points between pooled Δpower of tACS and control conditions. If the statistical comparison met an *a priori* defined-threshold ($p<0.05$), t-values of spatially adjacent grid points were combined to a cluster (minimum of two neighbouring channels). We permuted the data by randomizing the condition assignment (tACS or control), and on each permutation, the cluster with the maximum sum of t-values was retained. This procedure was repeated 1000 times, yielding 1000 summed cluster t-values, from which the probability of the observed cluster statistic was determined.

Post hoc, we investigated whether the observed increase in power was specific to ISF in the cluster. To this end, $\Delta power_{tACS}$ and $\Delta power_{control}$ for the respective blocks were pooled together. We averaged pooled Δpower across grid points in the significant cluster (see previous analysis). We performed a cluster-based permutation test as described above; here clusters were based on temporal and/or spectral adjacency. In a control analysis, we replicated this analysis, but we adjusted TFRs based on harmonic multiples of the ISF prior to calculating Δpower (see Fig. S1).

Further, we qualitatively separated the significant cluster into its frontal and somatosensory counterparts to test for region-specific effects. This separation was based on the spatial location of the grid points, as specified by the AAL atlas. The 10 s- and 30 s-blocks were first pooled together. Then we averaged pooled Δpower across grid points in the frontal and somatosensory clusters respectively. We used non-parametric permutation testing to statistically compare tACS and control conditions in the two distinct regions (see above).

Lastly, we tested the effects of train duration (10 s and 30 s) on power at ISF. In single participants, we first averaged Δpower across grid points in the entire significant spatial cluster. On group-level, we performed paired t-tests to contrast $\Delta power_{tACS}$ with $\Delta power_{control}$. We then

statistically compared the resulting t-values between the 10 s-block and 30 s-block using the Wilcoxon Rank Sum test.

Binning analysis of stimulation trains

We aimed to evaluate whether short tACS-trains were sufficient for enhancing power. We averaged power over trials and across time for the baseline period (denoted below as 'avg $power_{baseline}$'). We then calculated power-difference for each trial (n denotes the trial number):

$$Power\text{-}difference_{trial(n)} = \frac{power_{trial(n)} - avg\,power_{baseline}}{avg\,power_{baseline}}$$

Subsequently, we averaged power-difference (at ISF) across grid points in the significant cluster and over time in each participant, resulting in a single power-difference value per trial. All trials, in a given stimulation block, were divided into 5 equal-sized bins based on trial order (i.e., power-difference values of four consecutive post-stimulation trials were grouped into one bin). We used Friedman's tests to assess the effect of 'Bins' on power enhancement.

Exploratory analysis of rhythmic power modulations

Many participants exhibited rhythmic fluctuations in alpha power across time. Thus, we investigated whether this putative underlying rhythm, termed modulatory power, changed with the application of tACS. tACS may influence fluctuations of power in two ways. On one hand, the magnitude of the fluctuation i.e., how strongly power fluctuates at a given frequency, may be amplified by tACS. In this case, tACS merely amplifies the amplitude of alpha activity, without any changes in the modulation frequency. On the other hand, the regularity of these fluctuations i.e., the occurrence of burst-like activity, may be facilitated by tACS. For this analysis, TFRs of power were computed for a sliding window of 400 ms (in steps of 100 ms). All other steps were as described in Section 2.7. We computed power-difference for each trial by subtracting power of the preceding trial (averaged over time) from power of the current trial (n denotes trial number):

$$Power\text{-}difference_{trial(n)} = power_{trial(n)} - avg\,power_{trial(n-1)}$$

The first trial was excluded from this analysis since there is no preceding trial. In single-participants, we averaged power-difference over grid points in the significant cluster. We calculated the modulatory power in each trial for frequencies from 'ISF−2' to 'ISF+26' Hz (in steps on 1 Hz). We first filtered the power-difference values (filters between 0.1 and 2 Hz in steps of [0.1, 0.1, 0.1, 0.1, 0.25, 0.25, 0.25, 0.25, 0.25, 0.25] Hz). The filter frequencies were

non-uniform to reduce computational load while maintaining good spectral resolution at lower frequencies. We then applied a Hilbert transformation on the filtered data, extracted the modulatory power by computing the absolute value of the Hilbert transformation, and averaged the values across time. On group-level, modulatory power in each tACS block was contrasted with the corresponding control block via cluster-based permutation tests (see foregoing section).

Results

tACS and control session questionnaires

Five participants reported sensations on the scalp during the tACS session (confidence rating 3.80±2.49 [mean ± SD]), indicating that they were unsure whether tACS was administered. Three participants reported sensations during the control session (confidence rating 5.67±1.53). Across all participants, the mean confidence rating in the tACS session was 4.96±3.34, and 4.56±3.18 in the control session. Confidence ratings across sessions were not significantly different (Wilcoxon Rank Sum test; $p>0.05$). Overall, the topical anaesthetic was effective in eliminating peripheral stimulation and blinding the stimulation condition.

On the BL-VAS, participants scored 40.58±16.95 for alertness, 14.25±6.27 for contentedness, and 3.92±2.16 for calmness in the tACS session. In the control session, they scored 37.83±17.76 for alertness, 14.63±6.84 for contentedness, and 4.29±2.41 for calmness. Overall, BL-VAS scores did not significantly differ between the tACS and control sessions (Wilcoxon Rank Sum test; $p>0.05$). Further, all participants fulfilled at least a 70% detection rate on the vigilance task in both sessions.

tACS effects on alpha power

An increase in power was observed at individual stimulation frequency (ISF) after tACS compared to control ($p=0.007$; Fig. 18A). The power change in the tACS session was 31.68 ± 26.72% [mean ± SD], and 16.43 ± 22.46% in the control session. The cluster extended bilaterally in the somatosensory and frontal regions.

Next, we investigated whether the power increase was specific to the alpha-band. We found four significant time-frequency clusters ($p<0.030$; Fig. 18B). The clusters extended broadly across all frequencies, but the power increase was most prominent between ISF and 'ISF–2' Hz. In the control analysis, we aligned ISF to its first harmonic frequency to circumvent broad-

spectral effects. We found one significant positive cluster (p<0.031; Fig. S1), with a similar pattern of increase in power ~ISF, and analogous broadband effects at later timepoints.

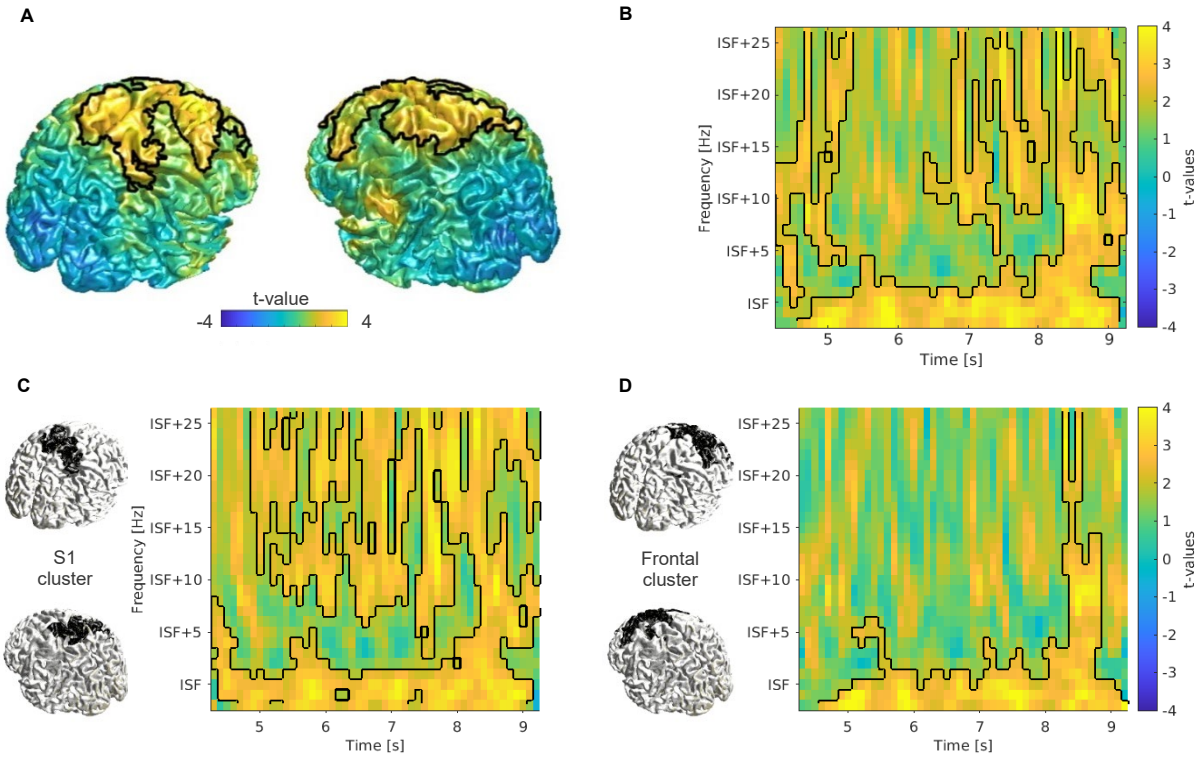

Figure 18. Analysis of power contrast between tACS and control conditions
A) t-values of Δpower contrast (see Section 2.8) projected on an MNI template brain. t-values were averaged across the post-stimulation period at individuals' stimulation frequency (ISF). A higher t-value signifies greater Δpower in tACS compared to control. We found one significant positive cluster ($p < .05$; outlined in black). **B)** Time-frequency representation (TFR) of t-values averaged across channels in the significant cluster shown in A). TFRs were aligned to ISF before averaging. We found four significant positive clusters (outlined in black). **C)** TFR of t-values averaged across channels in the somatosensory part of the cluster shown in A), as highlighted in the left panel. We found three significant positive clusters (black outlines in right panel). **D)** TFR of t-values averaged across channels in the frontal part of the cluster shown in A), as highlighted in the left panel. We found one significant positive cluster (black outlines in right panel).

Subsequently, the cluster was qualitatively separated into a somatosensory and a frontal cluster. We found one significant cluster in the frontal region (p=0.003, Fig. 18D), and three significant clusters in the somatosensory region (p<0.040, Fig. 18C). The time-frequency profile of the clusters in both regions matched closely; but in the frontal cluster, early effects at higher frequencies were not significant.

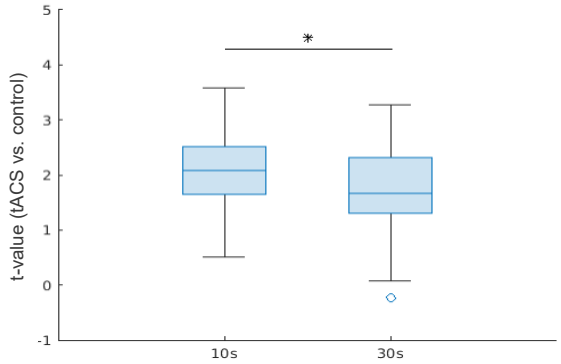

Figure 19. Modulation of power in 10s- & 30s-blocks. Boxplot shows t-values signifying the difference in Δpower between tACS and control conditions for the respective stimulation blocks. t-values were averaged within the significant cluster shown in Fig. 18A. *p < 0.05.

To investigate the effect of train duration on power, we compared Δpower at ISF between 10 s- and 30 s-blocks (Fig. S2 shows Δpower of individual participants). We found that the 10 s-block produced greater increases in power than the 30 s-block (p=0.020; Fig. 19).

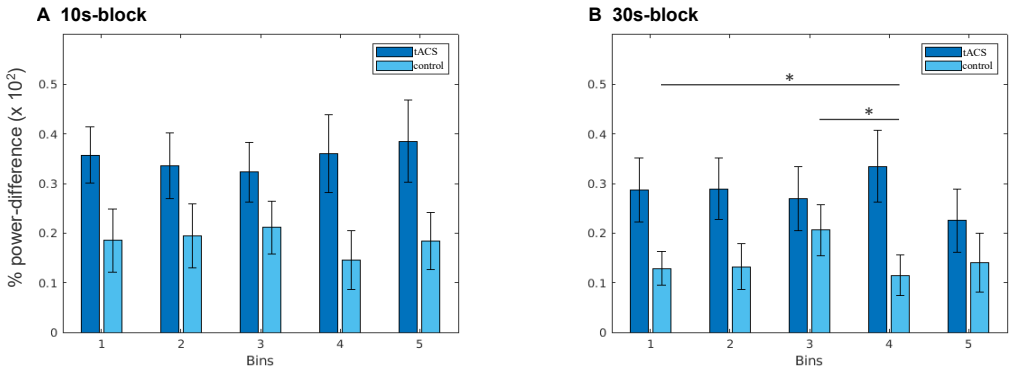

Figure 20. Modulation of power through the duration of the experiment
A) Bars represent the percentage of power-difference at ISF (relative to baseline) for the 10 s-block. Dark blue bars indicate power-difference in tACS, whereas light blue bars indicate power-difference in control. Error bars indicate standard deviation. Bin number increases with time on task. **B)** Same as A), but for the 30 s-block. *p < 0.05.

Binning analysis of stimulation trains

In the 10 s-block, there was no main effect of 'Bin' in tACS (X^2=7.50, p=0.112) or control conditions (X^2=7.93, p=0.094; Fig. 20A). Similarly, in the 30 s-block, there was no main effect of 'Bin' in the tACS condition (X^2=6.83, p=0.145); but a significant main effect of 'Bin' (X^2=15.00, p=0.005; Fig. 20B) in the control condition. A pairwise *post hoc* Conover test with Bonferroni correction showed a significant difference between the first and fourth bin (p=0.016) and the third and fourth bin (p=0.036).

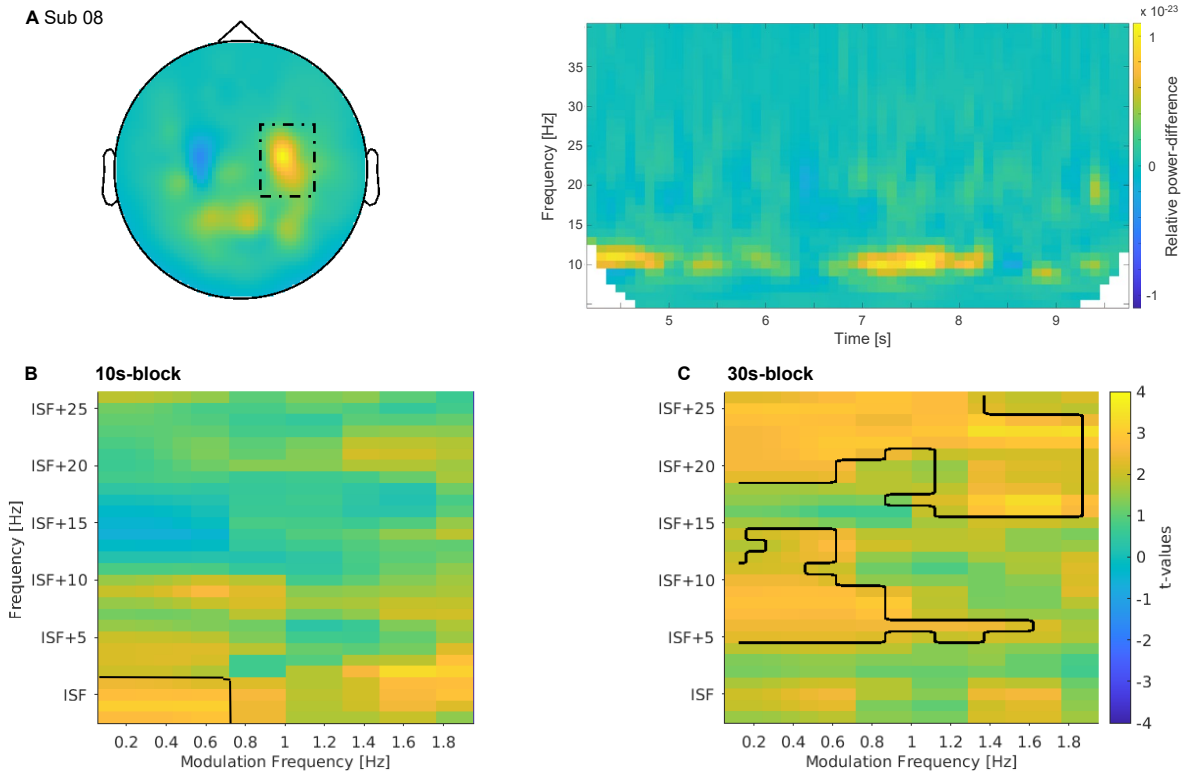

Figure 21. Exploratory analysis: Rhythmic fluctuation of power
A) Exemplary demonstration of slow fluctuation of power in a single participant. The left panel shows sensor-level topography of power change (relative to previous trial) at ISF±1. Dotted black outline indicates the somatosensory region of stimulation. The right panel shows TFR of power averaged over channels within the dotted outline. **B)** TFR of t-values on source-level. t-values signify the difference in modulatory power between tACS and control conditions for the 10 s-block. X-axis represents the modulatory frequencies. Y-axis represents the canonical frequencies and ranges from 'ISF-2' to 'ISF+26' Hz. We found one significant positive cluster (outlined in black). **C)** Same as in B), but for the 30 s-block. We found two significant clusters (outlined in black). TFRs (in B & C) were averaged across channels in the significant cluster (in Fig. 18A) for the respective stimulation blocks.

Exploratory analysis of rhythmic power modulations

We observed systematic fluctuations of alpha power with time in several participants (Fig. 21A); hence, we statistically evaluated whether the magnitude and/or regularity of these fluctuations is modulated by tACS. We found one significant positive cluster in the 10 s-block (p=0.031, Fig. 21B), which spanned from 0.1-0.75 Hz for the modulation frequency and between 'ISF±2' Hz for the power. For the 30 s-block, we found two significant clusters (p=0.006 and p=0.011, Fig. 21C). One cluster ranged from 0.1-1.75 Hz for the modulation frequency and from 'ISF+16' to 'ISF+26' Hz for the power. The other cluster ranged from 0.1-1.5 Hz for the modulation frequency and from ISF+5' to 'ISF+14' Hz for the power. In general, the modulatory power appears to be enhanced with tACS compared to the control condition.

Discussion

The heterogeneous effects of tACS are an ongoing challenge in the field of non-invasive brain stimulation. Our study was motivated by the lack of uniformity in stimulation parameters, which may in turn explain the heterogeneity in reported effects. To study the influence of stimulation duration, we intermittently applied tACS for short periods of 10 s and 30 s during simultaneous MEG. Our results demonstrate that short-period tACS enhanced alpha power at Individual Stimulation Frequency (ISF) in the somatosensory and frontal regions. Blocking transcutaneous stimulation via a topical anaesthetic did not hinder the modulation of power. Notably, short stimulation trains (10 s) produced a greater increase in alpha power than long stimulation trains (30 s).

Studies using short trains (8 s) of tACS to the parieto-occipital region have reported an increase in power (Stecher et al., 2021; Vossen et al., 2015). Whereas, the only study to administer intermittent tACS (6 s-trains) to the somatosensory cortex did not find any changes in alpha power (Sliva et al., 2018). On the contrary, Gundlach et al., (2017) showed a decrease in alpha amplitude following 5 minutes of tACS to the somatosensory cortex. Our results stand in contrast to both accounts, demonstrating the ability of tACS to enhance somatosensory alpha power. Discrepancies between our results and the others' may stem from variations in stimulation site and electrode placement, as the referenced studies used different setups: attaching electrodes to left S1 or bilaterally above left and right S1.

The power enhancement observed in our study spanned bilaterally over the somatosensory cortex, and surprisingly, it extended up to the frontal cortex. Similarly, Kasten et al., (2019) applied tACS over the parieto-occipital cortex and reported a widespread increase in alpha

power across parieto-occipital, temporal and frontal regions. Most studies only assess data from a selected region of interest; thus, little is known about dispersion of effects. New evidence suggests that tACS improves posterior-to-frontal alpha connectivity, implying that the widespread power increase might be due to altered network dynamics (Ahn et al., 2019; Clancy et al., 2022; Fuscà et al., 2018). Adding further credibility to this interpretation, we did not observe a congruent dispersion of electric fields in the current simulations. In general, our finding provides new insights into the spatial extent of tACS-induced after-effects.

Further, we found that the power increase induced by tACS extended beyond the alpha-band to the beta-band. This finding diverges from studies showing power modulation specifically at ISF (Randolph F. Helfrich et al., 2014; Zaehle et al., 2010). However, entrainment is a non-linear process and is not restricted to the frequency of stimulation. The frequency and intensity at which an entrainment is successful is characterised by a triangular region of synchronization, known as the "Arnold Tongue" (Pikovsky et al., 2002). For example, a neural oscillator with a peak in the beta frequency (~20 Hz) can be entrained by a 10 Hz rhythm (1:2 Arnold Tongue) and *vice versa*. Also, an increase in beta power can be explained by cross-frequency phase synchronization. A similar 1:2 relationship for 10 Hz Alpha and 20 Hz beta has been demonstrated extensively (Carlqvist et al., 2005; Nikulin & Brismar, 2006; Palva et al., 2005; Palva & Palva, 2018).

Power enhancement in beta frequencies persisted even after correcting individuals' TFRs by aligning ISF with its first harmonic frequency. This shows that the effect was not simply a result of spectral smearing. On the other hand, the power increase observed at higher frequencies might be driven by non-sinusoidal features of the somatosensory alpha rhythm (Cole & Voytek, 2017; Donoghue et al., 2022). We found power increase for harmonic frequencies in the somatosensory region, but less so in the frontal region. Stronger alpha band power, and greater deviation from sinusoidality coincides with stronger harmonics in the beta band (Donoghue et al., 2022; Schaworonkow, 2023). This might suggest that there is greater contamination of genuine beta-band activity in the somatosensory region due to its arc-shaped waveform. However, the concomitant changes in beta power and higher frequencies must be interpreted with caution, as the impact of alpha-tACS on other frequency bands and waveforms is grossly understudied.

Notably, we found 10 s-trains showed a larger increase of alpha power than 30 s-trains. Research employing transcranial Direct Current Stimulation (tDCS) has revealed similar non-linear effects (Ho et al., 2016; Mosayebi Samani et al., 2019). For example, 13 minutes of tDCS

increased cortical excitability; whereas applying it for 26 minutes attenuated excitability (Monte-Silva et al., 2013). Likewise, lower current intensities induced larger increases in alpha power than higher current intensities (4-6 mA; De Koninck et al., 2021). Longer stimulation times and higher current intensities might be counteracted by metaplasticity, which prevents over-excitation and over-inhibition of neural populations (Abraham, 2008). Thus, further research is required to understand the dose-dependent effects of tACS, especially in the somatosensory cortex.

Additionally, we split post-stimulation trials into equal-sized time bins to evaluate power modulation as a function of the number of tACS trains administered. We did not find statistically significant power-difference across all bins for both 10 s- and 30 s-tACS blocks. This finding reiterates that short trains of stimulation produce concurrent and consistent changes in alpha power. We found some variability in power modulation in the 30 s-control block, which may reflect a natural variation in alpha power due to increased mental fatigue (Boksem et al., 2005; Oken et al., 2006).

Additional exploratory analyses showed slow fluctuations in alpha power (~0.4 Hz), which are enhanced with tACS compared to control. It appears that tACS either facilitates rhythmicity in power (i.e., improves the occurrence of burst-like activity), or merely enhances the amplitude of the oscillation relative to control. In either case, we would observe a facilitation of modulatory power at the frequency of stimulation. While our analysis is not sufficient to delineate the nature of the observed changes, it presents an exciting opportunity for further study. The slow fluctuations of power might be driven by bodily rhythms (e.g., heartbeat and respiration; Kluger et al., 2021; Yuan et al., 2013). However, this interpretation warrants caution, as we did not measure ECG or respiration.

ISF (estimated at the beginning of each session) and alpha peak frequency (during the experiment) did not match for two thirds of our participants (Kasten et al., 2019; Stecher & Herrmann, 2018). Our target was somatosensory alpha oscillations, but since we estimated ISF from sensor-level data, it is possible that our estimates were contaminated by the dominant occipital alpha rhythm (Schaworonkow & Nikulin, 2022). Additionally, peak frequency has been shown to shift over time, further complicating its estimation (Benwell et al., 2019; Haegens et al., 2014). Eight participants had a matching peak frequency in the 10 s block, whereas ten participants had a matching peak frequency in the 30 s block. Therefore, the larger effect on power seen in the 10 s block is not attributable to disproportionate shifts in peak frequencies between the two stimulation blocks. Another limitation is loss of the first ~4 s post-

stimulation due to artefacts from the stimulation device. As entrainment echoes vanish a few milliseconds after stimulation offset, we could not assess the evidence for or against the entrainment hypothesis. Therefore, the role of plasticity and entrainment in producing the observed effects remains unclear. Future studies should consider employing the remote input available in DC-Stimulator PLUS (NeuroConn, Germany) to control the stimulation signal on a trial-by-trial basis.

In this study, we reiterate the potential of intermittent short-period tACS to induce oscillatory power changes. Importantly, we established that 10 s of tACS is sufficient for our intended use in a prospective study, and that longer stimulation periods are not a prerequisite for modulating power. Taken together, our findings strongly advocate the application of tACS to further our understanding of brain and behaviour.

4 STUDY 2

Title: Spontaneous Fluctuations in Alpha Peak Frequency Along the Posterior-to-Anterior Cortical Plane

Article information: Published on 19th December 2025 in eNeuro
DOI: https://doi.org/10.1523/ENEURO.0118-25.2025

Author names and contributions:
Vaishali Balaji: Formal Analysis, Investigation, Writing – Original Draft, Writing – Review & Editing, Visualisation. **Alfons Schnitzler:** Conceptualisation, Methodology, Resources, Writing – Review & Editing, Project administration. **Joachim Lange:** Conceptualisation, Methodology, Resources, Writing – Review & Editing, Supervision, Project administration, Funding acquisition.

Abstract

Alpha peak frequency (APF) is defined as a prominent spectral peak within the 8-12 Hz frequency range. Typically, an individual's alpha frequency is regarded as a stable neurophysiological marker. A wealth of recent evidence, however, indicates that APF shifts within short timescales in relation to task demands and even spontaneously so. Further, brain stimulation studies often report shifts in APF both within and between experimental sessions, directly contradicting the idea of a stable APF. To characterise the non-stationarities in spectral parameters, we estimated APFs from one-second epochs of resting-state magnetoencephalography (MEG) recordings from healthy adults of either sex. To enhance signal-to-noise ratio, without compromising on temporal resolution, we averaged power spectra within parcelled regions. Our findings indicate that variation in APFs exacerbates along the posterior-to-anterior cortical plane i.e., from the occipital to the frontal cortices. Further, by comparisons with amplitude-matched simulated signals, we demonstrated that the observed gradient is not attributable to measurement noise. Across the cortex, APFs showed poor temporal reliability, raising the question of whether APFs are more like a transient state than a trait. In general, our study elucidates the dynamic characteristics of alpha oscillations and reveals systematic regional differences which are, in part, shaped by underlying signal-to-noise ratio inherent to MEG recordings.

Introduction

Alpha oscillations, within the 8-12 Hz frequency range, are a prominent feature of electro - and magneto – encephalography (E/MEG) recordings (Berger, 1929). Parameters of the alpha oscillations, such as power and phase, have been studied extensively in the context of neural inhibition and excitation (Jensen et al., 2012; Jensen & Mazaheri, 2010; Klimesch et al., 2007; Lange et al., 2013; VanRullen, 2016). Typically, these studies examined power and phase in fixed or predefined frequencies or frequency bands. However, the practice of employing strict, *a priori* defined, frequency bands might overlook potentially meaningful variation within the alpha band (Donoghue et al., 2022; Jones et al., 2009; M. A. Sherman et al., 2016; Tallon-Baudry, 1999). Alpha peak frequency (APF), defined as the frequency having the maximum power, is a distinct measure of oscillatory activity. As APF is estimated per individual from the empirical data, it allows for flexible comparisons of intra- and inter- individual differences in behaviour and cognition (Baumgarten et al., 2023). Especially within the context of perception, APF has been widely implicated in the speed of processing information. APF is said to determine the temporal resolution of the visual system whereby fluctuations in APF dictate whether one perceives discrete visual stimuli as simultaneous or separate (Drewes et al., 2022; Samaha & Postle, 2015; Sharp et al., 2022). Similarly, top-down modulation of APF was demonstrated in the context of a working memory paradigm with an increase in APF in conjunction with increased memory load (Babu Henry Samuel et al., 2018; Haegens et al., 2014). Even in the absence of experimental manipulation, Benwell et al., (2019) found a difference in APF between two halves of an experimental session, whereas Cohen (2014) reported shifts in APFs within resting-state networks. Further, Mahjoory and colleagues (2020) showed a systematic decrease of APF across the cortex in the posterior to anterior direction, suggesting that APF varies spatially.

Contradictorily, it is assumed that APF is a stable 'trait' marker (Grandy et al., 2013; Haegens et al., 2014). This view is mainly driven by the longitudinal changes in APF across the lifespan in congruence with brain volume (Lindsley, 1939), and relative stability over test-retest intervals (Kondacs & Szabó, 1999) despite cognitive interventions (Grandy et al., 2013). APF is considered a neurophysiological fingerprint, especially due to its presumed heritability (Smit et al., 2006) and marked inter-individual differences (Klimesch, 1999; Posthuma et al., 2001). However, APF may resemble a state factor depending on the timescale of the investigation. Conventional analyses, which estimate APF from 2-5 minutes of resting-state M/EEG, capture the mean peak frequency over this time-period; however, the APF may spontaneously fluctuate

around the mean frequency in response to changes in physical stimuli or cognitive-state. In fact, numerous non-invasive brain stimulation studies report the notoriety of matching stimulation frequency to APF (Stecher & Herrmann, 2018; Vossen et al., 2015), highlighting the practical pitfalls of assuming that APF remains stationary over time.

Findings from computational studies collectively suggest that frequency transitions within the alpha band are likely a natural consequence of variation in synaptic input and concurrent firing rates of neural populations (Hutt et al., 2016; Lefebvre et al., 2015). When firing rates increase relative to baseline, cortical networks recruit non-linear feedback loops, in turn changing the system's response function and the features of its emergent dynamics (Mierau et al., 2017). Therefore, APF is a proxy for the activation-state of a population of neurons. As such, the fluctuations of frequency are a dynamic signature of low-frequency neural oscillations, but they are rarely accounted for in the analysis of experimental data.

Building on previous work by Smith et al., (2024), we aimed to analyse the stability of APF at short timescales. To this end, we estimated individual APFs from source-reconstructed power spectra derived from brief time-series (1s epochs) of resting-state magnetoencephalography (MEG). We decomposed the power spectrum into periodic and aperiodic components, ensuring that estimates of APF are unaffected by aperiodic activity. Since frequency of the intrinsic oscillator may vary spontaneously in conjunction with synaptic input, we hypothesised that APFs would show considerable variability within individuals. Further, brain areas vary in terms of spectral profiles (Keitel & Gross, 2016; Mahjoory et al., 2020; Mellem et al., 2017), developmental trajectories (Charvet & Finlay, 2014) and structural connections (Huntenburg et al., 2017); hence, we hypothesised that the variability of APFs would also be spatially heterogeneous.

Methods

Experimental design

In this study, we analysed a previously acquired dataset (manuscript has been submitted for publication), containing around four minutes of resting- state MEG recordings from 24 healthy participants (11 female, age 25.33 ± 2.81 [mean ± SD] years). The participants were seated upright in a dimly lit magnetically shielded room while we recorded neural activity using a 306-channel MEG system, with a sampling frequency of 1000 Hz (MEGIN Oy, Finland).

The MEG recordings are from a study where transcranial alternating current stimulation (tACS) was applied to the participants' somatosensory cortex. Each recording started with a baseline period of 2 min, followed by periods of either 10s or 30s of tACS, or no stimulation (control). The data used in the present study were collected during the control session. That is, tACS electrodes were placed at the participants' scalp, but no electrical stimulation was administered. The participants were unaware of the stimulation condition (10s, 30s, or control). Hence, we classify this dataset as resting-state MEG.

In addition, we instructed participants to focus on a white fixation-cross through the duration of the experiment. The cross was projected (PT-DW700E, Panasonic, Japan) on translucent screen placed ~57 cm in front of the participants. The fixation-cross rotated by 45° for 500 ms at random time points. Participants had to press a button within two seconds of the rotation. This task served merely as a vigilance task paradigm and was included to ensure sustained attention (Zaehle et al., 2010).

We acquired anatomical T1-weighted MRIs with a 3T Siemens scanner (Siemens Magnetom Tim Trio 3T, Siemens, Germany). We used the Polhemus Fastrak system (Polhemus, USA) to digitise HPI coils, fiducial markers, and ~50-100 additional points. We recorded electrooculogram (EOG) to monitor blinks and eye movements.

MEG data preprocessing

Entire preprocessing and analysis of the datasets were performed using the Fieldtrip toolbox (version 20240614) and custom-made scripts on MATLAB (R2023b; The MathWorks, Inc., USA).

We segmented the continuous MEG recording into trials, consisting of a single baseline trial (110 s) and 20 resting-state trials (of ~5.5 s). We restricted further preprocessing to 204 gradiometer channels. We applied a band-pass filter of 4-150 Hz and removed the linear trends and mean of every trial. We applied Fieldtrip's semi-automatic artefact detection approach to remove segments of trials containing artefacts (e.g., SQUID jumps, head and muscle movements). After visual inspection, we additionally removed noisy channels and trials containing artefacts. We used Independent Component Analysis (ICA) to remove any remaining electro-cardio and electro-ocular artefacts.

Source reconstruction

We reconstructed the sources of the time-series data measured by MEG sensors using Linearly Constrained Minimum Variance (LCMV) beamformers (Van Veen et al., 1997).

We generated a single-shell volume conduction model by performing co-registration of the sensors to participants' anatomical MRIs using fiducial markers, followed by segmentation of the brain surface (Nolte, 2003). Then we divided the brain volume into a regular 3D-grid with a 5 mm resolution, based on the MNI template brain (Montreal Neurological Institute, Canada).

We restricted the analysis to cortical regions resulting in 8384 grid points. We estimated spatial filters for each of the cortical grid points along the dipole direction with maximal power, with a regularisation parameter of 10%. By multiplying these filters with sensor-level data, we reconstructed time-series data at the source. Subsequently, source-level time-series were parcellated into 210 cortical regions of interest based on the Brainetome atlas (Fan et al., 2016).

Data analysis

We concatenated baseline and resting-state trials to create a continuous segment of the time series (~ 220 s) and then segmented parcel time-series into 1-s epochs. We computed power spectra for each epoch using a multi-tapered (3 tapers) Fast Fourier transform, based on discrete prolate spheroidal sequences (dpss), with 2 Hz spectral smoothing. We averaged power spectra over grid points within each parcel, resulting in ~220 power spectra per parcel and participant. We estimated the aperiodic 1/f component using the 'Fitting Oscillations One Over F' (FOOOF; Donoghue et al., 2020) algorithm in Python 3.7.2. Then we subtracted the 1/f component from the corresponding spectra and determined the spectral peaks in the alpha band (7-14 Hz), for each corrected spectrum of a parcel, using the '*findpeaks*' function on MATLAB. The frequency of the peak with the strongest power was regarded as the alpha peak frequency (APF) of a given spectrum. Epochs without a definitive spectral peak i.e., a flat peak with two neighbouring frequencies of the same power, were given the value of a 'NaN'.

Statistical analysis

First, we sought to replicate the results of Mahjoory et al., (2020). To this end, we performed a linear regression between time-averaged APF of 210 parcels and their corresponding Y-coordinate position, along the posterior-to-anterior direction. Second, to quantify the degree of variation in APFs within participants, we calculated the Coefficient of Variation (CV), for a given parcel, by dividing the standard deviation by the mean APF across 220 epochs.

For a given parcel, k:

$$CV_{parcel\ k} = \sigma_{epochs\ k} \div \mu_{epochs\ k}$$

To test the regional differences in CV along the posterior-anterior axis, we performed a linear regression between CV values of all parcels and their corresponding Y-coordinate position.

To check whether the spatial profile of alpha power confounded the estimation of APF, we calculated signal-to-noise ratio (SNR) and CV for each of the 8384 cortical grid points. We defined SNR as the ratio between the power of the APF and the average power of spectral peaks in all other frequencies. We averaged SNR and CV values within a spatial sliding window of 2.5 cm in increments of 0.25 cm (along the posterior to anterior direction), resulting in 61 SNR and CV values per participant. We concatenated the CV and SNR values across participants and performed a Pearson correlation.

To contrast the variation in APF with noise, we subjected 20 empty-room datasets to the same preprocessing and data analysis steps as detailed in the foregoing sections. Additionally, we added a 10 Hz alpha and a 20 Hz beta rhythm to the empty-room time series. The simulated alpha peaks decreased in amplitude along the posterior to anterior direction, thereby mimicking the physiological data (Fig. S4). The beta rhythm was added as a proxy to neuronal noise. We obtained CV values for the 210 parcels of physiological data, CV values for 204 MEG sensor channels of non-neuronal noise data and CV values for 204 MEG sensor channels of simulated noise data. We averaged CV values along the Y-axis gradient using a spatially sliding window as detailed above. Then we performed independent t-tests for each of the 61 Y-coordinate positions between signal and noise data. To circumvent the multiple comparison problem, we performed a non-parametric cluster-based permutation test. We permuted the data by shuffling the condition assignment (signal vs noise). Spatially adjacent Y-coordinate positions, which met *a priori* defined threshold ($\alpha = 0.05$), were combined to a cluster. On each permutation, we retained the cluster with the maximum sum of t-values. Given 1000 summed cluster t-values, obtained from 1000 permutations, we determined the probability of the empirical data.

To ensure that peaks identified from the physiological data reflected genuine neural activity rather than ambient noise, we estimated the distribution of spectral peak powers across the empty-room recordings (per MEG sensor), and we discarded epochs from physiological data, if the identified APF did not exceed the 99th percentile of this noise distribution (see Fig. S5). We then calculated CV values for all remaining APFs per parcel. To test whether the regional

differences in CV persisted after excluding APFs with low amplitudes, we performed a linear regression between the recalculated CV values and their corresponding Y-coordinate position.

Finally, we examined whether APF is a stable "trait-like" construct which is distinguishable between subjects. We used intra-class correlation (ICC) to measure the reliability of APF which akin to intra-rater reliability, quantifies the variation of data measured by 1 rater across 2 or more trials. In our study, it is the extent to which a single individual consistently produces the same APFs across epochs. Specifically, we implemented a single-rater two-way mixed-effects model and absolute agreement definition, or ICC(A,1) (McGraw & Wong, 1996; Shrout & Fleiss, 1979). Generally, ICC is calculated as a ratio,

$$\frac{MS_B - MS_E}{MS_B + (k-1)MS_E + \frac{k}{n}(MS_W - MS_E)}$$

where, MS_B is mean square between participants, representing the variance attributable to true differences between individuals, MS_E is mean square for error, representing the residual error variance (i.e., the variance not accounted for by participant or measurement), MS_W is the mean square within participants, representing the variance between measurements, k is the number of measurements (or epochs), and n is the number of participants. If the MS_E is equal to or larger than the variance of interest (MS_B), the reliability of APFs is evidently poor.

ICC estimates and their 95% confidence intervals were calculated using the Matlab Central file-exchange *ICC.m* function (Salarian, 2016). This ICC calculation was applied at every parcel to obtain spatially specific reliability estimates. In addition, we estimated APFs from epochs of 2 s and 5 s to chart out how ICC increases with longer periods of averaging (Fig. S7 and Fig. S8, respectively). ICC estimates range from 0 – 1, with values closer to 1 indicating higher reliability.

Results

We successfully replicated the key results of Mahjoory et al., (2020) showing that APF decreased significantly along the posterior-to-anterior axis ($R^2 = 0.646$, $p < 0.001$; Fig. S3). The left lateral occipital cortex had the highest APF of 10.57 ± 1.61 Hz [mean ± SD], whereas the left middle frontal gyrus had the lowest APF of 7.5 ± 0.74 Hz [mean ± SD].

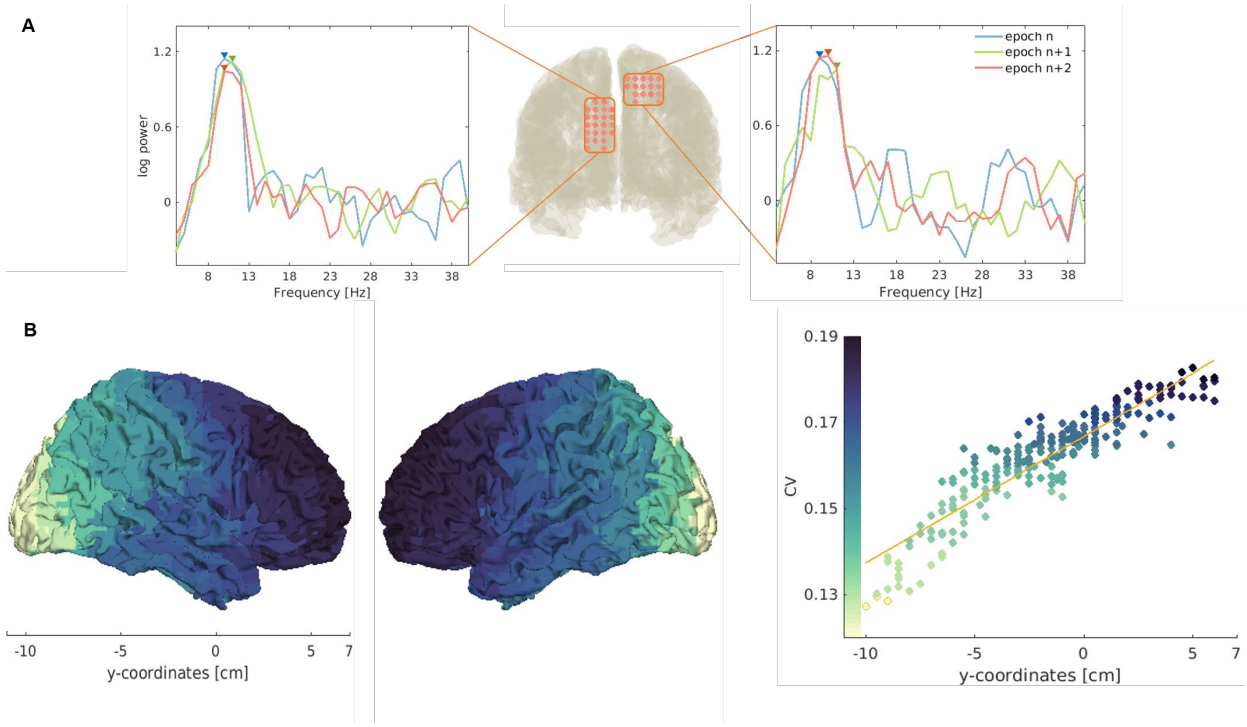

Figure 22. Variation in alpha peak frequency
A) Exemplary demonstration of shifts in alpha peak frequency (APF) in three consecutive epochs. The left panel shows shifts in APF in the left lateral Occipital cortex from 9 Hz to 10 Hz, and then back to 9 Hz, all within three seconds. The right panel shows shifts in APF in the right superior Parietal Lobule from 9 Hz to 11 Hz, and then to 10 Hz, again within three seconds. **B)** In the left panel, the degree of variation in APF, measured by Coefficient of Variation (CV), is projected on an MNI template brain. In the right panel, CV values were averaged along a spatially sliding window in the posterior-to-anterior direction. Y-coordinate position of the parcel significantly predicted CV ($R^2 = 0.841$, $p < 0.001$).

To quantify changes in APF within participants, we calculated the CV for all cortical parcels. CV values linearly increased along the posterior-to-anterior axis ($R^2 = 0.841$, $p < 0.001$; Fig. 22B). The lateral occipital cortices showed the least amount of variation in APF, with an average CV of 0.13 ± 0.03 [mean ± SD], whereas the superior and middle frontal gyri, showed the most variation, with an average CV of 0.18 ± 0.01. Among individuals, 70% showed a moderate positive correlation between Y-coordinate position and CV ($r > 0.6$).

We found a significant negative correlation between SNR and CV ($r = -0.87$, $p < 0.001$; Fig. 23). This suggests that low alpha power in the anterior regions may preclude the estimation of APF, resulting in seemingly high CV. *Alternatively, it could also be driven by the presence of multiple alpha-band oscillations of comparable magnitude occurring simultaneously in anterior regions, with APF switching between peaks as their relative prominence fluctuates.*

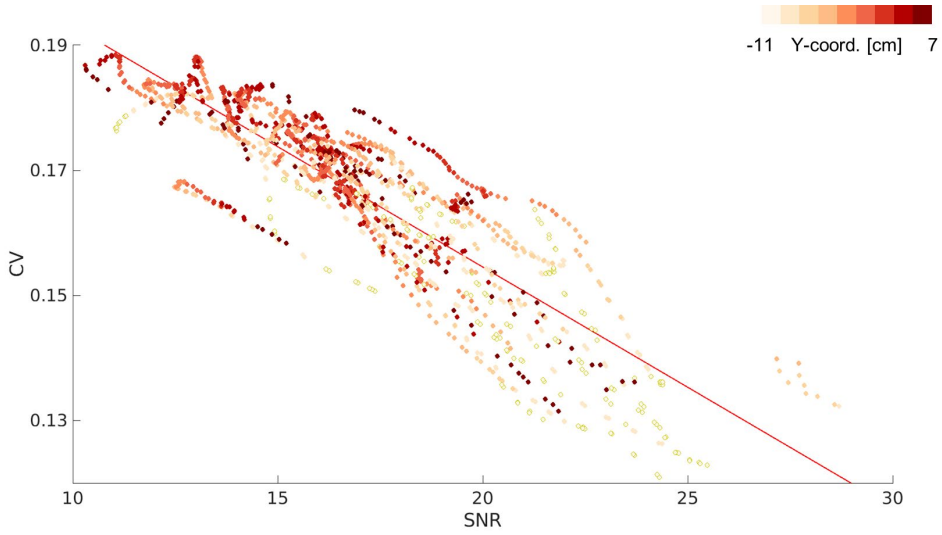

Figure 23. Correlation between CV and Signal-to-Noise ratio (SNR)
SNR of a parcel spectrum is the relative difference between the power of the APF and the average power of all other peak frequencies. The colour bar indicates the Y-coordinate position of each data point. Lighter colours lie caudally, whereas darker shades lie rostrally along the Y-coordinate axis. We found a significant negative correlation between SNR and CV, such that a lower SNR was associated with a higher degree of variation (CV) in APF ($r = -0.87$, $p < 0.001$).

To elucidate whether the temporal fluctuations in APF from second-to-second are simply a by-product of noise, we contrasted APFs estimated from physiological data with APFs estimated from empty-room measurements. CV of physiological signal was significantly lower than CV of empty-room noise between -10.5 cm and 0 cm on the y-axis plane (i.e., from the occipital cortex to pre-central gyri; Fig. 24A). In this significant spatial range, APF deviated by as much as -2.2 to +1.7 Hz from the median in the physiological signal (Fig. 24B). To evaluate the integrity of anterior APF estimates, we performed a control analysis in which we excluded epochs if the identified APF did not exceed the threshold derived from empty-room recordings. We found a substantial reduction in both the number of retained epochs and the CV

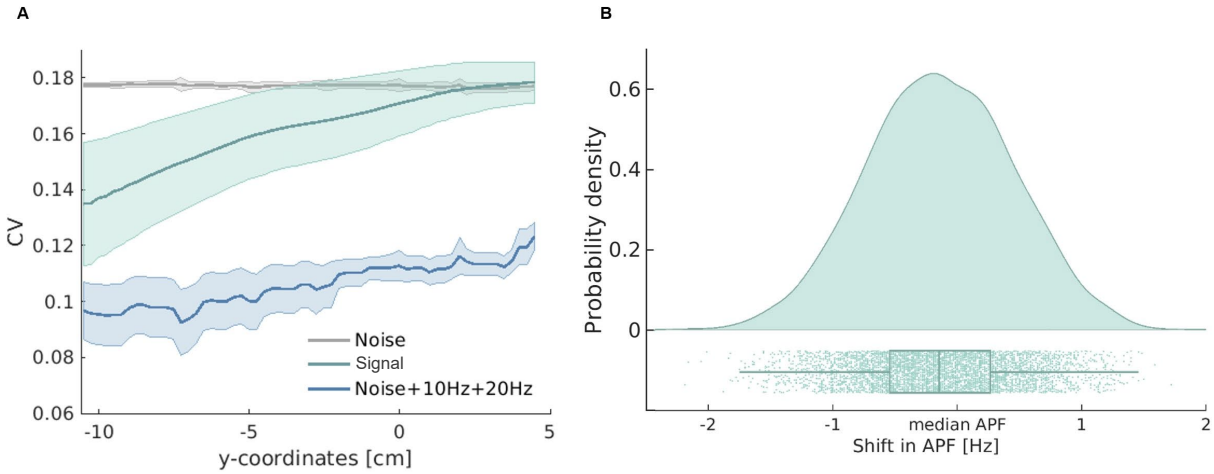

Figure 24. Analysis of CV in relation to simulated signal and noise
A) The CV of physiological signal (in teal), non-neuronal noise (in grey) and simulated noise+signal (in blue) is plotted along the Y-coordinate plane. The shaded region indicates the standard deviation across datasets. On comparing physiological signal with empty-room noise, we found a statistically significant cluster between -10.5 cm and 0 cm (i.e., from the occipital cortex to the pre-central gyri). On contrasting physiological signal with simulated noise (i.e., Noise + 10 Hz + 20Hz), we found a statistically significant cluster across the entire cortex. **B)** Probability density of APF, illustrating the distribution of APF shifts from the median APF of a parcel within the significant spatial cluster (between -10.5 cm and 0 cm).

values of the anteriorly located parcels (Fig. S5). Such that only ~7% of epochs were retained in the frontal cortices, whereas ~34% of epochs were retained in the occipital cortices. Notably, the linear increase in CV values along the posterior-to-anterior axis was still evident (R^2 = 0.359, p<0.001; Fig. S5).

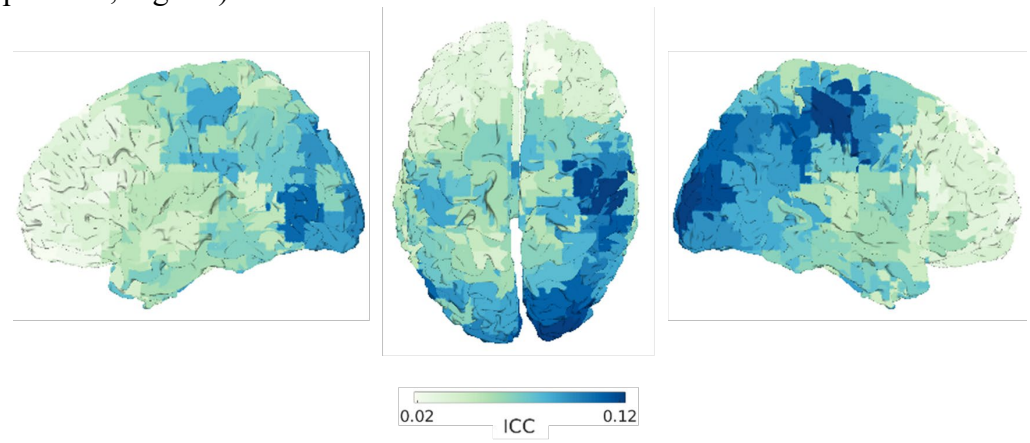

Figure 25. Estimates of Intra-Class Correlation (ICC)
ICC values of each parcel are projected on an MNI template brain. Lower estimates of ICC indicate poor reliability, whereas higher estimates are indicative of better reliability. Overall, APF shows poor reliability across the cortex reflecting substantial shifts in APF throughout. Distribution of APFs in the left lateral occipital cortex across participants (Fig. S6), show that low ICC values may reflect limited consistency within individuals and a lack of systematic differences between individuals. ICC estimates for 2-s (Fig. S7) and 5-s (Fig. S8) epochs reveal highest reliability in occipital regions and lowest in frontal regions.

ICC estimates at each of the parcels showed the highest reliability in right precentral (ICC = .121, 95% CI: .075-.216) and postcentral (ICC = .122, 95% CI: .075-.289) gyri, and the left lateral occipital cortex (ICC = .123, 95% CI: .076-.219). The right superior frontal gyrus (ICC = .018, 95% CI: .009-.040), and left middle frontal gyrus (ICC = .019, 95% CI: .010-.042; Fig. 25) had the lowest reliability. Overall, ICC values across the cortex were indicative of poor reliability of APF over epochs. The distribution of APFs in the left lateral occipital cortex of individual participants (Fig. S6) indicate that low ICC values may reflect both limited consistency within individuals and a lack of systematic differences between individuals. Despite averaging power over longer segments of time (2 s and 5 s), even regions with the highest ICC estimates (right lateral occipital cortex; ICC = 0.358, 95% CI: 0.244–0.531) fell short of having adequate reliability (i.e., ICC > 0.5) (Fig. S7; Fig. S8). Consistently across all epoch lengths, ICC estimates were highest in occipital regions and lowest in frontal regions.

Discussion

In recent years, alpha peak frequency (APF) has gained considerable attention as a potential marker of human cognition. On the one hand, APF is highly heritable and resistant to change over test-retest intervals, but on the other, it is extremely volatile and susceptible to changes in task demands and shifts in intrinsic states (Mierau et al., 2017). In the present study, we showed that such peak frequency transitions of APF occur at small timescales (i.e., within one second)

and the degree of variation in APF systematically increased from the caudal to rostral regions. We established that the observed fluctuations and the spatial gradient were not just an anomaly related to underlying noise. Further, we found that APFs show poor reliability across time over the entire cortex.

First and foremost, we confirmed that APF decreases along the posterior-to-anterior axis in a systematic fashion (in line with Mahjoory et al., 2020). The spatial gradient is governed by differences in the geometry of the cortex, in terms of cytoarchitecture and connectivity (Huntenburg et al., 2018), which in turn constrain the emergent dynamics (Demirtaş et al., 2019; Shafiei et al., 2023). The temporal dynamics of APF, however, has been largely overlooked. Therefore, we characterised the transient variations in APF to assess whether it more closely resembles a state- than a trait-marker. Our results illustrate that, not only APF, but also the degree of variation in APFs follows the posterior-to-anterior gradient, such that fluctuations in APFs exacerbates along this direction. This is in line with the findings of Salinsky et al., (1991) who provided evidence of variability on a similar timescale, but to a much smaller degree. Recent findings reveal that the APF shows temporal variations on a sub-second scale, evidently in the anterior regions (Smith et al., 2024), congruent with our findings. The temporal features of regional signals are likely governed by the anatomical and functional connectivity patterns with other cortical and subcortical regions. The caudal end of the gradient houses the lower sensorimotor functions, whereas the rostral end oversees higher cognitive functions. In effect, along the posterior-to-anterior direction, there is an increase in strength of synaptic excitation (Wang, 2020) and density of neurotransmitter receptors (Luppi et al., 2022), lengthening of timescales of information processing (Gao et al., 2020; Honey et al., 2012), and weakening of the coupling between structure and function (Larivière et al., 2020). By virtue of its neurobiological substrate, the rostral regions exhibit prolonged and flexible patterns of activity which complements its function, requiring the synergistic integration of diverse inputs (Suzuki et al., 2023). The results of our study are congruent in that respect. APF, reflecting intrinsic neural timescales, is higher in the caudal pole, whereas variations in APF, indexing input stochastics (Lefebvre et al., 2015) and neural malleability (Garrett et al., 2013), is higher in the rostral pole.

We found the signal-to-noise ratio (SNR) systematically decreased along the posterior-to-anterior axis, in relation to variations in APF. The alpha rhythm dominates the parieto-occipital region, whereas beta (13-30 Hz) and theta (4-8 Hz) oscillations are prominent in the sensorimotor and frontal regions, respectively (Groppe et al., 2013; Keitel & Gross, 2016). Due

to the variation in dominant peak frequency across the cortex, SNR varies on par. Given that low power precludes the true estimation of APF, the variation in APFs along the posterior-to-anterior axis may simply reflect an increment in noise/or a reduction in alpha power. However, if that were to be the case, we would not expect to see a gradient in the parieto-occipital region. We substantiated the variation in APFs along the gradient in comparison to noise, which was recorded from an empty magnetically shielded room. These findings reaffirm that there is a notable amount of variation in APFs from the occipital to the peri-central regions, following the gradient, which is not seen in empty-room noise. On adding a 10 Hz rhythm to empty-room noise, we found that the variation in empty room "APFs" was much lesser than APFs observed in the physiological data, despite matching the amplitude of the simulated alpha and beta rhythms. This leads us to believe that the variation in APFs did not arise from random fluctuations in measurement noise. In the frontal regions, however, the amount of variation was indistinguishable from non-neuronal noise, with the power of identified peaks being comparable to the spurious peaks observed in the empty-room data. Therefore, we cannot ascertain whether the degree of variation in the frontal regions is a manifestation of the intrinsic neural dynamics. Due to the highly variable dynamics of the frontal regions, it is advisable to exercise caution in conventional analyses, as estimates of alpha phase and coupling indices may also be distorted by poor SNR (Aru et al., 2015; Donoghue et al., 2022).

Further, we found that estimates of reliability, as indexed by intra-class correlations (ICC), were poor across the entire cortex in contrast to previous studies. A low ICC could be indicative of low degree of agreement between measurements (i.e., substantial variability in APFs over epochs) or a lack of difference in APFs between individuals (Koo & Li, 2016). Kondacs & Szabó (1999) showed that APF has excellent reliability on comparing odd and even epochs of the same EEG session. Another study found good reliability across two measurements, repeated over the span of 10 months (Gasser et al., 1985). However, this study included a sample of children, and as APFs and variability in neural signals changes over the course of development (Mišić et al., 2010), it does not offer a direct comparison. In addition, these studies used scalp recordings, which is inadequate to identify the sources of Alpha activity due to spatial mixing of signals (Schaworonkow & Nikulin, 2022). Notably, in our dataset, averaging power spectra over longer epochs drastically improved ICC estimates, but the observed values did not meet the threshold for adequate reliability (Koo & Li, 2016). Therefore, our findings challenge the reliability of APFs and suggest that it may not be a stable neurophysiological marker that qualifies as a trait.

Our results challenge the common assumption that APF represents a stable, trait-like characteristic—a premise that underlies many fixed-frequency stimulation protocols. Stimulation paradigms targeting anterior alpha oscillations may be particularly vulnerable to temporal variability, potentially failing to entrain neural oscillations. Furthermore, the dynamic nature of alpha activity raises critical concerns for closed-loop stimulation approaches. If the temporal resolution of such systems fails to capture the rapid shifts in endogenous oscillatory parameters, stimulation may be mismatched with the targeted neural dynamics, thereby compromising efficacy. In our study, participants were instructed to be seated such that the back of their head is leaning against the fixed helmet of the MEG; therefore, the occipital cortex lies closest to the SQUID sensor array, whereas the proximity of the frontal regions to the sensor array varies between individuals. As a result, the magnitude of the signal, in relation to background noise originating from non-neuronal sources, is much higher in the posterior regions. However, the low reliability of APFs cannot simply be attributed to measurement inaccuracies because despite good SNR, and a relatively low degree of variability in the occipital region, the ICC estimates were not adequate (Boutros et al., 1991). Moreover, since we only analysed datasets from a single measurement session, we cannot comment on the trait-likeliness of APF. Future studies would benefit from characterising the spatio-temporal variations in APF over multiple sessions.

In general, the spectral parameters of alpha oscillations appear to be non-stationary over time. Specifically, we showed that the degree of variation in APF increases along the posterior-to-anterior direction. From the occipital to the pericentral regions, the variation in APFs was evident in a substantial number of epochs, but still to a lesser extent than what is observed in empty-room measurements, suggesting that the observed gradient is not a feature of measurement noise. In the frontal regions, however, the degree of variation was indistinguishable from noise, which highlights the necessity to consider temporal variability and overall signal-to-noise ratio in the study of alpha oscillations. Further, the poor ICC estimates obtained in our data suggest that, depending on the timescale of the investigation, APF could transition rapidly, and to a similar extent across individuals, behaving more like a state than a trait.

5 GENERAL DISCUSSION

In the first study, we sought to alter oscillatory alpha activity in the right somatosensory cortex using short-period tACS. This was achieved by administering 10 s- and 30 s-trains of tACS and control (no-tACS) stimulation during simultaneous MEG recordings. We found that the increase in alpha power from pre-stimulation baseline levels was greater after tACS compared to the control condition. This increase was prominent in the bilateral somatosensory and frontal regions. Moreover, we found that 10 s-trains of tACS produced greater elevations in alpha power than 30 s-trains of tACS, suggesting that shorter stimulation durations are sufficient for modulating power at the stimulation frequency. Additionally, we split trials into equal-sized time bins to evaluate the evolution of power modulation with the number of tACS trains administered. We confirmed that short trains of stimulation produce concurrent and consistent changes in alpha power. We therefore established a valid stimulation protocol by which to modulate power within task-relevant timelines, for example, before stimulus presentation.

In the second study, we aimed to characterise spontaneous fluctuations in alpha peak frequency (APF) along the posterior-to-anterior cortical axis. This study was motivated by the limitations of Study 1, in which we failed to match stimulation frequency to individuals' APF for two-thirds of the participants. Guided by a recent publication showing a systematic reduction in APF from the caudal to rostral regions of the cortex, we hypothesised that the magnitude of fluctuations in APF would also vary along this cortical axis. To this end, we analysed resting-state data from the control condition of Study 1, in which no tACS was applied. Our results showed that APFs could vary from one second to the next to a great degree. Moreover, the magnitude of variation systematically exacerbated from the caudal to rostral regions such that, it was least in posterior-most occipital regions and greatest in the anterior-most frontal regions. We also confirmed that these fluctuations were not simply on account of measurement noise, by comparing it with pseudo-fluctuations of APFs in simulated data. Overall, the reliability estimates obtained from 1s epochs fell below the ideal threshold, suggesting that APFs more closely resemble a transient state rather than a stable trait.

Taken together, both studies demonstrate that alpha oscillations are highly volatile. In Study 1, we validated that they are susceptible to modulation of power via external perturbations, whereas in Study 2, we revealed that they exhibit fluctuations in frequency, even in the absence of stimulation. As such, both avenues of study indicate that the malleability of alpha oscillations is an inherent feature of its ongoing dynamics; in other words, alpha oscillations are invariably

variable. Yet the expression of this variability is not spatially uniform; instead, it could be shaped by cortical hierarchy and distribution of networks, as discussed below.

The power enhancement observed in Study 1 was not confined to the right-somatosensory cortex, which was the intended stimulation target. Instead, it extended bilaterally across somatosensory regions and, unexpectedly, into the frontal cortex, despite estimates of minimal electric field magnitudes in this region. Since any external perturbation, even with highly focal stimulation, inevitably propagates along anatomical and functional connections (Bergmann & Hartwigsen, 2021), such dispersion is not simply a methodological failure, but a consequence of the brain's integral architecture. Within this framework, the spatial profile of the tACS effects observed in Study 1 reflects not only the anatomical site of stimulation, but also that region's position within the cortical hierarchy and its connectivity to the broader network.

This points to the possibility that all cortical regions may not be equally susceptible to periodic perturbations. Propensity for malleability may be determined by the stimulation site's anatomical configuration such as folding, depth, and orientation (Huang et al., 2017; Opitz et al., 2015), which is in part shaped by its position along the cortical hierarchy. Modulation of the somatosensory cortex produces robust frequency-specific effects on tactile perception, as it is favourably positioned (Craddock et al., 2017; Fabbrini et al., 2022), and occipital alpha stimulation enhances visual learning when delivered over early visual areas with strong 10-Hz generators (He et al., 2022). In contrast, stimulation of less optimally oriented regions often yields attenuated or null effects due to limited laminar access and reduced local electric fields (Johnson et al., 2020; Manzo et al., 2020). Notably, primate electrophysiology shows that even modest shifts in electrode placement (of ~3–4 cm) abolishes single-neuron entrainment, underscoring the spatial specificity of tACS (Krause et al., 2019). These contrasts underscore that the propensity for perturbation and the activation of non-target areas may not be uniform across the cortex, but vary systematically with regional cytoarchitecture, resonance properties, and hierarchical network position.

Thus, one important dimension of Study 1 is that oscillatory perturbation extends beyond the stimulation site, reaching non-target regions in ways that appear to depend on the spatial organisation and connectivity of the cortical networks through which activity propagates. This spatial perspective sets the stage for understanding how location shapes not only the dispersion of induced activity, but also the intrinsic temporal dynamics of oscillatory signals themselves, which was observed in Study 2.

Although alpha activity is often conceptualised as an idle rhythm with stable oscillatory dynamics, computational work provides a mechanistic explanation for the existence of variability in frequency, as shown in Study 2. Lefebvre et al., (2015) demonstrated that a simple neural mass model generating stable alpha oscillations becomes spectrally nonstationary when it receives fluctuating synaptic input. Hutt et al., (2016) later extended this principle to a spiking network, showing that both stochastic noise and periodic external stimulation systematically accelerate alpha oscillations. Crucially, in both models, alpha frequency is not fixed to biophysical constants such as conduction delays; rather it is a dynamic variable that emerges from the interaction between the network's intrinsic architecture and the structure of its inputs. Moreover, intrinsic variability carries functional significance (Cohen, 2014). Fluctuations in oscillatory frequency modulate neural excitability, with slower alpha rhythms lowering spike thresholds, thereby improving the detection of weak synaptic inputs. Slower frequencies also yield more spikes per burst, expanding the analogue coding space and facilitating rapid reconfiguration of network dynamics. These models strengthen the plausibility of our results from Study 2 and support the claim that the temporal instability of alpha rhythms reflects genuine physiological processes rather than spurious fluctuations introduced by noise.

Recent work by Fehring et al., (2024) shows that intrinsic rhythms follow cortical hierarchy, contextualizing the effects observed in Study 2. Their results highlight that higher-order trans-modal regions display more variable and less periodic autocorrelation functions, reflecting inherently flexible, non-stationary temporal dynamics. Notably, they found that alpha-dependent periodicity, as reflected by autocorrelation at ~7–8 Hz, was strongest in occipital regions and systematically diminished with increasing hierarchical level. These findings reinforce that the posterior-to-anterior gradient found in Study 2 is not arbitrary, but might instead reflect the structural and functional organization of the cortical hierarchy.

Taken together, the two studies converge on a unifying insight: alpha rhythms propagate through, and are constrained by, the cortical hierarchy, with their susceptibility to tACS and their temporal variability governed by the same underlying hierarchical principles.

Limitations

A key limitation of Study 1 is the absence of a control stimulation frequency. We refrained from stimulating at a control frequency, as neural oscillators can be entrained not only at their intrinsic frequency, but also by harmonics or subharmonics. For example, Ali et al., (2013) demonstrated this mechanistically in a large-scale cortical model, showing that stimulation at a

harmonic frequency (6 Hz) entrained a network oscillating at 3 Hz, just as effectively as stimulation at its intrinsic frequency. Whereas, Helfrich et al., (2016) observed reduced alpha amplitude during 40 Hz tACS, showing cross-frequency interactions between alpha and gamma oscillations. Consequently, we cannot make definitive claims about the frequency specificity of the observed tACS effects.

In Study 2, we examined within-subject variability in APF, only in a single experimental session. This limited our ability to investigate the apparent trait-like stability of APF or lack thereof. It is possible that the administration of tACS enhanced the stability of power at the stimulation frequency; accordingly, it was necessary to restrict the analysis to data obtained during the control session. However, when considering the time-averaged APF estimates from Study 1 (Table S1), it is evident that APFs varied across stimulation blocks and between the tACS and control sessions.

Another limitation of Study 2 is that the empty-room data did not correspond to the exact dates on which the respective MEG recordings were acquired, which limits our ability to accurately capture the measurement noise conditions present during each recording session. Consequently, we compared shifts in APF between the physiological data and the empty-room data by treating them as independent groups rather than as paired (dependent) measures, which may have inflated or attenuated the apparent variability in the APF arising from session-specific non-neuronal noise fluctuations.

Outlook

The present findings raise the intriguing possibility that the magnitude of tACS-induced alpha modulation could be fundamentally constrained by the hierarchical position of the targeted cortical region. As demonstrated in Study 2, stimulation applied over somatosensory cortex interacts with a robust and periodic intrinsic alpha rhythm, whereas stimulation of higher-order associative regions would involve more broadband or variable rhythms. Future work should therefore systematically map how tACS influences oscillatory dynamics across the cortical hierarchy, probing whether regions differ in susceptibility to external modulations.

In Study 1, we found that the burst-like activity in the alpha band was enhanced by tACS, suggesting that externally applied rhythms may modulate not only the amplitude but also the stability and temporal regularity of intrinsic alpha events. This raises the possibility that tACS also alters the dynamics of spontaneous activity, potentially reducing variability in burst

timing, duration, or APF. Future studies will benefit from characterizing how rhythmic stimulation influences the spontaneous variability of oscillatory dynamics. Such work could reveal whether tACS primarily acts by entraining endogenous rhythms.

Beyond characterizing the neural effects, the validated stimulation protocol developed here provides a powerful tool for causal investigations into the role of alpha oscillations in perception and cognition. Future experiments could combine tACS with paradigms probing temporal integration, somatosensory discrimination, attentional gating, or multisensory integration to determine whether altering alpha dynamics predictably shifts behavioural thresholds or decision strategies.

Conclusions

In this thesis, I show that alpha oscillations are intrinsically dynamic rather than static rhythms. Study 1 demonstrates that somatosensory alpha activity is highly malleable even with stimulation trains as brief as 10 seconds. These effects extend further in space and frequency than what is commonly reported, and our findings point toward a multifaceted influence of tACS on alpha burst dynamics that warrants deeper investigation. Study 2, in turn, reveals that temporal variability, particularly fluctuations in peak frequency, is a fundamental property of alpha rhythms. Alpha frequency systematically shifts along the posterior–anterior axis in conjunction with changes in signal-to-noise ratio. This variability challenges assumptions built into many standard analytical approaches. In conclusion, the rhythms that shape our attention and perception are not fixed constraints, but flexible processes open to modulation.

6 REFERENCES

Abraham, W. C. (2008). Metaplasticity: Tuning synapses and networks for plasticity. *Nature Reviews Neuroscience*, *9*(5), 387–387. https://doi.org/10.1038/nrn2356

Ahn, S., Mellin, J. M., Alagapan, S., Alexander, M. L., Gilmore, J. H., Jarskog, L. F., & Fröhlich, F. (2019). Targeting reduced neural oscillations in patients with schizophrenia by transcranial alternating current stimulation. *NeuroImage*, *186*, 126–136. https://doi.org/10.1016/j.neuroimage.2018.10.056

Alamia, A., & VanRullen, R. (2019). Alpha oscillations and traveling waves: Signatures of predictive coding? *PLOS Biology*, *17*(10), e3000487. https://doi.org/10.1371/journal.pbio.3000487

Ali, M. M., Sellers, K. K., & Frohlich, F. (2013). Transcranial Alternating Current Stimulation Modulates Large-Scale Cortical Network Activity by Network Resonance. *Journal of Neuroscience*, *33*(27), Article 27. https://doi.org/10.1523/JNEUROSCI.5867-12.2013

Amzica, F., & Lopes da Silva, F. (2011). Cellular substrates of brain rhythms. *Niedermeyer's Electroencephalography: Basic Principles, Clinical Applications, and Related Fields*, *6*, 33–63.

Antal, A., Boros, K., Poreisz, C., Chaieb, L., Terney, D., & Paulus, W. (2008). Comparatively weak after-effects of transcranial alternating current stimulation (tACS) on cortical excitability in humans. *Brain Stimulation*, *1*(2), Article 2. https://doi.org/10.1016/j.brs.2007.10.001

Antal, A., & Herrmann, C. S. (2016). Transcranial Alternating Current and Random Noise Stimulation: Possible Mechanisms. *Neural Plasticity*, *2016*, 1–12. https://doi.org/10.1155/2016/3616807

Aru, Juhan, Aru, Jaan, Priesemann, V., Wibral, M., Lana, L., Pipa, G., Singer, W., & Vicente, R. (2015). Untangling cross-frequency coupling in neuroscience. *Current Opinion in Neurobiology*, *31*, 51–61. https://doi.org/10.1016/j.conb.2014.08.002

Asamoah, B., Khatoun, A., & Mc Laughlin, M. (2019). tACS motor system effects can be caused by transcutaneous stimulation of peripheral nerves. *Nature Communications*, *10*(1), Article 1. https://doi.org/10.1038/s41467-018-08183-w

Assaneo, M. F., & Orpella, J. (2024). Rhythms in Speech. In H. Merchant & V. De Lafuente (Eds), *Neurobiology of Interval Timing*, *1455*, 257–274. Springer International Publishing. https://doi.org/10.1007/978-3-031-60183-5_14

Averbeck, B. B., Latham, P. E., & Pouget, A. (2006). Neural correlations, population coding and computation. *Nature Reviews Neuroscience*, *7*(5), 358–366. https://doi.org/10.1038/nrn1888

Babu Henry Samuel, I., Wang, C., Hu, Z., & Ding, M. (2018). The frequency of alpha oscillations: Task-dependent modulation and its functional significance. *NeuroImage*, *183*, 897–906. https://doi.org/10.1016/j.neuroimage.2018.08.063

Bahramisharif, A., Van Gerven, M. A. J., Aarnoutse, E. J., Mercier, M. R., Schwartz, T. H., Foxe, J. J., Ramsey, N. F., & Jensen, O. (2013). Propagating Neocortical Gamma Bursts Are Coordinated by Traveling Alpha Waves. *The Journal of Neuroscience*, *33*(48), 18849–18854. https://doi.org/10.1523/JNEUROSCI.2455-13.2013

Baillet, S. (2017). Magnetoencephalography for brain electrophysiology and imaging. *Nature Neuroscience*, *20*(3), 327–339. https://doi.org/10.1038/nn.4504

Baillet, S., Mosher, J. C., & Leahy, R. M. (2001). Electromagnetic brain mapping. *IEEE Signal Processing Magazine*, *18*(6), 14–30. https://doi.org/10.1109/79.962275

Barnett, M. W., & Larkman, P. M. (2007). The action potential. *Practical Neurology*, *7*(3), 192.

Battaglini, L., Mena, F., Ghiani, A., Casco, C., Melcher, D., & Ronconi, L. (2020). The Effect of Alpha tACS on the Temporal Resolution of Visual Perception. *Frontiers in Psychology*, *11*, 1765. https://doi.org/10.3389/fpsyg.2020.01765

Baumgarten, T. J., Schnitzler, A., & Lange, J. (2016). Prestimulus Alpha Power Influences Tactile Temporal Perceptual Discrimination and Confidence in Decisions. *Cerebral Cortex*, *26*(3), 891–903. https://doi.org/10.1093/cercor/bhu247

Baumgarten, T. J., Wutz, A., & Samaha, J. (2023). Editorial: Peak frequencies in neural oscillatory activity and their connection to perception and cognition. *Frontiers in Psychology*, *14*, 1234955. https://doi.org/10.3389/fpsyg.2023.1234955

Benwell, C. S. Y., London, R. E., Tagliabue, C. F., Veniero, D., Gross, J., Keitel, C., & Thut, G. (2019). Frequency and power of human alpha oscillations drift systematically with time-on-task. *NeuroImage*, *192*, 101–114. https://doi.org/10.1016/j.neuroimage.2019.02.067

Berger, H. (1929). Über das elektroenkephalogramm des menschen. *Archiv Für Psychiatrie Und Nervenkrankheiten*, *87*(1), 527–570.

Bergmann, T. O., & Hartwigsen, G. (2021). Inferring Causality from Noninvasive Brain Stimulation in Cognitive Neuroscience. *Journal of Cognitive Neuroscience*, *33*(2), Article 2. https://doi.org/10.1162/jocn_a_01591

Bergmann, T. O., Karabanov, A., Hartwigsen, G., Thielscher, A., & Siebner, H. R. (2016). Combining non-invasive transcranial brain stimulation with neuroimaging and electrophysiology: Current approaches and future perspectives. *NeuroImage*, *140*, 4–19. https://doi.org/10.1016/j.neuroimage.2016.02.012

Bi, G., & Poo, M. (1998). Synaptic Modifications in Cultured Hippocampal Neurons: Dependence on Spike Timing, Synaptic Strength, and Postsynaptic Cell Type. *The Journal of Neuroscience*, *18*(24), 10464–10472. https://doi.org/10.1523/JNEUROSCI.18-24-10464.1998

Bishop, Geo. H. (1932). CYCLIC CHANGES IN EXCITABILITY OF THE OPTIC PATHWAY OF THE RABBIT. *American Journal of Physiology-Legacy Content*, *103*(1), 213–224. https://doi.org/10.1152/ajplegacy.1932.103.1.213

Boksem, M. A. S., Meijman, T. F., & Lorist, M. M. (2005). Effects of mental fatigue on attention: An ERP study. *Cognitive Brain Research*, *25*(1), 107–116. https://doi.org/10.1016/j.cogbrainres.2005.04.011

Bollimunta, A., Mo, J., Schroeder, C. E., & Ding, M. (2011). Neuronal Mechanisms and Attentional Modulation of Corticothalamic Alpha Oscillations. *The Journal of Neuroscience*, *31*(13), 4935–4943. https://doi.org/10.1523/JNEUROSCI.5580-10.2011

Bond, A., & Lader, M. (1974). The use of analogue scales in rating subjective feelings. *British Journal of Medical Psychology*, *47*(3), 211–218. https://doi.org/10.1111/j.2044-8341.1974.tb02285.x

Boutros, N. N., Overall, J., & Zouridakis, G. (1991). Test-retest reliability of the P50 mid-latency auditory evoked response. *Psychiatry Research*, *39*(2), 181–192. https://doi.org/10.1016/0165-1781(91)90086-5

Braboszcz, C., & Delorme, A. (2011). Lost in thoughts: Neural markers of low alertness during mind wandering. *NeuroImage*, *54*(4), 3040–3047. https://doi.org/10.1016/j.neuroimage.2010.10.008

Brus, J., Heng, J. A., Beliaeva, V., Gonzalez Pinto, F., Cassarà, A. M., Neufeld, E., Grueschow, M., Imbach, L., & Polanía, R. (2024). Causal phase-dependent control of non-spatial attention in human prefrontal cortex. *Nature Human Behaviour*, *8*(4), 743–757. https://doi.org/10.1038/s41562-024-01820-z

Burke, R., Maÿe, A., Misselhorn, J., Fiene, M., Engelhardt, F. J., Schneider, T. R., & Engel, A. K. (2025). The role of delta phase for temporal predictions investigated with bilateral parietal tACS. *Brain Stimulation*, *18*(1), 103–113. https://doi.org/10.1016/j.brs.2024.12.1476

Busch, N. A., Dubois, J., & VanRullen, R. (2009). The Phase of Ongoing EEG Oscillations Predicts Visual Perception. *Journal of Neuroscience*, *29*(24), 7869–7876. https://doi.org/10.1523/JNEUROSCI.0113-09.2009

Buzsáki, G., & Draguhn, A. (2004). Neuronal Oscillations in Cortical Networks. *Science*, *304*(5679), 1926–1929. https://doi.org/10.1126/science.1099745

Buzsáki, G., Lai-Wo S., L., & Vanderwolf, C. H. (1983). Cellular bases of hippocampal EEG in the behaving rat. *Brain Research Reviews*, *6*(2), 139–171. https://doi.org/10.1016/0165-0173(83)90037-1

Buzsáki, G., Logothetis, N., & Singer, W. (2013). Scaling Brain Size, Keeping Timing: Evolutionary Preservation of Brain Rhythms. *Neuron*, *80*(3), Article 3. https://doi.org/10.1016/j.neuron.2013.10.002

Buzsáki, G., & Wang, X.-J. (2012). Mechanisms of Gamma Oscillations. *Annual Review of Neuroscience*, *35*(1), 203–225. https://doi.org/10.1146/annurev-neuro-062111-150444

Cabrera-Álvarez, J., Sánchez-Claros, J., Carrasco-Gómez, M., Del Cerro-León, A., Gómez-Ariza, C. J., Maestú, F., Mirasso, C. R., & Susi, G. (2023). Understanding the effects of cortical gyrification in tACS: Insights from experiments and computational models. *Frontiers in Neuroscience*, *17*, 1223950. https://doi.org/10.3389/fnins.2023.1223950

Carlqvist, H., Nikulin, V. V., Strömberg, J. O., & Brismar, T. (2005). Amplitude and phase relationship between alpha and beta oscillations in the human electroencephalogram. *Medical & Biological Engineering & Computing*, *43*(5), 599–607. https://doi.org/10.1007/BF02351033

Cecere, R., Rees, G., & Romei, V. (2015). Individual Differences in Alpha Frequency Drive Crossmodal Illusory Perception. *Current Biology*, *25*(2), 231–235. https://doi.org/10.1016/j.cub.2014.11.034

Charvet, C. J., & Finlay, B. L. (2014). Evo-Devo and the Primate Isocortex: The Central Organizing Role of Intrinsic Gradients of Neurogenesis. *Brain, Behavior and Evolution*, *84*(2), 81–92. https://doi.org/10.1159/000365181

Clancy, K. J., Andrzejewski, J. A., You, Y., Rosenberg, J. T., Ding, M., & Li, W. (2022). Transcranial stimulation of alpha oscillations up-regulates the default mode network. *Proceedings of the National Academy of Sciences*, *119*(1), e2110868119. https://doi.org/10.1073/pnas.2110868119

Clarke, J. (2010). SQUIDs: THEN AND NOW. *International Journal of Modern Physics B*, *24*(20n21), 3999–4038. https://doi.org/10.1142/S0217979210056438

Clayton, M. S., Yeung, N., & Kadosh, R. C. (2015). The roles of cortical oscillations in sustained attention. *Trends in cognitive sciences*, *19*(4), 188-195. https://doi.org/10.1016/j.tics.2015.02.004

Cohen, D. (1972). Magnetoencephalography: Detection of the Brain's Electrical Activity with a Superconducting Magnetometer. *Science*, *175*(4022), 664–666. https://doi.org/10.1126/science.175.4022.664

Cohen, M. X. (2014). Fluctuations in Oscillation Frequency Control Spike Timing and Coordinate Neural Networks. *Journal of Neuroscience*, *34*(27), 8988–8998. https://doi.org/10.1523/JNEUROSCI.0261-14.2014

Cole, S. R., & Voytek, B. (2017). Brain Oscillations and the Importance of Waveform Shape. *Trends in Cognitive Sciences*, *21*(2), 137–149. https://doi.org/10.1016/j.tics.2016.12.008

Cotman, C. W., & McGaugh, J. L. (1980a). Basic Principles of Neuronal Signaling. *Behavioral Neuroscience*, 111–150. Elsevier. https://doi.org/10.1016/B978-0-12-191650-3.50009-X

Cotman, C. W., & McGaugh, J. L. (1980b). Synaptic Transmission. *Behavioral Neuroscience*, 151–208. Elsevier. https://doi.org/10.1016/B978-0-12-191650-3.50010-6

Craddock, M., Poliakoff, E., El-deredy, W., Klepousniotou, E., & Lloyd, D. M. (2017). Pre-stimulus alpha oscillations over somatosensory cortex predict tactile misperceptions. *Neuropsychologia*, *96*, 9–18. https://doi.org/10.1016/j.neuropsychologia.2016.12.030

Datta, A., Elwassif, M., Battaglia, F., & Bikson, M. (2008). Transcranial current stimulation focality using disc and ring electrode configurations: FEM analysis. *Journal of Neural Engineering*, *5*(2), 163–174. https://doi.org/10.1088/1741-2560/5/2/007

Dayan, P., & Abbott, L. F. (2005). *Theoretical neuroscience: Computational and mathematical modeling of neural systems*. MIT press.

De Koninck, B. P., Guay, S., Blais, H., & De Beaumont, L. (2021). Parametric study of transcranial alternating current stimulation for brain alpha power modulation. *Brain Communications*, *3*(2), Article 2. https://doi.org/10.1093/braincomms/fcab010

De Pesters, A., Coon, W. G., Brunner, P., Gunduz, A., Ritaccio, A. L., Brunet, N. M., De Weerd, P., Roberts, M. J., Oostenveld, R., Fries, P., & Schalk, G. (2016). Alpha power indexes task-related networks on large and small scales: A multimodal ECoG study in humans and a non-human primate. *NeuroImage*, *134*, 122–131. https://doi.org/10.1016/j.neuroimage.2016.03.074

Demirtaş, M., Burt, J. B., Helmer, M., Ji, J. L., Adkinson, B. D., Glasser, M. F., Van Essen, D. C., Sotiropoulos, S. N., Anticevic, A., & Murray, J. D. (2019). Hierarchical Heterogeneity across Human Cortex Shapes Large-Scale Neural Dynamics. *Neuron*, *101*(6), 1181-1194.e13. https://doi.org/10.1016/j.neuron.2019.01.017

Doesburg, S. M., Bedo, N., & Ward, L. M. (2016). Top-down alpha oscillatory network interactions during visuospatial attention orienting. *NeuroImage*, *132*, 512–519. https://doi.org/10.1016/j.neuroimage.2016.02.076

Donoghue, T., Haller, M., Peterson, E. J., Varma, P., Sebastian, P., Gao, R., Noto, T., Lara, A. H., Wallis, J. D., Knight, R. T., Shestyuk, A., & Voytek, B. (2020). Parameterizing neural power spectra into periodic and aperiodic components. *Nature Neuroscience*, *23*(12), 1655–1665. https://doi.org/10.1038/s41593-020-00744-x

Donoghue, T., Schaworonkow, N., & Voytek, B. (2022). Methodological considerations for studying neural oscillations. *European Journal of Neuroscience*, *55*(11–12), 3502–3527. https://doi.org/10.1111/ejn.15361

Drewes, J., Muschter, E., Zhu, W., & Melcher, D. (2022). Individual resting-state alpha peak frequency and within-trial changes in alpha peak frequency both predict visual dual-pulse segregation performance. *Cerebral Cortex*, *32*(23), 5455–5466. https://doi.org/10.1093/cercor/bhac026

Esghaei, M., Daliri, M. R., & Treue, S. (2018). Attention decouples action potentials from the phase of local field potentials in macaque visual cortical area MT. *BMC biology*, *16*(1), 86. https://doi.org/10.1186/s12915-018-0551-2

Fabbrini, A., Guerra, A., Giangrosso, M., Manzo, N., Leodori, G., Pasqualetti, P., Conte, A., Di Lazzaro, V., & Berardelli, A. (2022). Transcranial alternating current stimulation modulates cortical processing of somatosensory information in a frequency- and time-specific manner. *NeuroImage*, *254*, 119119. https://doi.org/10.1016/j.neuroimage.2022.119119

Fan, L., Li, H., Zhuo, J., Zhang, Y., Wang, J., Chen, L., Yang, Z., Chu, C., Xie, S., Laird, A. R., Fox, P. T., Eickhoff, S. B., Yu, C., & Jiang, T. (2016). The Human Brainnetome Atlas: A New Brain Atlas Based on Connectional Architecture. *Cerebral Cortex*, *26*(8), 3508–3526. https://doi.org/10.1093/cercor/bhw157

Fehring, J., Balestrieri, E., Focke, N., Dannlowski, U., Stier, C., & Gross, J. (2024). Neurophysiological correlates of cortical hierarchy across the lifespan. *bioRxiv*, 2024-27. https://doi.org/10.1101/2024.07.15.602693

Fiene, M., Radecke, J.-O., Misselhorn, J., Sengelmann, M., Herrmann, C. S., Schneider, T. R., Schwab, B. C., & Engel, A. K. (2022). tACS phase-specifically biases brightness perception of flickering light. *Brain Stimulation*, *15*(1), 244–253. https://doi.org/10.1016/j.brs.2022.01.001

Fries, P. (2005). A mechanism for cognitive dynamics: Neuronal communication through neuronal coherence. *Trends in Cognitive Sciences*, *9*(10), 474–480. https://doi.org/10.1016/j.tics.2005.08.011

Fries, P., Nikolić, D., & Singer, W. (2007). The gamma cycle. *Trends in Neurosciences*, *30*(7), 309–316. https://doi.org/10.1016/j.tins.2007.05.005

Fritsch, G., & Hitzig, E. (1870). The excitable cerebral cortex. Fritsch, G., Hitzig, E. Uber die elektrische Erregbarkeit des Grosshirns. *Arch. Anat. Physiol. Wissen*, *37*, 300–332.

Fröhlich, F., & McCormick, D. A. (2010). Endogenous Electric Fields May Guide Neocortical Network Activity. *Neuron*, *67*(1), 129–143. https://doi.org/10.1016/j.neuron.2010.06.005

Fuscà, M., Ruhnau, P., Neuling, T., & Weisz, N. (2018). Local Network-Level Integration Mediates Effects of Transcranial Alternating Current Stimulation. *Brain Connectivity*, *8*(4), 212–219. https://doi.org/10.1089/brain.2017.0564

Gao, R., Van Den Brink, R. L., Pfeffer, T., & Voytek, B. (2020). Neuronal timescales are functionally dynamic and shaped by cortical microarchitecture. *eLife*, *9*, e61277. https://doi.org/10.7554/eLife.61277

Garrett, D. D., Samanez-Larkin, G. R., MacDonald, S. W. S., Lindenberger, U., McIntosh, A. R., & Grady, C. L. (2013). Moment-to-moment brain signal variability: A next frontier in human brain mapping? *Neuroscience & Biobehavioral Reviews*, *37*(4), 610–624. https://doi.org/10.1016/j.neubiorev.2013.02.015

Gasser, T., Bächer, P., & Steinberg, H. (1985). Test-retest reliability of spectral parameters of the EEG. *Electroencephalography and Clinical Neurophysiology*, *60*(4), 312–319. https://doi.org/10.1016/0013-4694(85)90005-7

Geuzaine, C., & Remacle, J. (2009). Gmsh: A 3-D finite element mesh generator with built-in pre- and post-processing facilities. *International Journal for Numerical Methods in Engineering*, *79*(11), 1309–1331. https://doi.org/10.1002/nme.2579

Gould, I. C., Rushworth, M. F., & Nobre, A. C. (2011). Indexing the graded allocation of visuospatial attention using anticipatory alpha oscillations. *Journal of Neurophysiology*, *105*(3), 1318–1326. https://doi.org/10.1152/jn.00653.2010

Grandy, T. H., Werkle-Bergner, M., Chicherio, C., Schmiedek, F., Lövdén, M., & Lindenberger, U. (2013). Peak individual alpha frequency qualifies as a stable neurophysiological trait marker in healthy younger and older adults. *Psychophysiology*, *50*(6), Article 6. https://doi.org/10.1111/psyp.12043

Gray, C. M., & McCormick, D. A. (1996). Chattering Cells: Superficial Pyramidal Neurons Contributing to the Generation of Synchronous Oscillations in the Visual Cortex. *Science*, *274*(5284), 109–113. https://doi.org/10.1126/science.274.5284.109

Groppa, S., Oliviero, A., Eisen, A., Quartarone, A., Cohen, L. G., Mall, V., Kaelin-Lang, A., Mima, T., Rossi, S., Thickbroom, G. W., Rossini, P. M., Ziemann, U., Valls-Solé, J., & Siebner, H. R. (2012). A practical guide to diagnostic transcranial magnetic stimulation: Report of an IFCN committee. *Clinical Neurophysiology*, *123*(5), 858–882. https://doi.org/10.1016/j.clinph.2012.01.010

Groppe, D. M., Bickel, S., Keller, C. J., Jain, S. K., Hwang, S. T., Harden, C., & Mehta, A. D. (2013). Dominant frequencies of resting human brain activity as measured by the electrocorticogram. *NeuroImage*, *79*, 223–233. https://doi.org/10.1016/j.neuroimage.2013.04.044

Gross, J. (2019). Magnetoencephalography in Cognitive Neuroscience: A Primer. *Neuron*, *104*(2), 189–204. https://doi.org/10.1016/j.neuron.2019.07.001

Gundlach, C., Müller, M. M., Hoff, M., Ragert, P., Nierhaus, T., Villringer, A., & Sehm, B. (2020). Reduction of somatosensory functional connectivity by transcranial alternating current stimulation at endogenous mu-frequency. *NeuroImage*, *221*, 117175. https://doi.org/10.1016/j.neuroimage.2020.117175

Gundlach, C., Müller, M. M., Nierhaus, T., Villringer, A., & Sehm, B. (2016). Phasic Modulation of Human Somatosensory Perception by Transcranially Applied Oscillating Currents. *Brain Stimulation*, *9*(5), 712–719. https://doi.org/10.1016/j.brs.2016.04.014

Gundlach, C., Müller, M. M., Nierhaus, T., Villringer, A., & Sehm, B. (2017). Modulation of Somatosensory Alpha Rhythm by Transcranial Alternating Current Stimulation at Mu-Frequency. *Frontiers in Human Neuroscience*, *11*, 432. https://doi.org/10.3389/fnhum.2017.00432

Haegens, S., Barczak, A., Musacchia, G., Lipton, M. L., Mehta, A. D., Lakatos, P., & Schroeder, C. E. (2015). Laminar Profile and Physiology of the α Rhythm in Primary Visual, Auditory, and Somatosensory Regions of Neocortex. *The Journal of Neuroscience*, *35*(42), 14341–14352. https://doi.org/10.1523/JNEUROSCI.0600-15.2015

Haegens, S., Cousijn, H., Wallis, G., Harrison, P. J., & Nobre, A. C. (2014). Inter- and intra-individual variability in alpha peak frequency. *NeuroImage*, *92*, 46–55. https://doi.org/10.1016/j.neuroimage.2014.01.049

Haegens, S., Händel, B. F., & Jensen, O. (2011). Top-Down Controlled Alpha Band Activity in Somatosensory Areas Determines Behavioral Performance in a Discrimination Task. *The Journal of Neuroscience*, *31*(14), 5197–5204. https://doi.org/10.1523/JNEUROSCI.5199-10.2011

Haegens, S., Nácher, V., Luna, R., Romo, R., & Jensen, O. (2011). α-Oscillations in the monkey sensorimotor network influence discrimination performance by rhythmical inhibition of neuronal spiking. *Proceedings of the National Academy of Sciences*, *108*(48), 19377–19382. https://doi.org/10.1073/pnas.1117190108

Halbleib, A., Gratkowski, M., Schwab, K., Ligges, C., Witte, H., & Haueisen, J. (2012). Topographic Analysis of Engagement and Disengagement of Neural Oscillators in Photic Driving: A Combined Electroencephalogram/Magnetoencephalogram Study. *Journal of Clinical Neurophysiology*, *29*(1), 33–41. https://doi.org/10.1097/WNP.0b013e318246ad6e

Hallett, M. (2000). Transcranial magnetic stimulation and the human brain. *Nature*, *406*(6792), 147–150. https://doi.org/10.1038/35018000

Hallett, M. (2007). Transcranial Magnetic Stimulation: A Primer. *Neuron*, *55*(2), 187–199. https://doi.org/10.1016/j.neuron.2007.06.026

Hämäläinen, M., Hari, R., Ilmoniemi, R. J., Knuutila, J., & Lounasmaa, O. V. (1993). Magnetoencephalography—Theory, instrumentation, and applications to noninvasive studies of the working human brain. *Reviews of Modern Physics*, *65*(2), 413–497. https://doi.org/10.1103/RevModPhys.65.413

Hanslmayr, S., Matuschek, J., & Fellner, M.-C. (2014). Entrainment of Prefrontal Beta Oscillations Induces an Endogenous Echo and Impairs Memory Formation. *Current Biology*, *24*(8), 904–909. https://doi.org/10.1016/j.cub.2014.03.007

Hanslmayr, S., Volberg, G., Wimber, M., Dalal, S. S., & Greenlee, M. W. (2013). Prestimulus Oscillatory Phase at 7 Hz Gates Cortical Information Flow and Visual Perception. *Current Biology*, *23*(22), 2273–2278. https://doi.org/10.1016/j.cub.2013.09.020

Harada, T., Hara, M., Matsushita, K., Kawakami, Kenji, Kawakami, Keisuke, Anan, M., & Sugata, H. (2020). Off-line effects of alpha-frequency transcranial alternating current stimulation on a visuomotor learning task. *Brain and Behavior*, *10*(9), e01754. https://doi.org/10.1002/brb3.1754

Hari, R., Baillet, S., Barnes, G., Burgess, R., Forss, N., Gross, J., Hämäläinen, M., Jensen, O., Kakigi, R., Mauguière, F., Nakasato, N., Puce, A., Romani, G.-L., Schnitzler, A., & Taulu, S. (2018). IFCN-endorsed practical guidelines for clinical magnetoencephalography (MEG). *Clinical Neurophysiology*, *129*(8), 1720–1747. https://doi.org/10.1016/j.clinph.2018.03.042

Hari, R., & Puce, A. (2023). *MEG - EEG Primer* (2nd edn). Oxford University PressNew York. https://doi.org/10.1093/med/9780197542187.001.0001

Hari, R., & Salmelin, R. (2012). Magnetoencephalography: From SQUIDs to neuroscience. *NeuroImage*, *61*(2), 386–396. https://doi.org/10.1016/j.neuroimage.2011.11.074

Hari, R., Salmelin, R., Mäkelä, J. P., Salenius, S., & Helle, M. (1997). Magnetoencephalographic cortical rhythms. *International Journal of Psychophysiology*, *26*(1–3), 51–62. https://doi.org/10.1016/S0167-8760(97)00755-1

He, B. J., Snyder, A. Z., Zempel, J. M., Smyth, M. D., & Raichle, M. E. (2008). Electrophysiological correlates of the brain's intrinsic large-scale functional architecture. *Proceedings of the National Academy of Sciences*, *105*(41), 16039–16044. https://doi.org/10.1073/pnas.0807010105

He, Q., Yang, X.-Y., Gong, B., Bi, K., & Fang, F. (2022). Boosting visual perceptual learning by transcranial alternating current stimulation over the visual cortex at alpha frequency. *Brain Stimulation*, *15*(3), 546–553. https://doi.org/10.1016/j.brs.2022.02.018

Hebb, D. O. (1949). The first stage of perception: Growth of the assembly. *The Organization of Behavior*, *4*(60), 78–60.

Helfrich, R. F., Herrmann, C. S., Engel, A. K., & Schneider, T. R. (2016). Different coupling modes mediate cortical cross-frequency interactions. *NeuroImage*, *140*, 76–82. https://doi.org/10.1016/j.neuroimage.2015.11.035

Helfrich, Randolph F., Knepper, H., Nolte, G., Strüber, D., Rach, S., Herrmann, C. S., Schneider, T. R., & Engel, A. K. (2014). Selective Modulation of Interhemispheric Functional Connectivity by HD-tACS Shapes Perception. *PLoS Biology*, *12*(12), e1002031. https://doi.org/10.1371/journal.pbio.1002031

Helfrich, Randolph F., Schneider, T. R., Rach, S., Trautmann-Lengsfeld, S. A., Engel, A. K., & Herrmann, C. S. (2014). Entrainment of Brain Oscillations by Transcranial Alternating Current Stimulation. *Current Biology*, *24*(3), 333–339. https://doi.org/10.1016/j.cub.2013.12.041

Herrmann, C. S., Murray, M. M., Ionta, S., Hutt, A., & Lefebvre, J. (2016). Shaping Intrinsic Neural Oscillations with Periodic Stimulation. *The Journal of Neuroscience*, *36*(19), 5328–5337. https://doi.org/10.1523/JNEUROSCI.0236-16.2016

Hillebrand, A., & Barnes, G. R. (2005). Beamformer Analysis of MEG Data. In *International Review of Neurobiology, 68*, 149–171. Elsevier. https://doi.org/10.1016/S0074-7742(05)68006-3

Ho, K.-A., Taylor, J. L., Chew, T., Gálvez, V., Alonzo, A., Bai, S., Dokos, S., & Loo, C. K. (2016). The Effect of Transcranial Direct Current Stimulation (tDCS) Electrode Size and Current Intensity on Motor Cortical Excitability: Evidence From Single and Repeated Sessions. *Brain Stimulation*, *9*(1), 1–7. https://doi.org/10.1016/j.brs.2015.08.003

Honey, C. J., Thesen, T., Donner, T. H., Silbert, L. J., Carlson, C. E., Devinsky, O., Doyle, W. K., Rubin, N., Heeger, D. J., & Hasson, U. (2012). Slow Cortical Dynamics and the Accumulation of Information over Long Timescales. *Neuron*, *76*(2), 423–434. https://doi.org/10.1016/j.neuron.2012.08.011

Huang, Y., Liu, A. A., Lafon, B., Friedman, D., Dayan, M., Wang, X., Bikson, M., Doyle, W. K., Devinsky, O., & Parra, L. C. (2017). Measurements and models of electric fields in the in vivo human brain during transcranial electric stimulation. *eLife*, *6*, e18834. https://doi.org/10.7554/eLife.18834

Huntenburg, J. M., Bazin, P.-L., Goulas, A., Tardif, C. L., Villringer, A., & Margulies, D. S. (2017). A Systematic Relationship Between Functional Connectivity and Intracortical Myelin in the Human Cerebral Cortex. *Cerebral Cortex*, *27*(2), 981–997. https://doi.org/10.1093/cercor/bhx030

Huntenburg, J. M., Bazin, P.-L., & Margulies, D. S. (2018). Large-Scale Gradients in Human Cortical Organization. *Trends in Cognitive Sciences*, *22*(1), 21–31. https://doi.org/10.1016/j.tics.2017.11.002

Hutt, A., Mierau, A., & Lefebvre, J. (2016). Dynamic Control of Synchronous Activity in Networks of Spiking Neurons. *PLOS ONE*, *11*(9), e0161488. https://doi.org/10.1371/journal.pone.0161488

Jensen, O., Bonnefond, M., & VanRullen, R. (2012). An oscillatory mechanism for prioritizing salient unattended stimuli. *Trends in Cognitive Sciences*, *16*(4), 200–206. https://doi.org/10.1016/j.tics.2012.03.002

Jensen, O., & Colgin, L. L. (2007). Cross-frequency coupling between neuronal oscillations. *Trends in Cognitive Sciences*, *11*(7), 267–269. https://doi.org/10.1016/j.tics.2007.05.003

Jensen, O., & Mazaheri, A. (2010). Shaping Functional Architecture by Oscillatory Alpha Activity: Gating by Inhibition. *Frontiers in Human Neuroscience*, *4*. https://doi.org/10.3389/fnhum.2010.00186

Johnson, L., Alekseichuk, I., Krieg, J., Doyle, A., Yu, Y., Vitek, J., Johnson, M., & Opitz, A. (2020). Dose-dependent effects of transcranial alternating current stimulation on spike timing in awake nonhuman primates. *Science Advances*, *6*(36), eaaz2747. https://doi.org/10.1126/sciadv.aaz2747

Jones, S. R., Pritchett, D. L., Sikora, M. A., Stufflebeam, S. M., Hämäläinen, M., & Moore, C. I. (2009). Quantitative Analysis and Biophysically Realistic Neural Modeling of the MEG Mu Rhythm: Rhythmogenesis and Modulation of Sensory-Evoked Responses. *Journal of Neurophysiology*, *102*(6), 3554–3572. https://doi.org/10.1152/jn.00535.2009

Kasten, F. H., Dowsett, J., & Herrmann, C. S. (2016). Sustained Aftereffect of α-tACS Lasts Up to 70 min after Stimulation. *Frontiers in Human Neuroscience*, *10*. https://doi.org/10.3389/fnhum.2016.00245

Kasten, F. H., Duecker, K., Maack, M. C., Meiser, A., & Herrmann, C. S. (2019). Integrating electric field modeling and neuroimaging to explain inter-individual variability of tACS effects. *Nature Communications*, *10*(1), 5427. https://doi.org/10.1038/s41467-019-13417-6

Keitel, A., & Gross, J. (2016). Individual Human Brain Areas Can Be Identified from Their Characteristic Spectral Activation Fingerprints. *PLOS Biology*, *14*(6), e1002498. https://doi.org/10.1371/journal.pbio.1002498

Kemmerer, S. K., Sack, A. T., De Graaf, T. A., Ten Oever, S., De Weerd, P., & Schuhmann, T. (2020). Frequency-specific transcranial neuromodulation of oscillatory alpha power alters and predicts human visuospatial attention performance. *BioRxiv*, 2020-08. https://doi.org/10.1101/2020.08.04.236109

Khamechian, M. B., Daliri, M. R., Treue, S., & Esghaei, M. (2024). Coupled oscillations orchestrate selective information transmission in visual cortex. *PNAS Nexus*, *3*(8), pgae288. https://doi.org/10.1093/pnasnexus/pgae288

Klimesch, W. (1999). EEG alpha and theta oscillations reflect cognitive and memory performance: A review and analysis. *Brain Research Reviews*, *29*(2–3), 169–195. https://doi.org/10.1016/S0165-0173(98)00056-3

Klimesch, W. (2012). Alpha-band oscillations, attention, and controlled access to stored information. *Trends in Cognitive Sciences*, *16*(12), 606–617. https://doi.org/10.1016/j.tics.2012.10.007

Klimesch, W., Sauseng, P., & Hanslmayr, S. (2007). EEG alpha oscillations: The inhibition–timing hypothesis. *Brain Research Reviews*, *53*(1), Article 1. https://doi.org/10.1016/j.brainresrev.2006.06.003

Kluger, D. S., Balestrieri, E., Busch, N. A., & Gross, J. (2021). Respiration aligns perception with neural excitability. *eLife*, *10*, e70907. https://doi.org/10.7554/eLife.70907

Kondacs, A., & Szabó, M. (1999). Long-term intra-individual variability of the background EEG in normals. *Clinical Neurophysiology*, *110*(10), 1708–1716. https://doi.org/10.1016/S1388-2457(99)00122-4

Koo, T. K., & Li, M. Y. (2016). A Guideline of Selecting and Reporting Intraclass Correlation Coefficients for Reliability Research. *Journal of Chiropractic Medicine*, *15*(2), 155–163. https://doi.org/10.1016/j.jcm.2016.02.012

Krause, M. R., Vieira, P. G., Csorba, B. A., Pilly, P. K., & Pack, C. C. (2019). Transcranial alternating current stimulation entrains single-neuron activity in the primate brain. *Proceedings of the National Academy of Sciences*, *116*(12), 5747–5755. https://doi.org/10.1073/pnas.1815958116

Krause, M. R., Vieira, P. G., Thivierge, J.-P., & Pack, C. C. (2022). Brain stimulation competes with ongoing oscillations for control of spike timing in the primate brain. *PLOS Biology*, *20*(5), Article 5. https://doi.org/10.1371/journal.pbio.3001650

Lakatos, P., Gross, J., & Thut, G. (2019). A New Unifying Account of the Roles of Neuronal Entrainment. *Current Biology*, *29*(18), R890–R905. https://doi.org/10.1016/j.cub.2019.07.075

Lange, J., Oostenveld, R., & Fries, P. (2013). Reduced Occipital Alpha Power Indexes Enhanced Excitability Rather than Improved Visual Perception. *The Journal of Neuroscience*, *33*(7), 3212–3220. https://doi.org/10.1523/JNEUROSCI.3755-12.2013

Larivière, S., Vos De Wael, R., Hong, S.-J., Paquola, C., Tavakol, S., Lowe, A. J., Schrader, D. V., & Bernhardt, B. C. (2020). Multiscale Structure–Function Gradients in the Neonatal Connectome. *Cerebral Cortex*, *30*(1), 47–58. https://doi.org/10.1093/cercor/bhz069

Larkum, M. (2013). A cellular mechanism for cortical associations: An organizing principle for the cerebral cortex. *Trends in Neurosciences*, *36*(3), 141–151. https://doi.org/10.1016/j.tins.2012.11.006

Lefebvre, J., Hutt, A., Knebel, J.-F., Whittingstall, K., & Murray, M. M. (2015). Stimulus Statistics Shape Oscillations in Nonlinear Recurrent Neural Networks. *The Journal of Neuroscience*, *35*(7), 2895–2903. https://doi.org/10.1523/JNEUROSCI.3609-14.2015

Liang, H., Bressler, S. L., Ding, M., Truccolo, W. A., & Nakamura, R. (2002). Synchronized activity in prefrontal cortex during anticipation of visuomotor processing: *NeuroReport*, *13*(16), 2011–2015. https://doi.org/10.1097/00001756-200211150-00004

Lima, B., Singer, W., Chen, N.-H., & Neuenschwander, S. (2010). Synchronization dynamics in response to plaid stimuli in monkey V1. *Cerebral Cortex*, *20*(7), 1556–1573. https://doi.org/10.1093/cercor/bhp218

Lindsley, D. B. (1939). A Longitudinal Study of the Occipital Alpha Rhythm in Normal Children: Frequency and Amplitude Standards. *The Pedagogical Seminary and Journal of Genetic Psychology*, *55*(1), 197–213. https://doi.org/10.1080/08856559.1939.10533190

Lopes Da Silva, F. H., Hoeks, A., Smits, H., & Zetterberg, L. H. (1974). Model of brain rhythmic activity: The alpha-rhythm of the thalamus. *Kybernetik*, *15*(1), 27–37. https://doi.org/10.1007/BF00270757

Lopes Da Silva, F. H., Van Lierop, T. H. M. T., Schrijer, C. F., & Storm Van Leeuwen, W. (1973). Organization of thalamic and cortical alpha rhythms: Spectra and coherences. *Electroencephalography and Clinical Neurophysiology*, *35*(6), 627–639. https://doi.org/10.1016/0013-4694(73)90216-2

Lopes da Silva, F. (2013). EEG and MEG: Relevance to Neuroscience. *Neuron*, *80*(5), 1112–1128. https://doi.org/10.1016/j.neuron.2013.10.017

Luczak, A., Bartho, P., & Harris, K. D. (2013). Gating of Sensory Input by Spontaneous Cortical Activity. *The Journal of Neuroscience*, *33*(4), 1684–1695. https://doi.org/10.1523/JNEUROSCI.2928-12.2013

Lundqvist, M., Herman, P., & Lansner, A. (2013). Effect of Prestimulus Alpha Power, Phase, and Synchronization on Stimulus Detection Rates in a Biophysical Attractor Network Model. *Journal of Neuroscience*, *33*(29), 11817–11824. https://doi.org/10.1523/JNEUROSCI.5155-12.2013

Luppi, A. I., Mediano, P. A. M., Rosas, F. E., Holland, N., Fryer, T. D., O'Brien, J. T., Rowe, J. B., Menon, D. K., Bor, D., & Stamatakis, E. A. (2022). A synergistic core for human brain evolution and cognition. *Nature Neuroscience*, *25*(6), 771–782. https://doi.org/10.1038/s41593-022-01070-0

Mahjoory, K., Schoffelen, J.-M., Keitel, A., & Gross, J. (2020). The frequency gradient of human resting-state brain oscillations follows cortical hierarchies. *eLife*, *9*, e53715. https://doi.org/10.7554/eLife.53715

Makeig, S., & Inlow, M. (1993). Lapse in alertness: Coherence of fluctuations in performance and EEG spectrum. *Electroencephalography and Clinical Neurophysiology*, *86*(1), 23–35. https://doi.org/10.1016/0013-4694(93)90064-3

Maldonado, P., Babul, C., Singer, W., Rodriguez, E., Berger, D., & Grün, S. (2008). Synchronization of Neuronal Responses in Primary Visual Cortex of Monkeys Viewing Natural Images. *Journal of Neurophysiology*, *100*(3), 1523–1532. https://doi.org/10.1152/jn.00076.2008

Manzo, N., Guerra, A., Giangrosso, M., Belvisi, D., Leodori, G., Berardelli, A., & Conte, A. (2020). Investigating the effects of transcranial alternating current stimulation on primary somatosensory cortex. *Scientific Reports*, *10*(1), 17129. https://doi.org/10.1038/s41598-020-74072-2

Maris, E., & Oostenveld, R. (2007). Nonparametric statistical testing of EEG- and MEG-data. *Journal of Neuroscience Methods*, *164*(1), 177–190. https://doi.org/10.1016/j.jneumeth.2007.03.024

Masquelier, T., Hugues, E., Deco, G., & Thorpe, S. J. (2009). Oscillations, Phase-of-Firing Coding, and Spike Timing-Dependent Plasticity: An Efficient Learning Scheme. *The Journal of Neuroscience*, *29*(43), 13484–13493. https://doi.org/10.1523/JNEUROSCI.2207-09.2009

Mathewson, K. E., Gratton, G., Fabiani, M., Beck, D. M., & Ro, T. (2009). To See or Not to See: Prestimulus α Phase Predicts Visual Awareness. *The Journal of Neuroscience*, *29*(9), Article 9. https://doi.org/10.1523/JNEUROSCI.3963-08.2009

McGraw, K. O., & Wong, S. P. (1996). Forming inferences about some intraclass correlation coefficients. *Psychological Methods*, *1*(1), 30–46. https://doi.org/10.1037/1082-989X.1.1.30

Mehta, A. R., Pogosyan, A., Brown, P., & Brittain, J.-S. (2015). Montage Matters: The Influence of Transcranial Alternating Current Stimulation on Human Physiological Tremor. *Brain Stimulation*, *8*(2), 260–268. https://doi.org/10.1016/j.brs.2014.11.003

Mellem, M. S., Wohltjen, S., Gotts, S. J., Ghuman, A. S., & Martin, A. (2017). Intrinsic frequency biases and profiles across human cortex. *Journal of Neurophysiology*, *118*(5), 2853–2864. https://doi.org/10.1152/jn.00061.2017

Michalareas, G., Vezoli, J., van Pelt, S., Schoffelen, J.-M., Kennedy, H., & Fries, P. (2016). Alpha-Beta and Gamma Rhythms Subserve Feedback and Feedforward Influences among Human Visual Cortical Areas. *Neuron*, *89*(2), 384–397. https://doi.org/10.1016/j.neuron.2015.12.018

Mierau, A., Klimesch, W., & Lefebvre, J. (2017). State-dependent alpha peak frequency shifts: Experimental evidence, potential mechanisms and functional implications. *Neuroscience*, *360*, 146–154. https://doi.org/10.1016/j.neuroscience.2017.07.037

Mišić, B., Mills, T., Taylor, M. J., & McIntosh, A. R. (2010). Brain Noise Is Task Dependent and Region Specific. *Journal of Neurophysiology*, *104*(5), 2667–2676. https://doi.org/10.1152/jn.00648.2010

Monte-Silva, K., Kuo, M.-F., Hessenthaler, S., Fresnoza, S., Liebetanz, D., Paulus, W., & Nitsche, M. A. (2013). Induction of Late LTP-Like Plasticity in the Human Motor Cortex by Repeated Non-Invasive Brain Stimulation. *Brain Stimulation*, *6*(3), 424–432. https://doi.org/10.1016/j.brs.2012.04.011

Mosayebi Samani, M., Agboada, D., Jamil, A., Kuo, M.-F., & Nitsche, M. A. (2019). Titrating the neuroplastic effects of cathodal transcranial direct current stimulation (tDCS) over the primary motor cortex. *Cortex*, *119*, 350–361. https://doi.org/10.1016/j.cortex.2019.04.016

Neuling, T., Rach, S., & Herrmann, C. S. (2013). Orchestrating neuronal networks: Sustained after-effects of transcranial alternating current stimulation depend upon brain states. *Frontiers in Human Neuroscience*, *7*. https://doi.org/10.3389/fnhum.2013.00161

Nikulin, V. V., & Brismar, T. (2006). Phase synchronization between alpha and beta oscillations in the human electroencephalogram. *Neuroscience*, *137*(2), 647–657. https://doi.org/10.1016/j.neuroscience.2005.10.031

Nitsche, M. A., & Paulus, W. (2000). Excitability changes induced in the human motor cortex by weak transcranial direct current stimulation. *The Journal of Physiology*, *527*(3), 633–639. https://doi.org/10.1111/j.1469-7793.2000.t01-1-00633.x

Nolte, G. (2003). The magnetic lead field theorem in the quasi-static approximation and its use for magnetoencephalography forward calculation in realistic volume conductors. *Physics in Medicine and Biology*, *48*(22), 3637–3652. https://doi.org/10.1088/0031-9155/48/22/002

Noury, N., Hipp, J. F., & Siegel, M. (2016). Physiological processes non-linearly affect electrophysiological recordings during transcranial electric stimulation. *NeuroImage*, *140*, 99–109. https://doi.org/10.1016/j.neuroimage.2016.03.065

Nunez, P. L., & Srinivasan, R. (2006). *Electric fields of the brain: The neurophysics of EEG*. Oxford university press.

Oken, B. S., Salinsky, M. C., & Elsas, S. M. (2006). Vigilance, alertness, or sustained attention: Physiological basis and measurement. *Clinical Neurophysiology*, *117*(9), 1885–1901. https://doi.org/10.1016/j.clinph.2006.01.017

Oostenveld, R., Fries, P., Maris, E., & Schoffelen, J.-M. (2011). FieldTrip: Open Source Software for Advanced Analysis of MEG, EEG, and Invasive Electrophysiological Data. *Computational Intelligence and Neuroscience*, *2011*, 1–9. https://doi.org/10.1155/2011/156869

Opitz, A., Paulus, W., Will, S., Antunes, A., & Thielscher, A. (2015). Determinants of the electric field during transcranial direct current stimulation. *NeuroImage*, *109*, 140–150. https://doi.org/10.1016/j.neuroimage.2015.01.033

Opitz, A., Windhoff, M., Heidemann, R. M., Turner, R., & Thielscher, A. (2011). How the brain tissue shapes the electric field induced by transcranial magnetic stimulation. *NeuroImage*, *58*(3), 849–859. https://doi.org/10.1016/j.neuroimage.2011.06.069

Osipova, D., Hermes, D., & Jensen, O. (2008). Gamma Power Is Phase-Locked to Posterior Alpha Activity. *PLoS ONE*, *3*(12), e3990. https://doi.org/10.1371/journal.pone.0003990

Ozen, S., Sirota, A., Belluscio, M. A., Anastassiou, C. A., Stark, E., Koch, C., & Buzsáki, G. (2010). Transcranial Electric Stimulation Entrains Cortical Neuronal Populations in Rats. *The Journal of Neuroscience*, *30*(34), 11476–11485. https://doi.org/10.1523/JNEUROSCI.5252-09.2010

Palva, J. M., Monto, S., Kulashekhar, S., & Palva, S. (2010). Neuronal synchrony reveals working memory networks and predicts individual memory capacity. *Proceedings of the National Academy of Sciences*, *107*(16), 7580–7585. https://doi.org/10.1073/pnas.0913113107

Palva, J. M., & Palva, S. (2018). Functional integration across oscillation frequencies by cross-frequency phase synchronization. *European Journal of Neuroscience*, *48*(7), 2399–2406. https://doi.org/10.1111/ejn.13767

Palva, J. M., Palva, S., & Kaila, K. (2005). Phase Synchrony among Neuronal Oscillations in the Human Cortex. *The Journal of Neuroscience*, *25*(15), 3962–3972. https://doi.org/10.1523/JNEUROSCI.4250-04.2005

Palva, S., & Palva, J. M. (2007). New vistas for α-frequency band oscillations. *Trends in Neurosciences*, *30*(4), 150–158. https://doi.org/10.1016/j.tins.2007.02.001

Palva, S., & Palva, J. M. (2011). Functional Roles of Alpha-Band Phase Synchronization in Local and Large-Scale Cortical Networks. *Frontiers in Psychology*, *2*. https://doi.org/10.3389/fpsyg.2011.00204

Paulus, W. (2011). Transcranial electrical stimulation (tES – tDCS; tRNS, tACS) methods. *Neuropsychological Rehabilitation*, *21*(5), 602–617. https://doi.org/10.1080/09602011.2011.557292

Pfurtscheller, G., Stancák, A., & Neuper, Ch. (1996). Event-related synchronization (ERS) in the alpha band — an electrophysiological correlate of cortical idling: A review. *International Journal of Psychophysiology*, *24*(1–2), 39–46. https://doi.org/10.1016/S0167-8760(96)00066-9

Pikovsky, A., Kurths, J., & Rosenblum, M. (2001). *Synchronization: A universal concept in nonlinear sciences*. Cambridge University Press.

Pikovsky, A., Rosenblum, M., Kurths, J., & Hilborn, R. C. (2002). *Synchronization: A Universal Concept in Nonlinear Science*. *American Journal of Physics*, *70*(6), 655–655. https://doi.org/10.1119/1.1475332

Posthuma, D., Neale, M. C., Boomsma, D. I., & De Geus, E. J. C. (2001). [No title found]. *Behavior Genetics*, *31*(6), 567–579. https://doi.org/10.1023/A:1013345411774

Purves, D. (Ed.). (2008). *Neuroscience* (4th ed). Sinauer.

Ray, S., & Maunsell, J. H. R. (2010). Differences in Gamma Frequencies across Visual Cortex Restrict Their Possible Use in Computation. *Neuron*, *67*(5), 885–896. https://doi.org/10.1016/j.neuron.2010.08.004

Ray, S., & Maunsell, J. H. R. (2015). Do gamma oscillations play a role in cerebral cortex? *Trends in Cognitive Sciences*, *19*(2), 78–85. https://doi.org/10.1016/j.tics.2014.12.002

Rohenkohl, G., & Nobre, A. C. (2011). Alpha Oscillations Related to Anticipatory Attention Follow Temporal Expectations. *The Journal of Neuroscience*, *31*(40), 14076–14084. https://doi.org/10.1523/JNEUROSCI.3387-11.2011

Ruhnau, P., Neuling, T., Fuscá, M., Herrmann, C. S., Demarchi, G., & Weisz, N. (2016). Eyes wide shut: Transcranial alternating current stimulation drives alpha rhythm in a state dependent manner. *Scientific Reports*, *6*(1), Article 1. https://doi.org/10.1038/srep27138

Saalmann, Y. B., Pinsk, M. A., Wang, L., Li, X., & Kastner, S. (2012). The Pulvinar Regulates Information Transmission Between Cortical Areas Based on Attention Demands. *Science*, *337*(6095), 753–756. https://doi.org/10.1126/science.1223082

Sadaghiani, S., & Kleinschmidt, A. (2016). Brain Networks and α-Oscillations: Structural and Functional Foundations of Cognitive Control. *Trends in Cognitive Sciences*, *20*(11), 805–817. https://doi.org/10.1016/j.tics.2016.09.004

Saito, K., Otsuru, N., Yokota, H., Inukai, Y., Miyaguchi, S., Kojima, S., & Onishi, H. (2021). α-tACS over the somatosensory cortex enhances tactile spatial discrimination in healthy subjects with low alpha activity. *Brain and Behavior*, *11*(3), Article 3. https://doi.org/10.1002/brb3.2019

Salarian, A. (2016). *„MATLAB Central File Exchange. Intraclass Correlation Coefficient (ICC),”*.

Salinsky, M. C., Oken, B. S., & Morehead, L. (1991). Test-retest reliability in EEG frequency analysis. *Electroencephalography and Clinical Neurophysiology*, *79*(5), 382–392. https://doi.org/10.1016/0013-4694(91)90203-G

Samaha, J., Bauer, P., Cimaroli, S., & Postle, B. R. (2015). Top-down control of the phase of alpha-band oscillations as a mechanism for temporal prediction. *Proceedings of the National Academy of Sciences*, *112*(27), 8439–8444. https://doi.org/10.1073/pnas.1503686112

Samaha, J., & Postle, B. R. (2015). The Speed of Alpha-Band Oscillations Predicts the Temporal Resolution of Visual Perception. *Current Biology*, *25*(22), Article 22. https://doi.org/10.1016/j.cub.2015.10.007

Saturnino, G. B., Puonti, O., Nielsen, J. D., Antonenko, D., Madsen, K. H. H., & Thielscher, A. (2018). *SimNIBS 2.1: A Comprehensive Pipeline for Individualized Electric Field Modelling for Transcranial Brain Stimulation*. https://doi.org/10.1101/500314

Sauseng, P., Klimesch, W., Doppelmayr, M., Pecherstorfer, T., Freunberger, R., & Hanslmayr, S. (2005). EEG alpha synchronization and functional coupling during top-down processing in a working memory task. *Human Brain Mapping*, *26*(2), 148–155. https://doi.org/10.1002/hbm.20150

Schaworonkow, N. (2023). Overcoming harmonic hurdles: genuine beta-band rhythms vs. contributions of alpha-band waveform shape. *Imaging Neuroscience*, *1*, 1-8. https://doi.org/10.1162/imag_a_00018

Schaworonkow, N., & Nikulin, V. V. (2022). Is sensor space analysis good enough? Spatial patterns as a tool for assessing spatial mixing of EEG/MEG rhythms. *NeuroImage*, *253*, 119093. https://doi.org/10.1016/j.neuroimage.2022.119093

Schoffelen, J.-M., Pesci, U. G., & Noppeney, U. (2024). Alpha Oscillations and Temporal Binding Windows in Perception—A Critical Review and Best Practice Guidelines. *Journal of Cognitive Neuroscience*, *36*(4), 655–690. https://doi.org/10.1162/jocn_a_02118

Schubert, C., Dabbagh, A., Classen, J., Krämer, U. M., & Tzvi, E. (2021). Alpha oscillations modulate premotor-cerebellar connectivity in motor learning: Insights from transcranial alternating current stimulation. *Neuroimage*, *241*, 118410. https://doi.org/10.1016/j.neuroimage.2021.118410

Schuhmann, T., Kemmerer, S. K., Duecker, F., De Graaf, T. A., Ten Oever, S., De Weerd, P., & Sack, A. T. (2019). Left parietal tACS at alpha frequency induces a shift of visuospatial attention. *PLOS ONE*, *14*(11), e0217729. https://doi.org/10.1371/journal.pone.0217729

Schwab, B. C., König, P., & Engel, A. K. (2021). Spike-timing-dependent plasticity can account for connectivity aftereffects of dual-site transcranial alternating current stimulation. *NeuroImage*, *237*, 118179. https://doi.org/10.1016/j.neuroimage.2021.118179

Schwab, B. C., Misselhorn, J., & Engel, A. K. (2019). Modulation of large-scale cortical coupling by transcranial alternating current stimulation. *Brain Stimulation*, *12*(5), 1187–1196. https://doi.org/10.1016/j.brs.2019.04.013

Shafiei, G., Fulcher, B. D., Voytek, B., Satterthwaite, T. D., Baillet, S., & Misic, B. (2023). Neurophysiological signatures of cortical micro-architecture. *Nature Communications*, *14*(1), 6000. https://doi.org/10.1038/s41467-023-41689-6

Sharp, P., Gutteling, T., Melcher, D., & Hickey, C. (2022). Spatial attention tunes temporal processing in early visual cortex by speeding and slowing alpha oscillations. *The Journal of Neuroscience*, *42*(41), 7824-7832. https://doi.org/10.1523/JNEUROSCI.0509-22.2022

Sherman, M. A., Lee, S., Law, R., Haegens, S., Thorn, C. A., Hämäläinen, M. S., Moore, C. I., & Jones, S. R. (2016). Neural mechanisms of transient neocortical beta rhythms: Converging evidence from humans, computational modeling, monkeys, and mice. *Proceedings of the National Academy of Sciences*, *113*(33). https://doi.org/10.1073/pnas.1604135113

Sherman, M. T., Kanai, R., Seth, A. K., & VanRullen, R. (2016). Rhythmic Influence of Top–Down Perceptual Priors in the Phase of Prestimulus Occipital Alpha Oscillations. *Journal of Cognitive Neuroscience*, *28*(9), 1318–1330. https://doi.org/10.1162/jocn_a_00973

Shrout, P. E., & Fleiss, J. L. (1979). Intraclass correlations: Uses in assessing rater reliability. *Psychological Bulletin*, *86*(2), 420–428. https://doi.org/10.1037/0033-2909.86.2.420

Singer, W. (1993). Synchronization of Cortical Activity and its Putative Role in Information Processing and Learning. *Annual Review of Physiology*, *55*(1), 349–374. https://doi.org/10.1146/annurev.ph.55.030193.002025

Singer, W. (1999). Neuronal Synchrony: A Versatile Code for the Definition of Relations? *Neuron*, *24*(1), 49–65. https://doi.org/10.1016/S0896-6273(00)80821-1

Singer, W. (2018). Neuronal oscillations: Unavoidable and useful? *European Journal of Neuroscience*, *48*(7), 2389–2398. https://doi.org/10.1111/ejn.13796

Singer, W., & Gray, C. M. (1995). Visual Feature Integration and the Temporal Correlation Hypothesis. *Annual Review of Neuroscience*, *18*(1), 555–586. https://doi.org/10.1146/annurev.ne.18.030195.003011

Sliva, D. D., Black, C. J., Bowary, P., Agrawal, U., Santoyo, J. F., Philip, N. S., Greenberg, B. D., Moore, C. I., & Jones, S. R. (2018). A Prospective Study of the Impact of Transcranial Alternating Current Stimulation on EEG Correlates of Somatosensory Perception. *Frontiers in Psychology*, *9*, 2117. https://doi.org/10.3389/fpsyg.2018.02117

Smit, C. M., Wright, M. J., Hansell, N. K., Geffen, G. M., & Martin, N. G. (2006). Genetic variation of individual alpha frequency (IAF) and alpha power in a large adolescent twin sample. *International Journal of Psychophysiology*, *61*(2), 235–243. https://doi.org/10.1016/j.ijpsycho.2005.10.004

Smith, M. K., Grabowekcy, M., & Suzuki, S. (2024). Dynamic formation of a posterior-to-anterior peak-alpha-frequency gradient driven by two distinct processes. *eneuro 11*(8). https://doi.org/10.1101/2024.01.31.578276

So, P. P. M., Stuchly, M. A., & Nyenhuis, J. A. (2004). Peripheral Nerve Stimulation by Gradient Switching Fields in Magnetic Resonance Imaging. *IEEE Transactions on Biomedical Engineering*, *51*(11), 1907–1914. https://doi.org/10.1109/TBME.2004.834251

Stecher, H. I., & Herrmann, C. S. (2018). Absence of Alpha-tACS Aftereffects in Darkness Reveals Importance of Taking Derivations of Stimulation Frequency and Individual Alpha Variability Into Account. *Frontiers in Psychology*, *9*, 984. https://doi.org/10.3389/fpsyg.2018.00984

Stecher, H. I., Notbohm, A., Kasten, F. H., & Herrmann, C. S. (2021). A Comparison of Closed Loop vs. Fixed Frequency tACS on Modulating Brain Oscillations and Visual Detection. *Frontiers in Human Neuroscience*, *15*, 661432. https://doi.org/10.3389/fnhum.2021.661432

Stonkus, R., Braun, V., Kerlin, J. R., Volberg, G., & Hanslmayr, S. (2016). Probing the causal role of prestimulus interregional synchrony for perceptual integration via tACS. *Scientific Reports*, *6*(1), 32065. https://doi.org/10.1038/srep32065

Strüber, D., Rach, S., Neuling, T., & Herrmann, C. S. (2015). On the possible role of stimulation duration for after-effects of transcranial alternating current stimulation. *Frontiers in Cellular Neuroscience*, *9*. https://doi.org/10.3389/fncel.2015.00311

Supek, S., & Aine, C. J. (Eds). (2019). *Magnetoencephalography: From Signals to Dynamic Cortical Networks*. Springer International Publishing. https://doi.org/10.1007/978-3-030-00087-5

Suzuki, S., Grabowecky, M., & Menceloglu, M. (2023). Characteristics of spontaneous anterior-posterior oscillation-frequency convergences in the alpha band. *eneuro, 12*(3). https://doi.org/10.1101/2023.09.12.557455

Tallon-Baudry, C. (1999). Oscillatory gamma activity in humans and its role in object representation. *Trends in Cognitive Sciences*, *3*(4), 151–162. https://doi.org/10.1016/S1364-6613(99)01299-1

Thielscher, A., Antunes, A., & Saturnino, G. B. (2015). Field modeling for transcranial magnetic stimulation: A useful tool to understand the physiological effects of TMS? *2015 37th Annual International Conference of the IEEE Engineering in Medicine and Biology Society (EMBC)*, 222–225. https://doi.org/10.1109/EMBC.2015.7318340

Tröndle, M., Popov, T., Pedroni, A., Pfeiffer, C., Barańczuk-Turska, Z., & Langer, N. (2023). Decomposing age effects in EEG alpha power. *Cortex*, *161*, 116–144. https://doi.org/10.1016/j.cortex.2023.02.002

Tzourio-Mazoyer, N., Landeau, B., Papathanassiou, D., Crivello, F., Etard, O., Delcroix, N., Mazoyer, B., & Joliot, M. (2002). Automated Anatomical Labeling of Activations in SPM Using a Macroscopic Anatomical Parcellation of the MNI MRI Single-Subject Brain. *NeuroImage*, *15*(1), 273–289. https://doi.org/10.1006/nimg.2001.0978

Van Diepen, R. M., Foxe, J. J., & Mazaheri, A. (2019). The functional role of alpha-band activity in attentional processing: The current zeitgeist and future outlook. *Current Opinion in Psychology*, *29*, 229–238. https://doi.org/10.1016/j.copsyc.2019.03.015

Van Dijk, H., Schoffelen, J.-M., Oostenveld, R., & Jensen, O. (2008). Prestimulus Oscillatory Activity in the Alpha Band Predicts Visual Discrimination Ability. *The Journal of Neuroscience*, *28*(8), 1816–1823. https://doi.org/10.1523/JNEUROSCI.1853-07.2008

Van Ede, F., Van Pelt, S., Fries, P., & Maris, E. (2015). Both ongoing alpha and visually induced gamma oscillations show reliable diversity in their across-site phase-relations. *Journal of Neurophysiology*, *113*(5), 1556–1563. https://doi.org/10.1152/jn.00788.2014

Van Veen, B. D., Van Drongelen, W., Yuchtman, M., & Suzuki, A. (1997). Localization of brain electrical activity via linearly constrained minimum variance spatial filtering. *IEEE Transactions on Biomedical Engineering*, *44*(9), 867–880. https://doi.org/10.1109/10.623056

VanRullen, R. (2016). Perceptual Cycles. *Trends in Cognitive Sciences*, *20*(10), 723–735. https://doi.org/10.1016/j.tics.2016.07.006

VanRullen, R., Delorme, A., & Thorpe, S. (2001). Feed-forward contour integration in primary visual cortex based on asynchronous spike propagation. *Neurocomputing*, *38–40*, 1003–1009. https://doi.org/10.1016/S0925-2312(01)00445-3

VanRullen, R., Guyonneau, R., & Thorpe, S. J. (2005). Spike times make sense. *Trends in Neurosciences*, *28*(1), 1–4. https://doi.org/10.1016/j.tins.2004.10.010

Vieira, P. G., Krause, M. R., & Pack, C. C. (2020). tACS entrains neural activity while somatosensory input is blocked. *PLOS Biology*, *18*(10), Article 10. https://doi.org/10.1371/journal.pbio.3000834

Vogeti, S., Boetzel, C., & Herrmann, C. S. (2022). Entrainment and Spike-Timing Dependent Plasticity – A Review of Proposed Mechanisms of Transcranial Alternating Current Stimulation. *Frontiers in Systems Neuroscience*, *16*, 827353. https://doi.org/10.3389/fnsys.2022.827353

Voloh, B., & Womelsdorf, T. (2018). Cell-Type Specific Burst Firing Interacts with Theta and Beta Activity in Prefrontal Cortex During Attention States. *Cerebral Cortex*, *28*(12), 4348–4364. https://doi.org/10.1093/cercor/bhx287

Von Der Malsburg, C., Phillips, W. A., & Singer, W. (2010). *Dynamic coordination in the brain: From neurons to mind* (Vol. 5). MIT press.

Von Stein, A., Chiang, C., & König, P. (2000). Top-down processing mediated by interareal synchronization. *Proceedings of the National Academy of Sciences*, *97*(26), 14748–14753. https://doi.org/10.1073/pnas.97.26.14748

Vöröslakos, M., Takeuchi, Y., Brinyiczki, K., Zombori, T., Oliva, A., Fernández-Ruiz, A., Kozák, G., Kincses, Z. T., Iványi, B., Buzsáki, G., & Berényi, A. (2018). Direct effects of transcranial electric stimulation on brain circuits in rats and humans. *Nature Communications*, *9*(1), Article 1. https://doi.org/10.1038/s41467-018-02928-3

Vorwerk, J., Cho, J.-H., Rampp, S., Hamer, H., Knösche, T. R., & Wolters, C. H. (2014). A guideline for head volume conductor modeling in EEG and MEG. *NeuroImage*, *100*, 590–607. https://doi.org/10.1016/j.neuroimage.2014.06.040

Vossen, A., Gross, J., & Thut, G. (2015). Alpha Power Increase After Transcranial Alternating Current Stimulation at Alpha Frequency (α-tACS) Reflects Plastic Changes Rather Than Entrainment. *Brain Stimulation*, *8*(3), Article 3. https://doi.org/10.1016/j.brs.2014.12.004

Vosskuhl, J., Strüber, D., & Herrmann, C. S. (2018). Non-invasive Brain Stimulation: A Paradigm Shift in Understanding Brain Oscillations. *Frontiers in Human Neuroscience*, *12*, 211. https://doi.org/10.3389/fnhum.2018.00211

Wang, X.-J. (2020). Macroscopic gradients of synaptic excitation and inhibition in the neocortex. *Nature Reviews Neuroscience*, *21*(3), 169–178.

Whittington, M. A., Traub, R. D., Kopell, N., Ermentrout, B., & Buhl, E. H. (2000). Inhibition-based rhythms: Experimental and mathematical observations on network dynamics. *International Journal of Psychophysiology*, *38*(3), 315–336. https://doi.org/10.1016/S0167-8760(00)00173-2

Windhoff, M., Opitz, A., & Thielscher, A. (2013). Electric field calculations in brain stimulation based on finite elements: An optimized processing pipeline for the generation and usage of accurate individual head models. *Human Brain Mapping*, *34*(4), 923–935. https://doi.org/10.1002/hbm.21479

Wischnewski, M., Engelhardt, M., Salehinejad, M. A., Schutter, D. J. L. G., Kuo, M.-F., & Nitsche, M. A. (2019). NMDA Receptor-Mediated Motor Cortex Plasticity After 20 Hz Transcranial Alternating Current Stimulation. *Cerebral Cortex*, *29*(7), 2924–2931. https://doi.org/10.1093/cercor/bhy160

Wittenberg, M. A., Morr, M., Schnitzler, A., & Lange, J. (2019). 10 Hz tACS Over Somatosensory Cortex Does Not Modulate Supra-Threshold Tactile Temporal Discrimination in Humans. *Frontiers in Neuroscience*, *13*, 311. https://doi.org/10.3389/fnins.2019.00311

Yuan, H., Zotev, V., Phillips, R., & Bodurka, J. (2013). Correlated slow fluctuations in respiration, EEG, and BOLD fMRI. *NeuroImage*, *79*, 81–93. https://doi.org/10.1016/j.neuroimage.2013.04.068

Zaehle, T., Rach, S., & Herrmann, C. S. (2010). Transcranial Alternating Current Stimulation Enhances Individual Alpha Activity in Human EEG. *PLoS ONE*, *5*(11), Article 11. https://doi.org/10.1371/journal.pone.0013766

Zareian, B., Maboudi, K., Daliri, M. R., Abrishami Moghaddam, H., Treue, S., & Esghaei, M. (2020). Attention strengthens across-trial pre-stimulus phase coherence in visual cortex, enhancing stimulus processing. *Scientific Reports*, *10*(1), 4837. https://doi.org/10.1038/s41598-020-61359-7

Zarubin, G., Gundlach, C., Nikulin, V., Villringer, A., & Bogdan, M. (2020). Transient Amplitude Modulation of Alpha-Band Oscillations by Short-Time Intermittent Closed-Loop tACS. *Frontiers in Human Neuroscience*, *14*, 366. https://doi.org/10.3389/fnhum.2020.00366

Zhang, F., Wang, F., Yue, L., Zhang, H., Peng, W., & Hu, L. (2019). Cross-species investigation on resting state electroencephalogram. *Brain Topography*, *32*(5), 808-824. https://doi.org/10.1007/s10548-019-00723-x

Zhang, Yanyu, Zhang, Yifei, Cai, P., Luo, H., & Fang, F. (2019). The causal role of α-oscillations in feature binding. *Proceedings of the National Academy of Sciences*, *116*(34), 17023–17028. https://doi.org/10.1073/pnas.1904160116

7 APPENDIX

Eidesstattliche Erklärung

An Eides statt erkläre ich, dass ich die vorgelegte Dissertation selbstständig und ohne unzulässige fremde Hilfe unter der Beachtung der "Grundsätze zur Sicherheit guter wissenschaftlicher Praxis an der Heinrich-Heine-Universität Düsseldorf" angefertigt habe und dass ich diese in der jetzigen oder einer ähnlichen Form noch keiner anderen Fakultät eingereicht habe.

Düsseldorf, den

VAISHALI BALAJI

Supplementary Material

Table S1: Individual Stimulation Frequency (ISF) and Alpha Peak Frequency (APF) per block

Subject	*ISF (Hz)*	*10s-tACS (Hz)*	*30s-tACS (Hz)*	*10s-control (Hz)*	*30s-control (Hz)*
1	8	9/10	9	11	10
2	10	10	10	10	9
3	12	8/10	9	11	9
4	9	9	9	9	9
5	14	10	8	11	9
6	9	10	9	10	10
7	10	13	10	12	8
8	10	10	10	9	8
9	9	9/10	10	11	10
10	7	9	9	9	9
11	11	12	11	11	11
12	13	8	12	9	13
13	10	11	12	12	11
14	11	11	8/11	9	12
15	11	12	not available	12	12
16	8	9	9	8	10
17	9	10	10	9	10
18	12	12	12	12	12
19	10	9	9	10	8
20	10	11	11	11	11
21	10	10/11	10	9	10
22	10	9	9	9	10
23	9	10	9	10	8
24	11	11	11	11	11

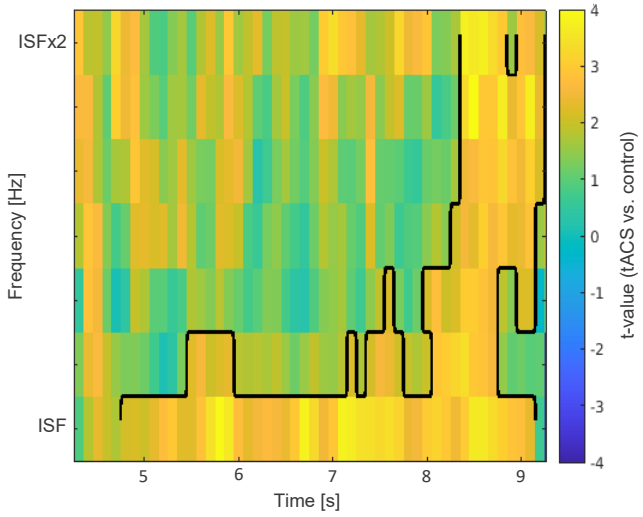

Figure S1. Control Analysis
On uniformly shifting the TFR to align ISFs to 10 Hz, the harmonic frequencies are misaligned. To circumvent broadband-spectral increase in power and thereby delineate harmonic effects, we recomputed the analysis in Fig. 2B. In the control analysis, we restricted the frequency range between ISF and its first harmonic frequency. Hence, for an ISF of 10 Hz, the frequencies ranged from 10 to 20 Hz, and for an ISF of 7 Hz, from 7 to 14 Hz. Five intermediate frequencies were selected between ISF and the first harmonic of ISF. Y-axis ranges from 'ISF' to 'ISFx2' Hz (first harmonic frequency). t-values were averaged over channels in the significant cluster shown in Fig 17A. We found one significant positive cluster (outlined in black).

A 10s-block

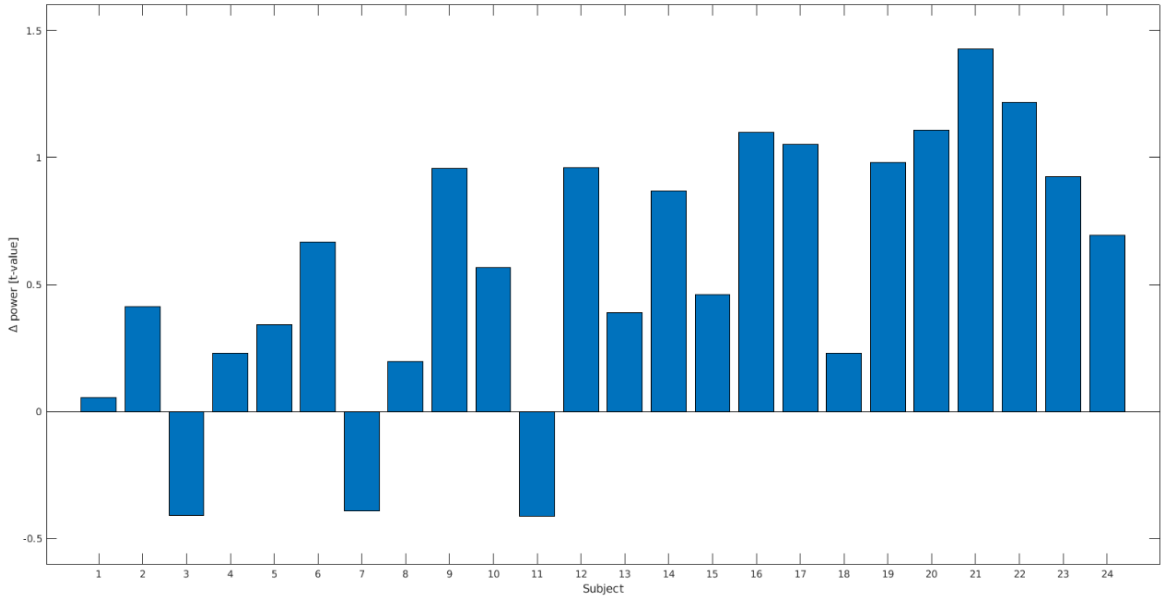

B 30s-block

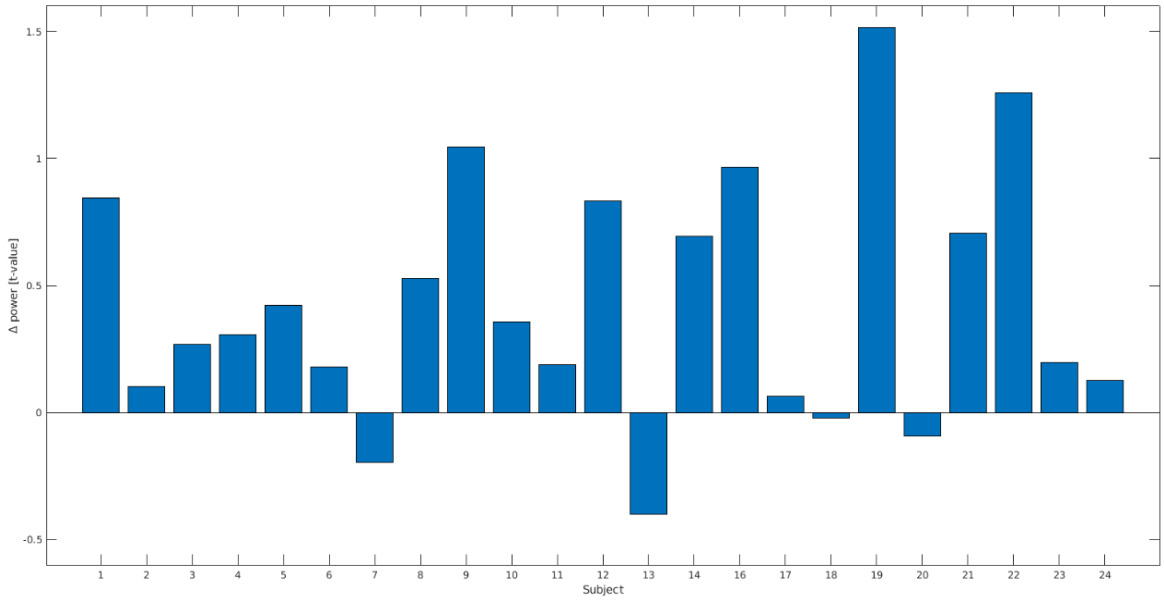

Figure S2. Inter-individual variation in response to tACS
A) Bar graph illustrates Δpower for the 10 s-tACS block. Δpower (at ISF) was averaged over channels in the significant cluster shown in Fig. 17A, and over time. Each bar represents a single subject. **B)** Same as in A), but for 30 s-tACS block.

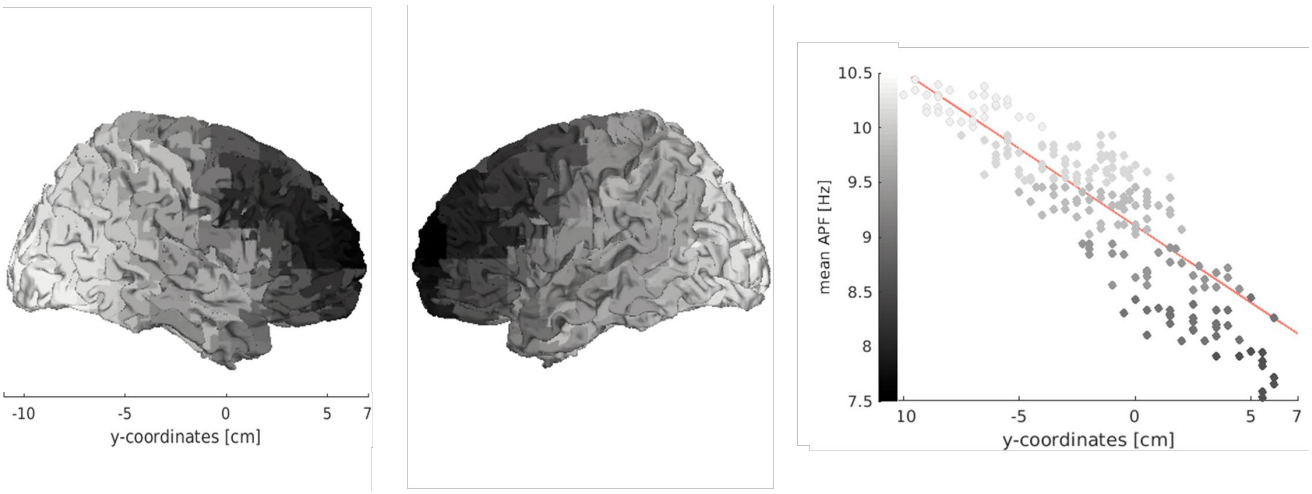

Figure S3. Distribution of time-averaged APF
In the left panel, time-averaged APF for each parcel is projected on an MNI template brain. In the right panel, APF values were averaged along a spatially sliding window in the posterior-to-anterior direction. We found that the Y-coordinate position of the parcel significantly predicted APF ($R^2 = 0.646$, $p < 0.001$).

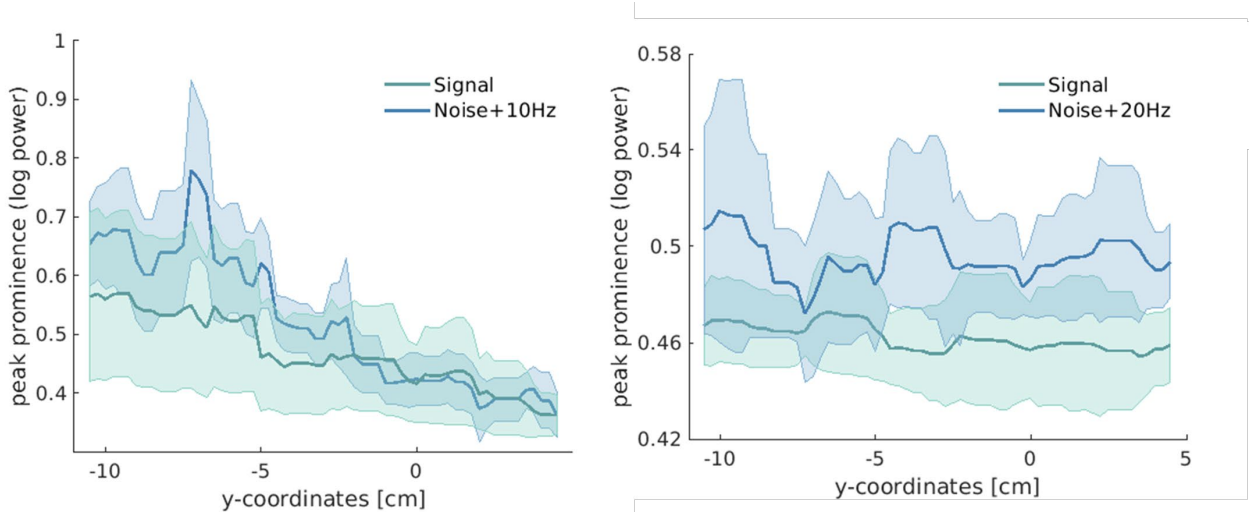

Figure S4. Amplitude of simulated peaks
Log power of APF of physiological signal (in teal) and simulated signal (in blue) is plotted along the y-coordinate plane.

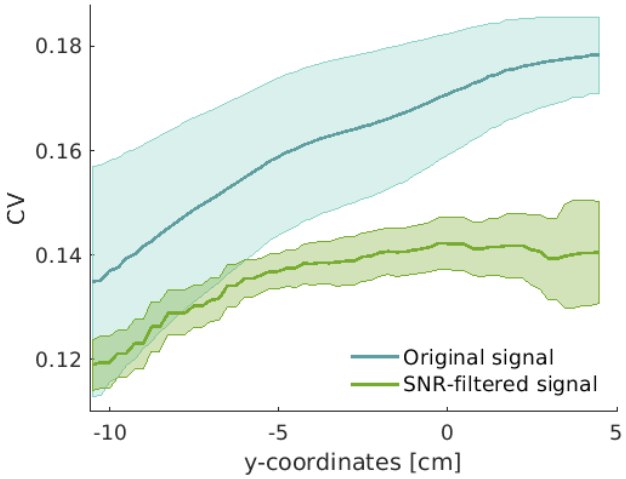

Figure S5. Control analysis: SNR-based thresholding of APFs
The CV of physiological signal (in teal) and SNR-filtered signal (in green) is plotted along the Y-coordinate plane. The shaded region indicates the standard deviation across datasets. We found that the Y-coordinate position of the parcel significantly predicted the CV of the SNR-filtered APFs (R^2 = 0.359, p<0.001).

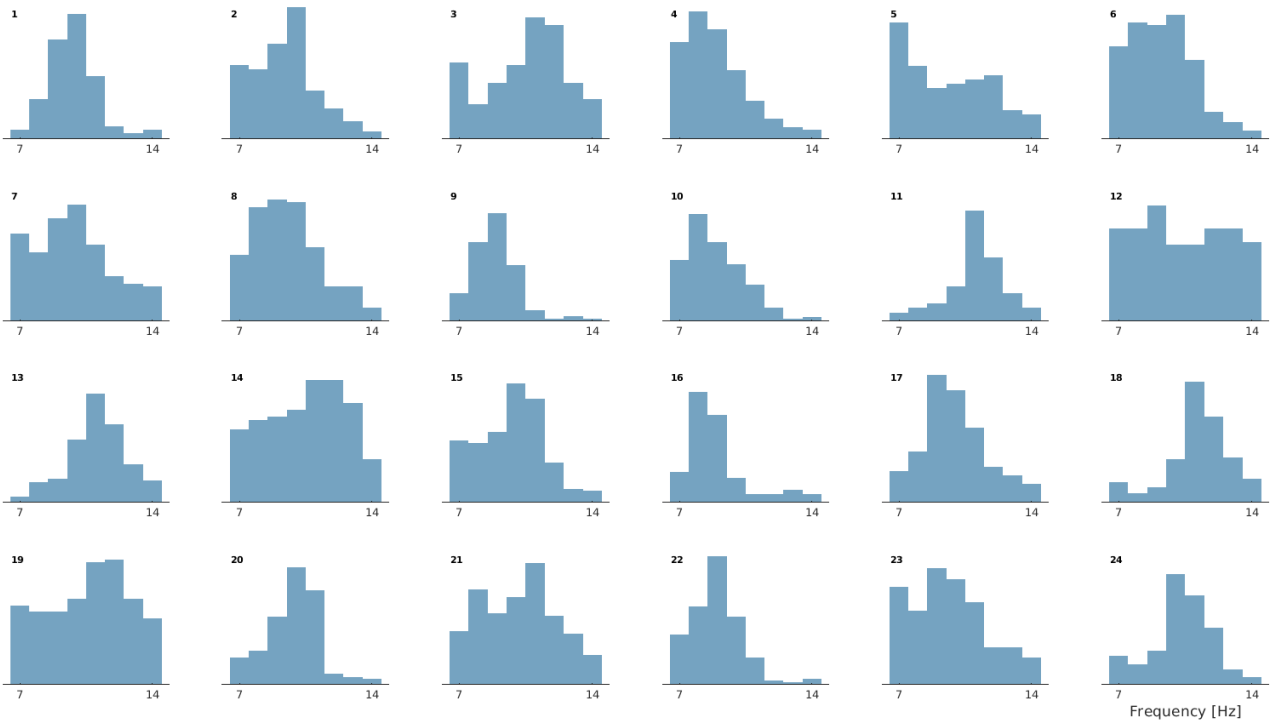

Figure S6. Distribution of APFs in the left lateral occipital cortex
Histogram of individual alpha peak frequencies (APFs) across all participants (n = 24). The x-axis shows APF values in Hz, and the y-axis indicates the number of epochs in which each frequency was identified as the APF in the left lateral occipital cortex.

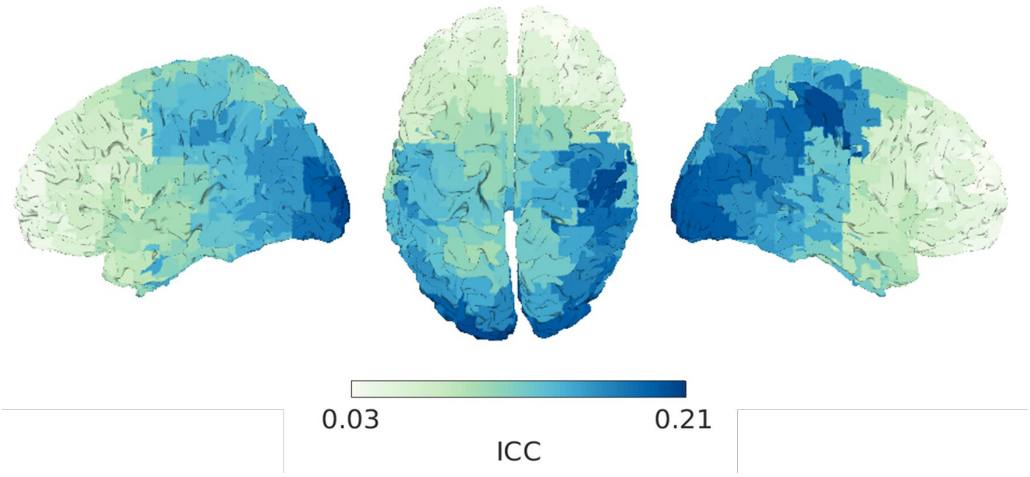

Figure S7. Estimates of Intra-Class Correlation (ICC) from 2 s epochs
Parcel-wise ICC values are projected onto an MNI template brain. The lowest reliability was observed in the right middle frontal gyrus (ICC = 0.024, 95% CI: 0.011–0.056), while the highest was found in the left ventromedial occipital cortex (ICC = 0.207, 95% CI: 0.133–0.345). The colour bar is scaled to the maximum ICC value observed across parcels.

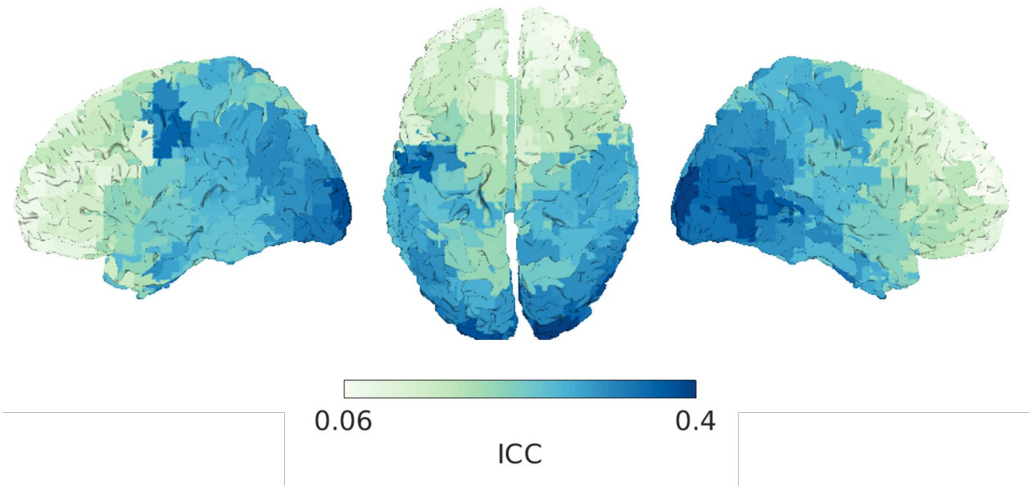

Figure S8. Estimates of Intra-Class Correlation (ICC) from 5 s epochs
Parcel-wise ICC values are projected onto an MNI template brain. The lowest reliability was observed in the right middle frontal gyrus (ICC = 0.056, 95% CI: 0.019–0.134), while the highest occurred in the right lateral occipital cortex (ICC = 0.358, 95% CI: 0.244–0.531). The colour bar is scaled to the maximum ICC value observed across parcels.